NAVAL POSTGRADUATE SCHOOL

MONTEREY, CALIFORNIA

THESIS

EXPERIMENTAL INVESTIGATION OF PITCH CONTROL ENHANCEMENT TO THE FLAPPING WING MICRO AIR VEHICLE

by

Chin Chee Kian

December 2006

Thesis Advisor: Kevin D. Jones
Second Reader: Christopher Brophy

Approved for public release; distribution is unlimited

THIS PAGE INTENTIONALLY LEFT BLANK

REPORT DOCUMENTATION PAGE		Form Approved OMB No. 0704-0188

1. AGENCY USE ONLY *(Leave blank)*	2. REPORT DATE	3. REPORT TYPE AND DATES COVERED
	December 2006	Master's Thesis

4. TITLE AND SUBTITLE: Experimental Investigation of Pitch Control Enhancement to the Flapping Wing Micro Air Vehicle.	**5. FUNDING NUMBERS**
6. AUTHOR(S) Chin Chee Kian	
7. PERFORMING ORGANIZATION NAME(S) AND ADDRESS(ES) Naval Postgraduate School Monterey, CA 93943-5000	**8. PERFORMING ORGANIZATION REPORT NUMBER**
9. SPONSORING /MONITORING AGENCY NAME(S) AND ADDRESS(ES) N/A	**10. SPONSORING/MONITORING AGENCY REPORT NUMBER**
11. SUPPLEMENTARY NOTES The views expressed in this thesis are those of the author and do not reflect the official policy or position of the Department of Defense or the U.S. Government.	
12a. DISTRIBUTION / AVAILABILITY STATEMENT Approved for public release; distribution is unlimited	**12b. DISTRIBUTION CODE** A

13. ABSTRACT (maximum 200 words)

The mechanical pitching characteristic of the NPS flapping-wing Micro Air Vehicle (MAV) developed by Professor Kevin D. Jones are studied experimentally through the use of constant temperature anemometry and force balance techniques. The MAV without the main fixed-wing is placed in a laminar flow field within a low speed wind tunnel with the wake after the flapping wings characterized with a constant temperature anemometer and thrust generation measured by a load cell at various neutral angles, flapping frequencies and free stream velocities. The experiments seek to determine the effects on the MAV propulsion when the neutral angle of attack of the flapping wings is varied. Flow visualization is also performed to better enhance understanding of the flow field across the pitched flapping wings.

14. SUBJECT TERMS Flapping-wing Propulsion, Micro Air Vehicle, Unmanned Systems, Constant Temperature Anemometer, Low Reynolds Number			**15. NUMBER OF PAGES** 135 **16. PRICE CODE**
17. SECURITY CLASSIFICATION OF REPORT Unclassified	**18. SECURITY CLASSIFICATION OF THIS PAGE** Unclassified	**19. SECURITY CLASSIFICATION OF ABSTRACT** Unclassified	**20. LIMITATION OF ABSTRACT** UL

NSN 7540-01-280-5500 Standard Form 298 (Rev. 2-89)
Prescribed by ANSI Std. 239-18

THIS PAGE INTENTIONALLY LEFT BLANK

Approved for public release; distribution is unlimited

EXPERIMENTAL INVESTIGATION OF PITCH CONTROL ENHANCEMENT TO THE FLAPPING WING MICRO AIR VEHICLE

Chin Chee Kian
Defence Science & Technology Agency, Singapore
B.Eng., University of Glasgow (UK), 1997

Submitted in partial fulfillment of the
requirements for the degree of

**MASTER OF SCIENCE IN ENGINEERING SCIENCE
(MECHANICAL ENGINEERING)**

from the

**NAVAL POSTGRADUATE SCHOOL
December 2006**

Author: Chin Chee Kian

Approved by: Dr. Kevin D. Jones
Thesis Advisor

Dr. Christopher Brophy
Second Reader

Dr. Anthony Healey
Chairman, Department of Mechanical and Astronautical Engineering

THIS PAGE INTENTIONALLY LEFT BLANK

ABSTRACT

The mechanical pitching characteristic of the NPS flapping-wing Micro Air Vehicle (MAV) developed by Professor Kevin D. Jones are studied experimentally through the use of constant temperature anemometry and force balance techniques. The MAV without the main fixed-wing is placed in a laminar flow field within a low speed wind tunnel with the wake after the flapping wings characterized with a constant temperature anemometer and thrust generation measured by a load cell at various neutral angles, flapping frequencies and free stream velocities. The experiments seek to determine the effects on the MAV propulsion when the neutral angle of attack of the flapping wings is varied. Flow visualization is also performed to better enhance understanding of the flow field downstream of the pitched flapping wings.

THIS PAGE INTENTIONALLY LEFT BLANK

TABLE OF CONTENTS

LIST OF FIGURES

LIST OF TABLES

THIS PAGE INTENTIONALLY LEFT BLANK

ACKNOWLEDGMENTS

The author would like to express his sincerest appreciation to Dr. Kevin Jones for his time and effort supervising and assisting in the completion of this project. His expertise in this field was essential. Additionally, the author would like to thank Dr. Christopher Brophy and CAPT Patrick Hutcheson (USAF) for their shared expertise in the mysterious world of the StreamWare continuous temperature anemometery and Mr. Thomas Christian for his work on the creation of the National instruments Labview 7.1 Virtual Instrument blocks.

Finally, the author would like to thank his family for their continuing support and encouragement throughout this process, without which this would not have been possible.

THIS PAGE INTENTIONALLY LEFT BLANK

I. INTRODUCTION

A. BACKGROUND

The advancement of science and technology in the last century brought a new facet to this civilization. Man has begun to experience what their forefathers could only have dreamed. Spears and sword no longer command the war of the modern world but technologies and weapons beyond the reach of a non-civilized society. The increasing need for small autonomous aerial vehicles draws the attention of modern scientists and researcher to the field of low Reynolds number aerodynamics. In this perspective the prototype flapping-wing propelled MAV developed by NPS has since been successful. Attention now shifts to the performance optimization of the vehicle since actual flight experience and experimental data show the possibility of further aerodynamic enhancement, predominantly in areas with regard to the flapping wings of the MAV.

Garrick [Ref. 10] showed that plunging wings produce thrust at any frequency and propulsion is also possible for purely pitching airfoils but only at high frequencies. Using linear theory, it was found that the addition of pitching motion reduces thrust and sets a maximum speed for which thrust is produced [Ref. 2]. Nevertheless, the NPS model found a combination of plunge motion with elastic pitching advantageous and for the NPS model a pitch degree of freedom was apparently necessary. This highlights the limit of linear theory in modeling the physics of the phenomena and emphasizes the need of a more realistic approach to analyze the phenomena.

Further research on effects of mechanical pitch control on the flapping wing micro air vehicle is desired and a heuristic approach by experimenting may be an option since numerical simulation may be too expensive an option to be part of the iterative optimization process.

B. OBJECTIVE

The primary goal of this work is to examine the geometric effects of varying the flapping wing neutral angle of attack and aero-elastic pitching on the NPS flapping-wing MAV and its influence on aerodynamic properties. It is also of interest to investigate the effect of varying flapping frequency and free stream conditions on the experimental model.

C. CHALLENGES / MOTIVATION

The full potential of the existing MAV has yet to be realized; many parameters that affect the performance of the existing flying model have not been optimized. Earlier findings by Jones and Platzer [Ref. 11] recognized that at reasonable frequencies, a large portion of the energy used in flapping was lost in the form of vortices shed in the wake. It is therefore the interest of this work to conduct an experimental investigation in the area of varying flapping wing spring neutral or simply the neutral angle of attack to better understand the aerodynamic properties affecting the performance of the flapping wings so as to improve performance and control of the existing MAV.

II. EQUIPMENTS

A. WIND TUNNEL

The NPS MAV wind tunnel [Ref. 3] utilizes an open circuit design with the intake and test section mounted horizontally on a wooden frame with casters for mobility. Air flow within the test facility is driven by a 4-blade axial fan powered by a Minarik Electric direct current motor and speed variation controlled by a Motor Master 100 controller. The facility has an overall length of 13 feet and is 84 inches tall at the tip of the 9 blades exhaust stator cone. The intake section or settling chamber consists of an aluminum honeycomb section with approximately 38,800 cells, each cell size of 0.25 inches, thickness of 1.375 inches and a length to size ratio at 5.5. The honeycomb section is followed with two layers of screen and their associated settling regions connected to a bellmouth. Screens in the settling chamber are made of 0.01 inch diameter wire with a mesh size of 0.05 inches. They are spaced at 3.25 inches in their mounting frames for a spacing of 65 mesh diameters. The screen improves airflow uniformity and reduces turbulence intensity by imposing a pressure drop proportional to the velocity squared. The bellmouth is further connected to a three dimensional contraction 40 inches long, 45 inches high and 54 inches wide yielding a contraction ratio of 6.75 and a length to height ratio at 0.89. It serves to reduce variation in the mean and fluctuating air velocity to an even smaller fraction of the average mean air velocity supplied to the test section. The rectangular plexi-glass test section is 53 inches long, 15 inches high and 24 inches wide and has a top access ceiling to facilitate equipment mounting and dismounting. The Wind tunnel is as illustrated in Figure 2-1 to Figure 2-4.

Figure 2- 1 NPS MAV Wind Tunnel

Figure 2- 2 Honeycomb Intake Screen and Bell-mouth contraction

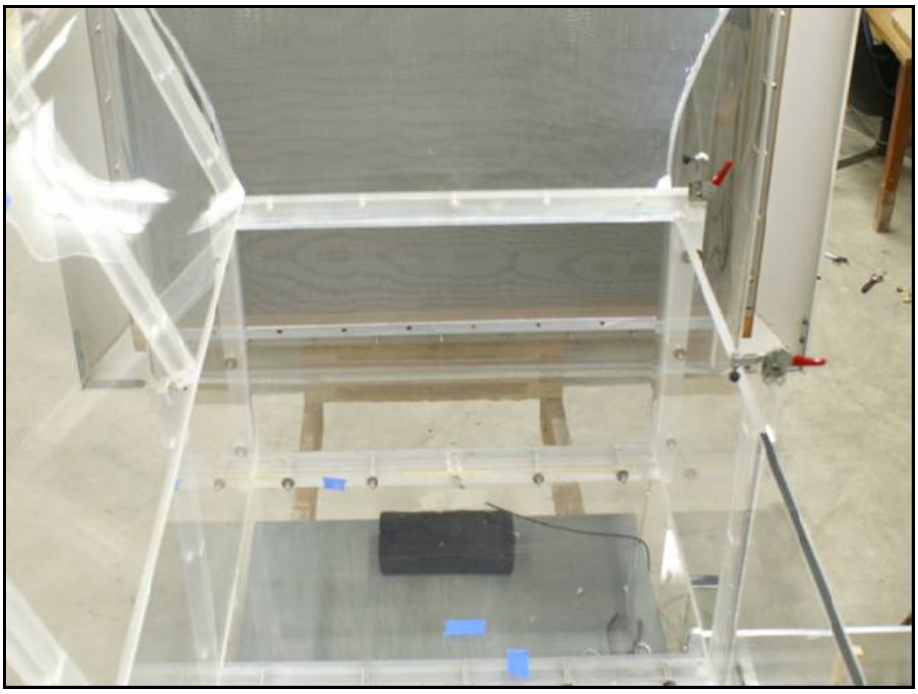

Figure 2- 3 Test Section

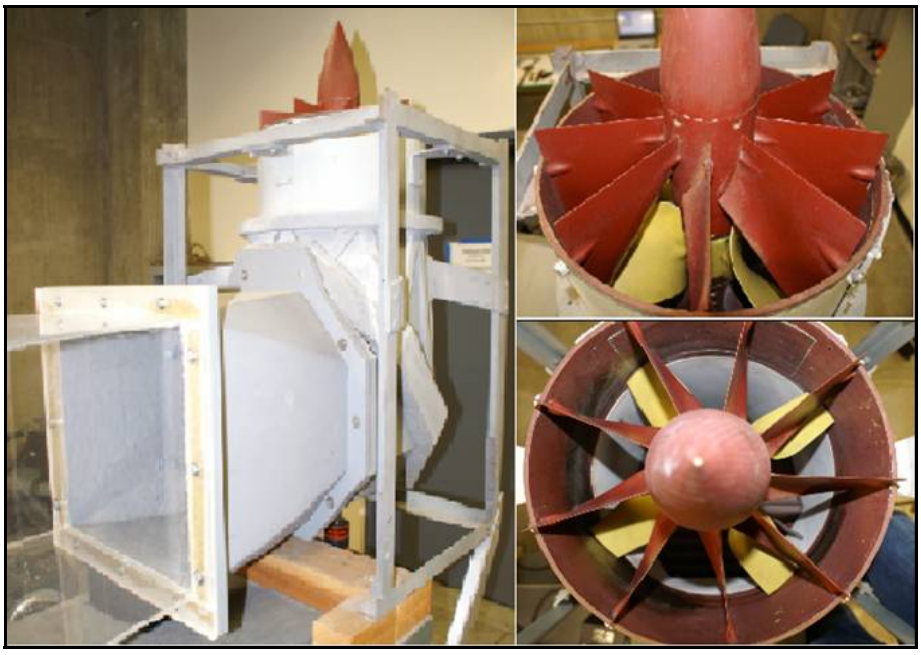

Figure 2- 4 4-Blade Axial Fan with 9-Blades Exhaust Stator Cone

B. NPS MAV MODEL

The NPS MAV model [Ref. 3] used for the experiment was constructed by Professor Kevin D. Jones. The experimental model without the main fixed wing is illustrated in Figure 2-5. The experimental model generally consisted of a fuselage to house a miniature DC motor, self-developed miniature electronic circuitry, a set of planetary transmission gears for speed reduction and crankshaft for converting rotational motion to linear motion of the flapping beams. The flapping beams were attached to the front of the fuselage on one end and a pair of flexible wing mounts on the other. The flapping wings were driven by the flapping beams in a plunge motion connected via a pair of elastic carbon fiber tabs.

The pair of flapping wings with span at 9.84 inches was identical in construction, each having a chord of 1.57 inches in the midspan and tapering to 1.18 inch at the ends to limit spanwise oscillations of the wing. The tapered wing provided no noticeable decrease in thrust [Ref. 3]. The leading edge was constructed of a balsawood dowel and the surface was covered with thin plastic film supported at seven points with chordwise ribs of carbon fiber ply construction. A set of crankshaft and connecting rods were used in the experiment to adjust the plunging amplitude and mean separation; the centerline to bottom-dead-center is 0.5 inches with a max separation of 4 inches and plunge amplitude of 0.75” or 0.48 Chord.

The crankshaft and connecting rods drive the flapping wings in a counter-phase manner to eliminate the inertial and aerodynamic effects of a single wing moving in plunge motion. Primary pitch control of the flapping wings was achieved by varying two miniature servo-motors housed within the fuselage via a connecting rod to a control horn at the flapping wing attach point. Secondary or aero-elastic pitching was further induced by allowing free bending motion of the flexible carbon fiber strips connecting the beams and the flapping wings.

The physical dimensions of the standard model and its flapping wings are illustrated in Figure 2-6 to Figure 2-8.

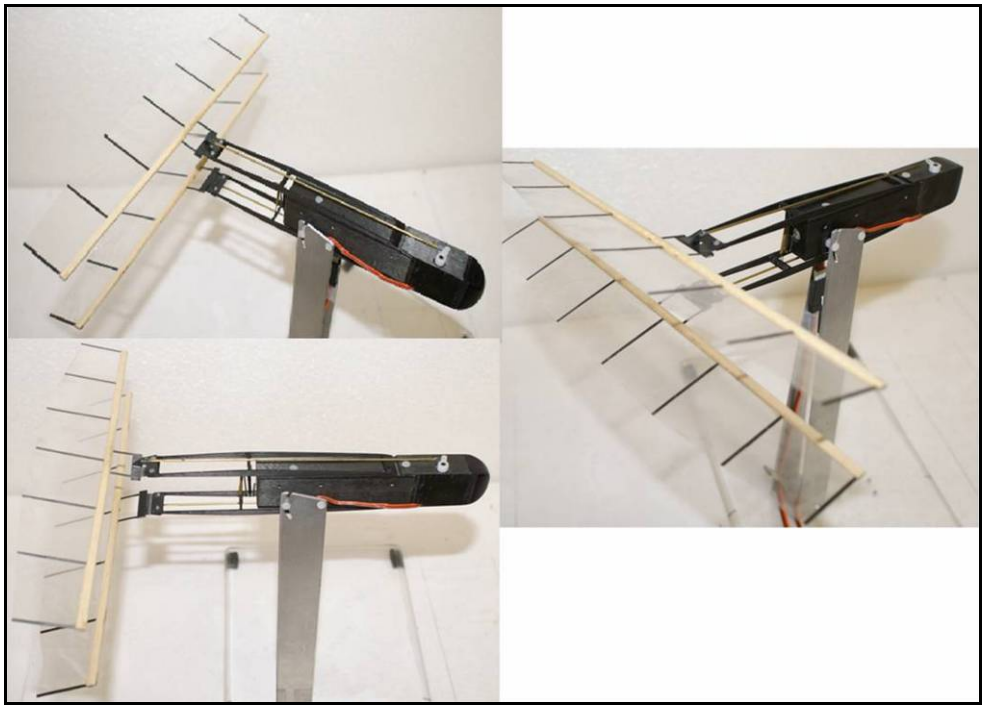

Figure 2- 5 Experimental Model with Flapping Wings

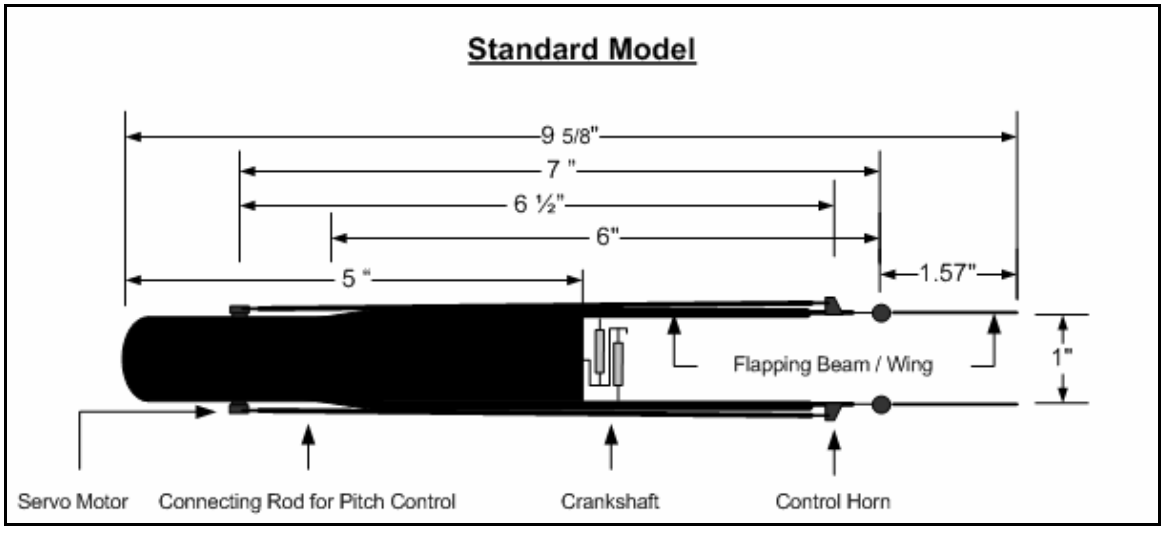

Figure 2- 6 Standard Experimental Model (Part a)

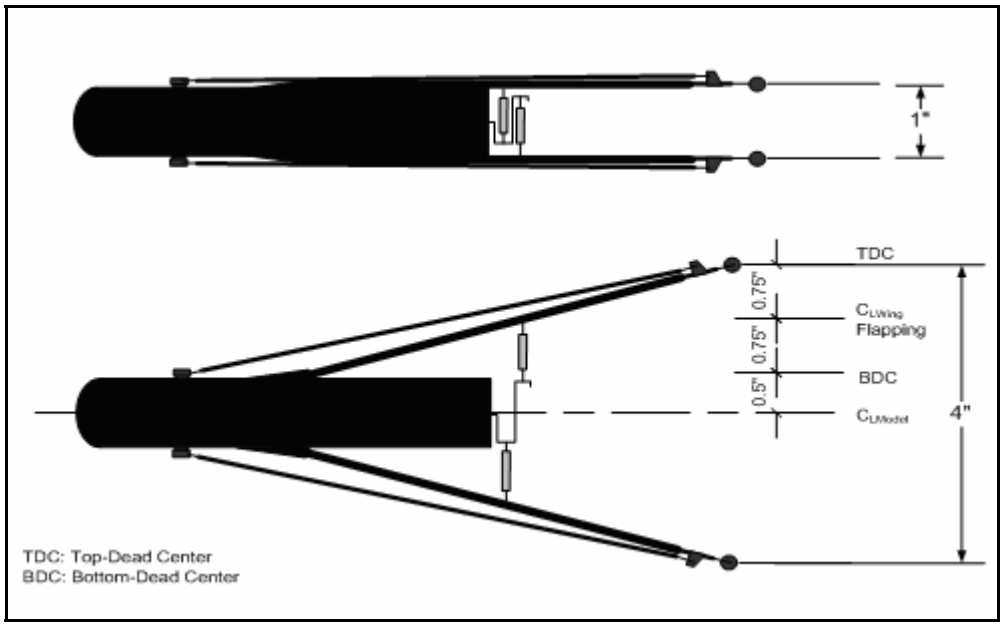

Figure 2- 7 Standard Experimental Model (Part b)

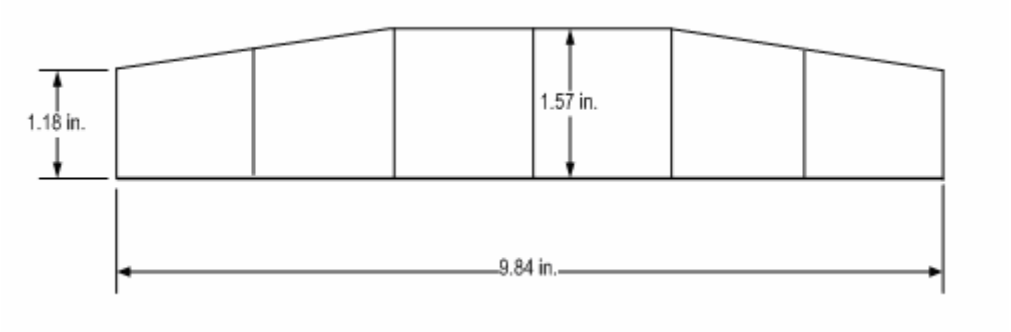

Figure 2- 8 Flapping Wing of Standard Experimental Model

The experimental model was powered by an external Elenco (model MX-9300) power supply. The flapping frequency was controlled by adjusting the voltage from the Elenco MX-9300 with frequency fluctuation within ±0.5% set point. The actual frequency was monitored using a HP (model 54600B) 100 MHz oscilloscope monitoring a once-per-revolution square wave generator.

C. TRAVERSE MECHANISM

The traverse mechanism [Ref. 3] consists of 3 directional axes on Velmex Unislide, each driven by a standalone drive motor capable of 200 steps per revolution and 16,000 counts per inch of movement on a pitched lead screw. The x-axis was supported by a Velmex Unislide (model B4026P40J) with a Bodine Electric DC stepping motor (model 34T1BEHD). The y-direction was supported by Velmex Unislide (model B4027P40J) with a Superior Electric stepping motor (model M091-FD09), and the z-axis was regulated by a Velmex Unislide (model B2515 P40J) with an attached Bodine Electric DC stepping motor (model 23T2BEHD). The motors control was integrated and master controlled by a Velmex VP 9003 controller. The traverse mechanism is illustrated in Figure 2-9.

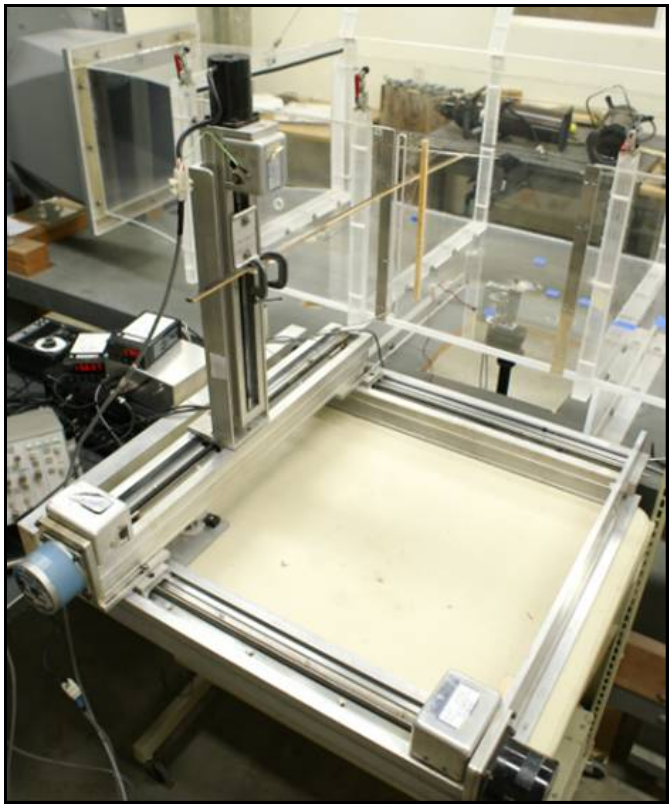

Figure 2- 9 3-Directional Axes Traverse Mechanism

D. HOT WIRE ANEMOMETER

A Dantec Measurement Technology Streamline 90N10 main frame with controller and temperature monitor was used for the experiment [Refs. 4 and 5]. The system consists of a controller, five 90C10 CTA (Constant Temperature Anemometer) modules, a temperature probe, a 55R11 single sensor wire probe and a 90H02 flow unit. The complete system is operated by the StreamWare application software operating on a Pentium II-450 MHz PC, which performs module set-up, automatic probe calibration, acquisition of data, data conversion and data reduction. Both raw and reduced data can be presented in StreamWare. A schematic of the hot-wire measurement system is illustrated in Figure 2-10.

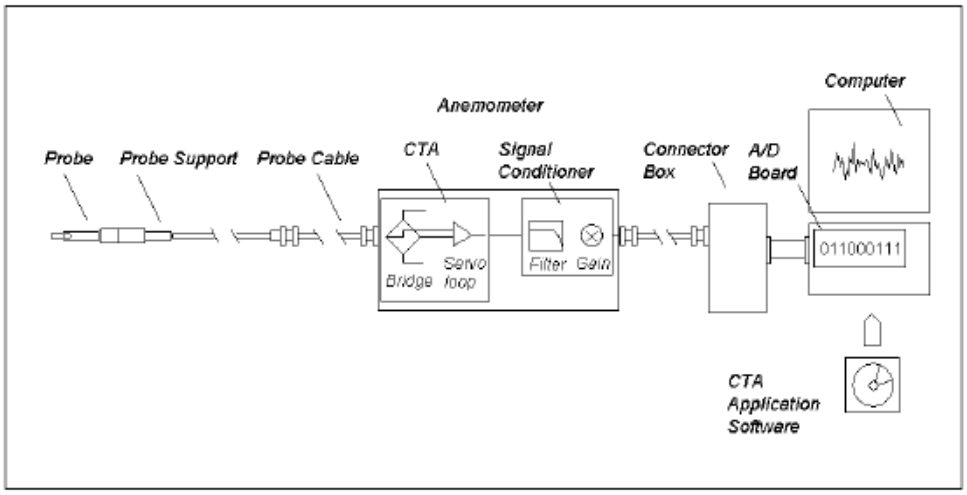

Figure 2- 10 Schematic of Typical CTA Measuring Chain [Ref. 4]

The controller manages communications between the hardware modules and the PC via a serial comport. The controller also includes a temperature circuit for a system temperature probe. It is used to monitor the ambient temperature during overheat set-up and data acquisition. The ambient temperature is then used by the application software to correct the anemometer voltages before conversion

The five channel 90C10 CTA provides efficient mapping of velocity and turbulence fields in air flow calibration when used with StreamWare application software and Streamline 90H02 flow unit. The 90H02 flow unit, an automatic calibrator is an important part of the system as it facilitates fast and accurate probe calibrations prior to experiments. The calibrator produces a free air jet via a high resolution control valve and a selection of exit nozzles for accurate calibration of hot-wire probes in air at velocities from a few cm/s up to Mach 1 when supplied with a normal pressurized air supply between 0.7 MPa to 0.9 MPa. During calibration, the probe is placed in a free jet with a flat, low-turbulence velocity profile.

Real-time analog velocity and temperature measurements were made possible with the Streamline main frame and StreamWare application software. The acquired raw data were post-processed by StreamWare after being fed through a 15 channel National Instruments BNC-2090 A/D board.

The 55R11 single sensor wire probe [Ref. 3, 4 and 5] capable of high flow sensitivity and frequency response was recommended for the measurement of unidirectional gas flows with low turbulence intensity. The 55R11 wire probe with a sensitivity of 0.42% consists of a 5µm diameter tungsten wire 1 mm long supported by ceramic coated stainless steel prongs at each end. The prongs supported by a probe support connect via a Streamline probe cable to the CTA modules. The probe operates by measuring the change in its wire resistance with temperature. The system’s thermocouple in the flow field next to the hot wire probe provides for temperature compensation. When the bridge is in balance, no voltage difference exists across its diagonal. If the flow velocity were to increase, more heat would be transferred away from the wire and its resistance reduces with reduced temperature. Since, the probe current is calculated by the voltage drop across the bridge, reduction in resistance results in an error voltage at the

input of the current regulating amplifier, which then increases the probe's operating current. The increase in current heats the wire and increases its resistance until balance is restored. The current regulating amplifier operates with a very high gain so a condition of bridge balance exists almost independent of the flow velocity past the wire. The response time of the wire is thus reduced to a few micro seconds. In this way, velocity profile evaluation at very high frequencies is made possible when system calculations are based on real-time heat transfer from the hot-wire. The system setup is illustrated in Figure 2-11 to Figure 2-13.

Figure 2- 11 90C10 CTA Modules with BNC 2090 ADC board

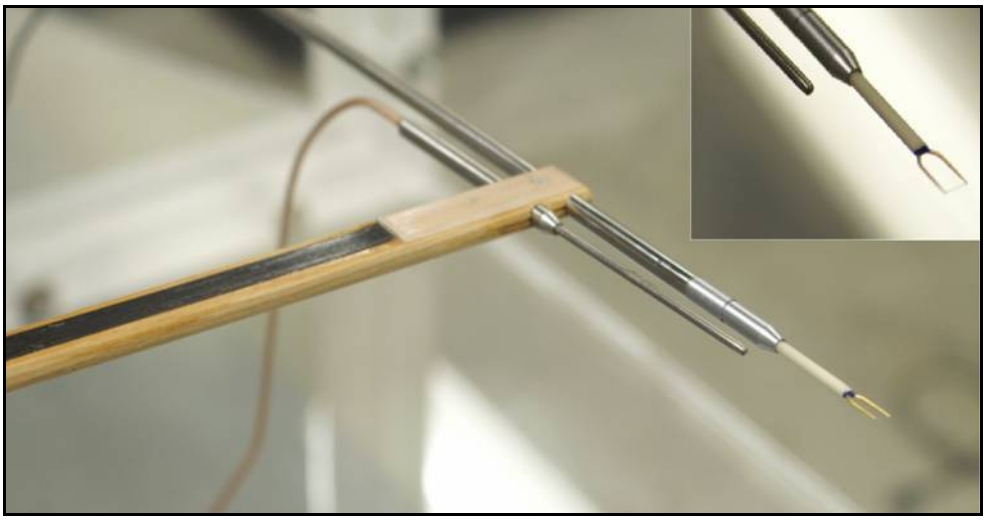

Figure 2- 12 Temperature Probe and 55R11 Single Sensor Wire Probe

Figure 2- 13 90H02 Flow Unit

THIS PAGE INTENTIONALLY LEFT BLANK

III. EXPERIMENTAL SETUP

A. TEST GRID

The test section of the wind tunnel measures 53 inches long, 15 inches tall and 24 inches wide. In view of boundary layer effects near the wall, the desired test area with minimal air flow fluctuation was mapped into an 11 row by 9 column grid system measuring 5 inches tall by 13.12 inches wide. The center of the grid coincides with the center of the model fuselage located at row 6, column 5. Each vertical gridline/ point is space 1.64 inches apart and each horizontal gridline/ point is spaced 0.5 inches apart. Division of the flapping wing in 9 columns is illustrated in Figure 3-1 and the 11 row x 9 column test grid for the model in Figure 3-2 to Figure 3-4.

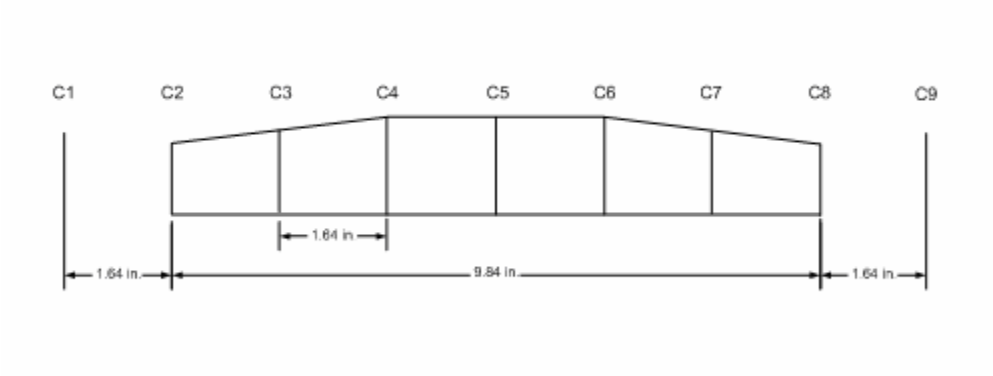

Figure 3- 1 Nine Horizontal Divisions of the Flapping Wing

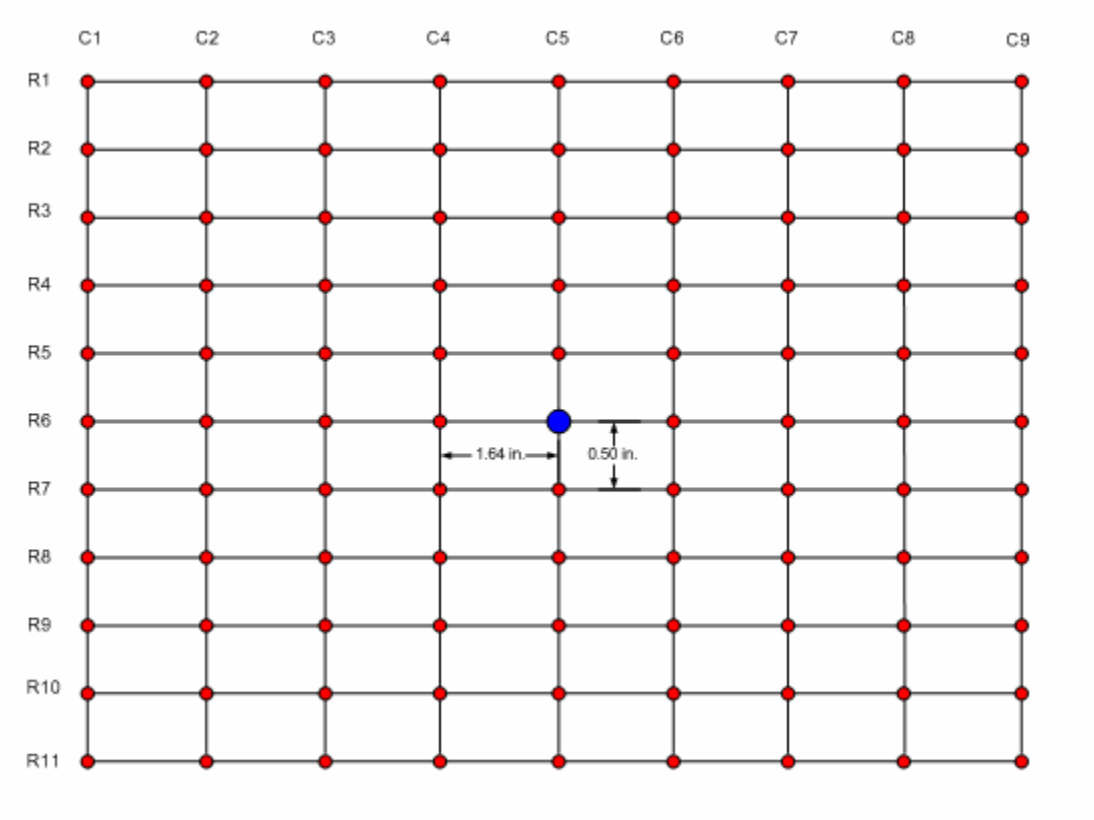

Figure 3- 2 11 Row x 9 Columns Test Grid

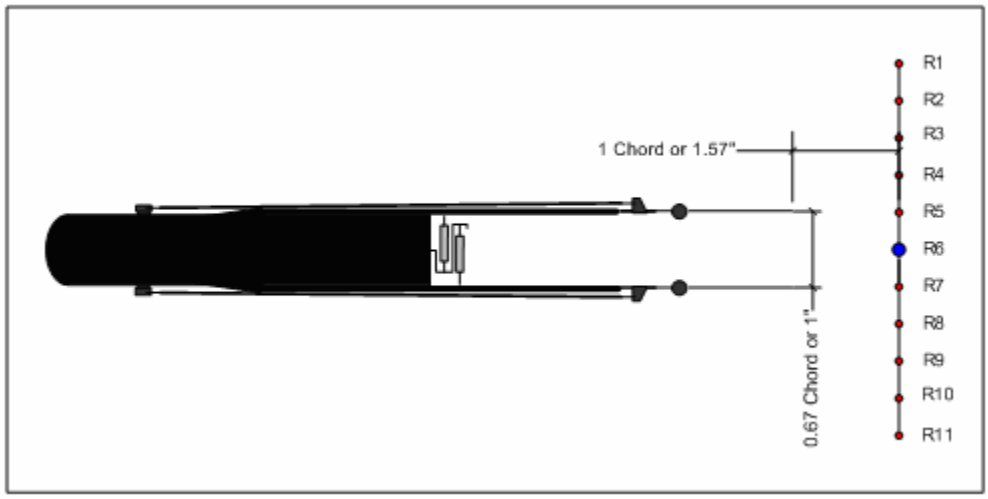

Figure 3- 3 Experimental Model (Fully Closed Position)

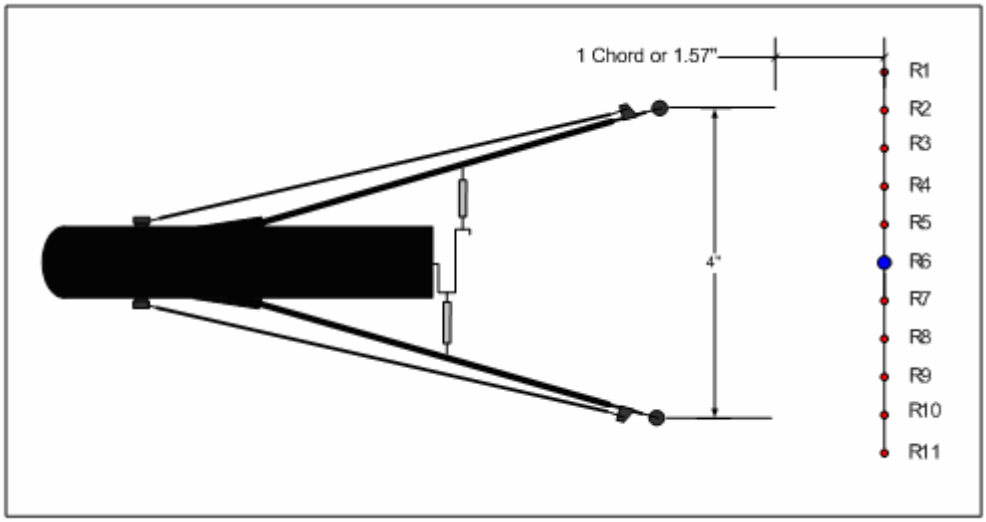

Figure 3- 4 Experimental Model (Fully Extended Position)

B. CALIBRATION

1. Hot-Wire Anemometer

The 55R11 single sensor wire probe was calibrated with the Streamline 90H02 flow unit and with an exit nozzle for air velocity referenced at 0.5m/s to 60m/s. The probe and thermocouple were attached to the flow module with the hotwire sensor positioned directly in the flow stream. The module was set to calibrate from 1 to 10 m/s in accordance with the testing velocities of interest in 10 points arranged logarithmically as recommended by the system manufacturer. The calibration results with a fourth order polynomial fit according to the equation;

$$U = C_0 + C_1 E_{corr} + C_2 E_{corr}^{\ 2} + C_3 E_{corr}^{\ 3} + C_4 E_{corr}^{\ 4}.$$

are tabulated in Appendix A. The coefficients differ for each calibration, but typical values are;

C_0= -11.63; C_1= 56.69; C_2= -92.80; C_3= 51.99; C_4= -0.00.

2. Test Grid Air Flow Verification

Earlier wind tunnel air flow verification tests by Hickle, C. [Ref. 3] are shown in Table 3-1.

S/N	Test Speed (m/s)	Average Turbulence Intensity (%)	Average Velocity Variation (%)
1.	2 m/s	0.712	0.251
2.	3 m/s	0.569	0.165
3.	5 m/s	0.511	0.125

Table 3- 1 Wind Tunnel Air Flow Verification (From: Ref. 3)

Hickle indicated that the percentage velocity variation was well within velocity variation across good quality wind tunnel test sections often quoted in the .2 - .3% range [Refs. 3 and 7].

The test grid was further verified with air flow sampled at 40 KHz, 10,000 points per sample taken at 5 locations within the test grid, i.e., at 4 corners and center of test area. Samples were taken for 2m/s, 3m/s, 4m/s and 5m/s respectively. The average velocity variation was computed by averaging the sum of percent difference between the velocity at a point and the mean velocity. The average velocity variations are shown in Table 3-2.

S/N	Test Speed (m/s)	Average Velocity Variation (%)
1.	2 m/s	0.262
2.	3 m/s	0.155
3.	4 m/s	0.139
4.	5 m/s	0.118

Table 3- 2 Average Velocity Variation for Varying Free Stream Velocities

The results showed that the velocity variation across the test area was well within standards [Refs. 3 and 7].

3. NPS MAV Model

Earlier studies conducted on the model were primarily pure plunge motion with uncontrolled secondary pitching induced by the aero-elastic carbon fiber joint. In this experiment, a miniature servo motor was housed in the model fuselage connected via connecting rods to provide primary mechanical pitch (controlled) motion at the flexible joint flapping wings, i.e., the flapping wings were controlled to pitch mechanically and also allowed to pitch elastically under the influence of the aero-elastic carbon fiber joint. The mechanical pitch deflection on the model was made possible by an external pulse-width modulation input to the servo motor via a HiTEC HFP-10 digital servo programmer. Three neutral pitch settings were desired; 0°, 10° and 20°. The pitch settings on the model are illustrated in Figure 3-5 to Figure 3-7.

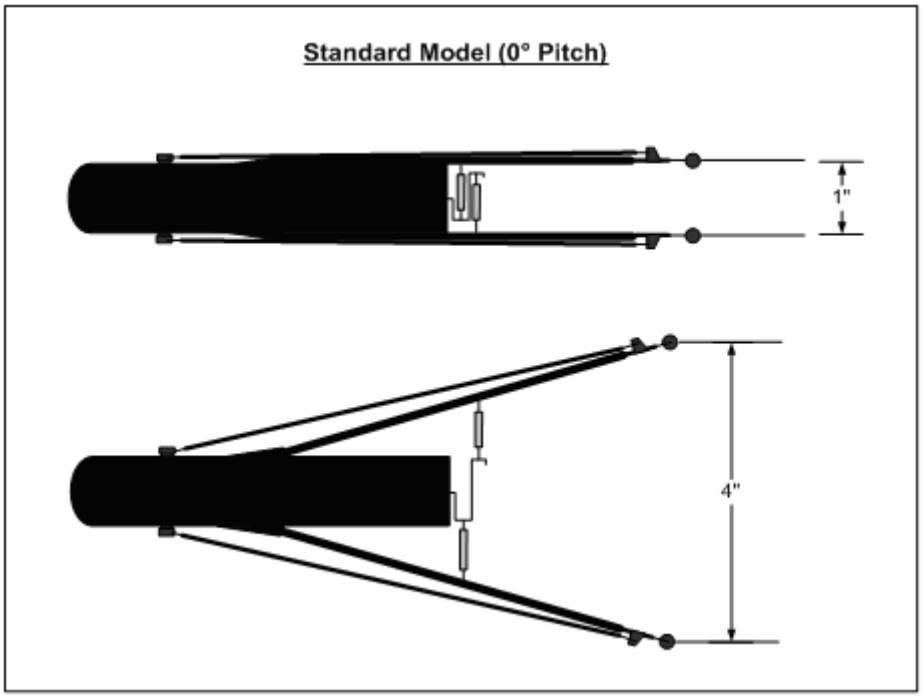

Figure 3- 5 Experimental Model with 0 Degree Neutral Angle

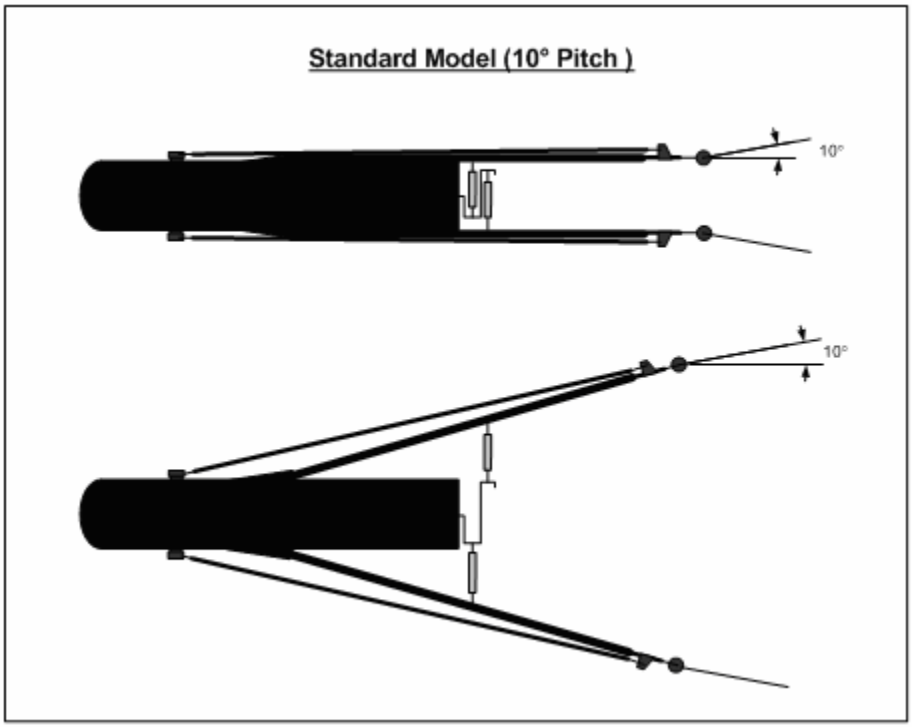

Figure 3- 6 Experimental Model with 10 Degree Neutral Angle

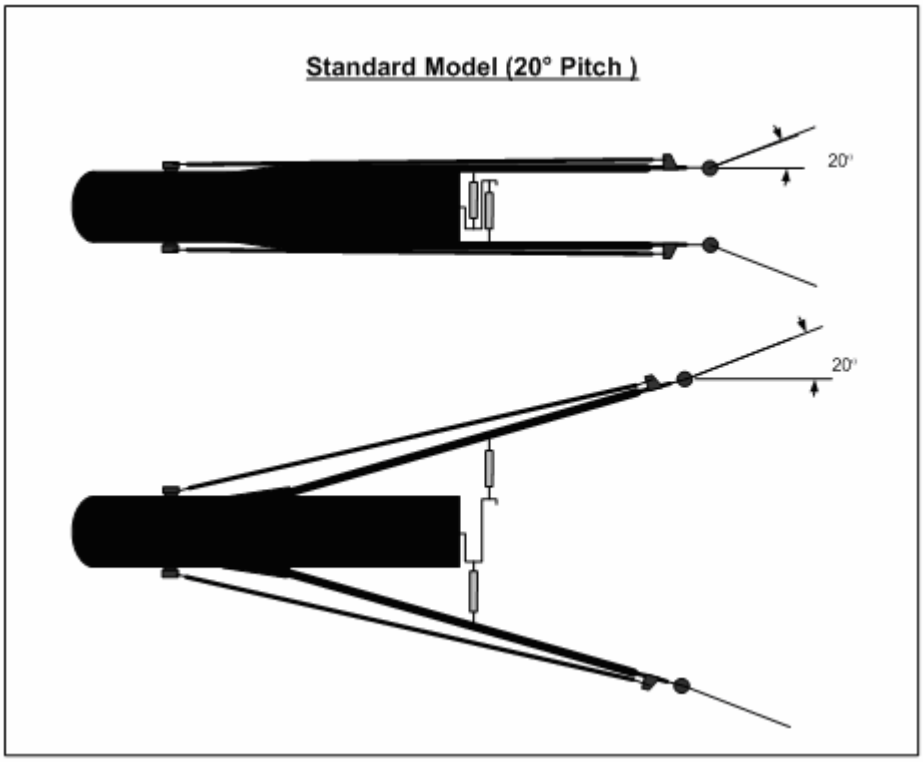

Figure 3- 7 Experimental Model with 20 Degree Neutral Angle

4. Force Balance

A set of weights weighing 1 gram to 20 grams were used for the calibration of the force balance. The model was mounted on a stand equipped with two OMEGA LC703-10 load cells incorporated with a DP41-S-A conditioner that turns measured strain into voltage; one cell was mounted in the horizontal position to measure lift and another in the vertical position to measure thrust and drag. An almost frictionless pulley fixture was setup upstream of the model to allow for test load to be applied. Weight was added at one end of fixture where the other end was connected to the model's support located near the model C.G position.

The voltage reading registered by the cell representing the equivalent weight-force (gram-force) for the stationary model was recorded and used as datum for each experimental run. Each new weight added upstream of the model caused the stationary model with its support to impress upon the load cell to register a new reference voltage. A total of eight runs were conducted for each weight and the respective datum and voltages registered. The detailed results for the calibration are tabulated in Appendix D: Tabulation of Force Balance Calibration. The Omega Load cells with conditioner are illustrated in Figure 3-8 and the force balance calibration setup is illustrated in Figure 3-9. The average gradient was evaluated to be 0.0271 V/g as illustrated graphically in Figure 3-10.

Figure 3- 8 OMEGA LC703-10 load cells with a DP41-S-A conditioner

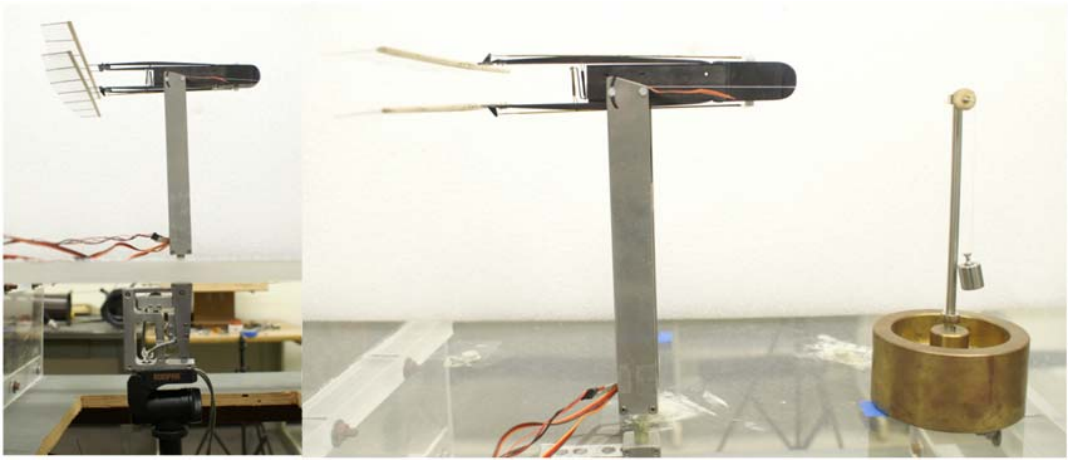

Figure 3- 9 Force Balance Calibration Setup

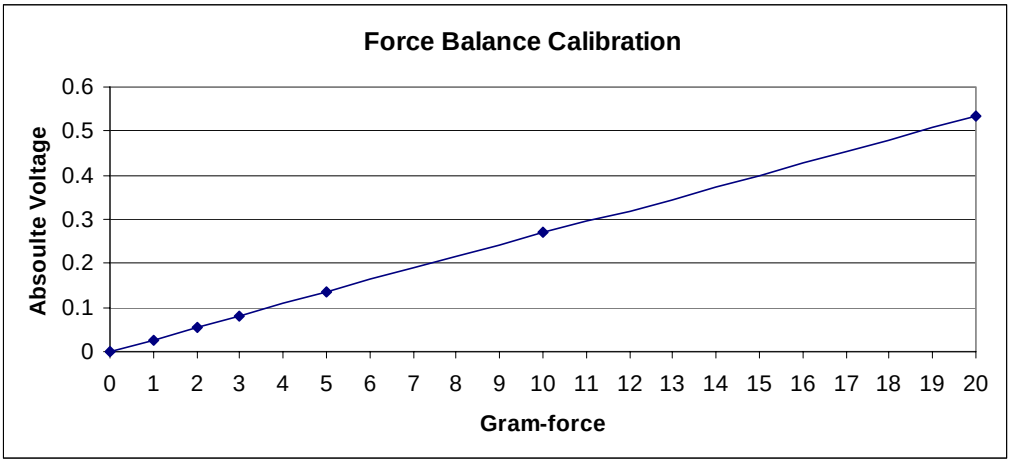

Figure 3- 10 Force Balance Calibration with Linear Curve Fit

5. Traverse Mechanism

Settings on the traverse mechanism were taken in the order that all position to the left and above the center of the test grid are considered as all negative zone while positions to the right and below centroid are considered as all positive zone. The other two zones outside the above designated are considered as combination zones with either the row being positive or the column being positive and vice versa. Each row is spaced 0.5 inch apart and each column is spaced 1.64 inch apart. The traverse motor is capable of 200 steps per revolution and 16,000 counts per inch of movement on a pitched lead screw. This translates to a horizontal traverse setting of -104,960 to +104,960 counts with a separation of 26,240 counts per column division. The vertical traverse setting ranges from -40,000 to +40,000 counts with a separation of 8,000 counts per row division.

C. SOFTWARE

1. StreamWare

StreamWare [Ref. 6] is an application software designed to communicate with the StreamLine main frame system. The software operates in the Microsoft Windows environment to provide a system capability to organize and document flow measurements and results. It performs the complete task from system configuration and experiment layout to data acquisition, reduction and storage.

The normal routine is to calibrate the probe before and after an experiment. Default set-up parameters for the 55R11 wire probe; supporting the automatic velocity calibration and curve fitting to convert CTA output voltages into velocities, and the software driver for Analog-to-Digital signal conversion via National Instruments BNC-2090 15 Channel A/D board are stored in the system dedicated libraries. System configuration and information related to individual experiment inclusive of set-up, calibration, experiment layout, raw and final reduced data are stamped into a user defined project manager which provides traceability of data related to the respective experiment. The project manager can be started and re-used as need be, as data are always stored with headers pointing to the default user defined experiment set-up.

Data acquisition, conversion and reduction are managed by StreamWare. During acquisition and prior to linearization; StreamWare uses system routines for temperature correction of raw data, based on temperature input from the system temperature probe. Raw data acquired are then converted into velocity samples with data reduction process comprising component analysis in both the amplitude and the time (spectral) domain. The reduced data are stored separately and can be exported for further analysis and better graphical presentation.

2. National Instrument LabVIEW

National Instruments LabVIEW [Ref. 8] provides a powerful graphical development environment for signal acquisition, measurement analysis, and data presentation by simplifying the measurement hardware interface with an interactive virtual instrumental (VI) building block. Two VI blocks used for the project were namely the Test.VI and Waveforms2spreadsheet.VI.

Time-varying temperatures and wake velocities behind the flapping wings were captured in binary form by the Test VI, recording 30,000 samples at 40 KHz. The binary data were converted to ASCII form by the Waveforms2spreadsheet.VI for further signal post-processing. The Test and Waveforms2spread VI's front panels are illustrated in Figure 3-9 and 3-10.

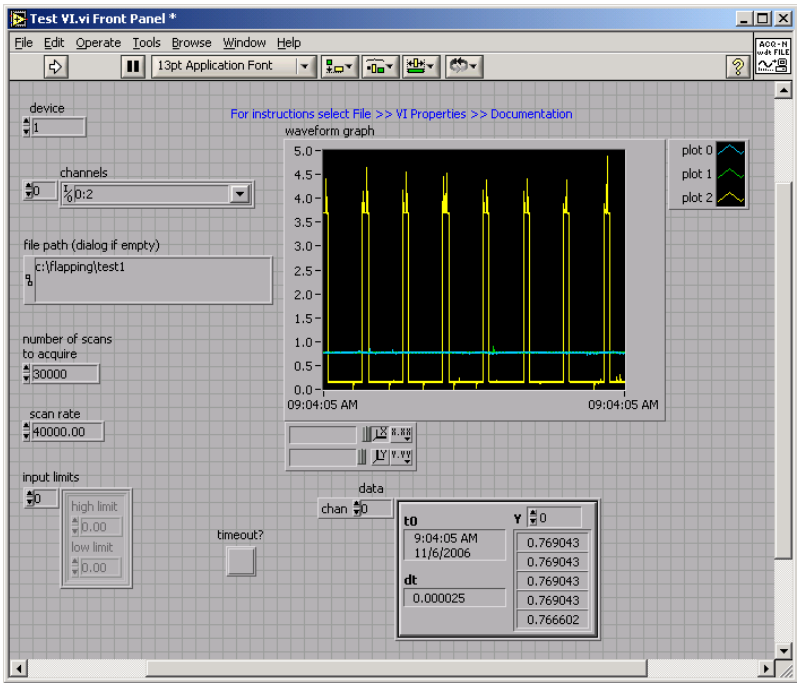

Figure 3- 11 Virtual Instrument block used for data acquisition

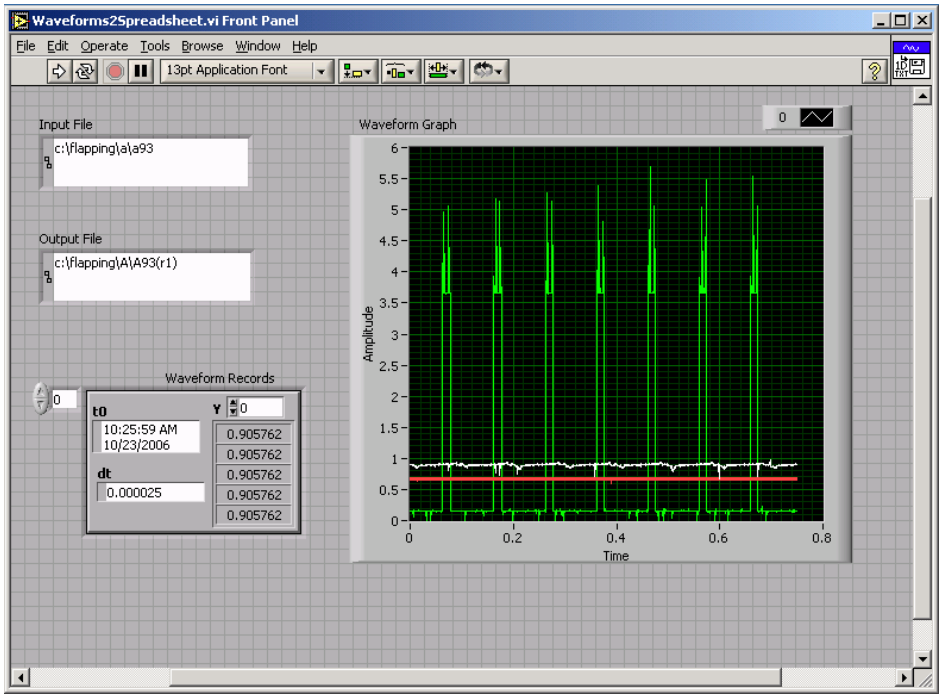

Figure 3- 12 Virtual Instrument block for Binary to ASCII conversion

IV. EXPERIMENTAL PROCEDURES

The entire work was conducted in four phases. The first phase was to conduct a flow visualization to identify the degree and effects of flexing for a combination of varying neutral angle of attack and aero-elastic pitching of the flapping wings. The second phase was to map the time-averaged velocities behind the flapping wings; the third phase was to map the time-dependant velocity during a flapping stroke along the C3 plane, and the last phase was to identify the thrust generated by the experimental model using the force balance. Details of the experimental procedures are further elaborated in the relevant sections below.

A. PHASE 1: FLOW VISUALIZATION OF THE EFFECT OF VARYING NEUTRAL ANGLE OF ATTACK AND AERO-ELASTIC PITCHING OF FLAPPING WINGS

The model fuselage is aligned along grid (R6,C5). Images for aero-elastic pitching with varying neutral angle of attack were photographed for test conditions as follow

S/N	Free Stream conditions	Flapping Frequency	Neutral Pitch
1.	Static (0 m/s)	10, 15, 20 and 25 Hz	0°, 10° and 20°

Images from flow visualization with free stream velocity at 2m/s were also photographed and all results were illustrated in Section V with further discussion in Section VI.

B. PHASE 2: TIME-AVERAGED VELOCITY PROFILE MAPPING

The model fuselage was aligned along grid (R6,C5). Data were collected for 99 positions, i.e., over the entire grid with test conditions for

S/N	Free Stream conditions	Flapping Velocity	Neutral Pitch
1.	2 m/s	10 and 15 Hz	0°, 10° and 20°
2.	3 m/s		
3.	4 m/s		

A total of 1782 samples were recorded and time-averaged by StreamWare and the non-dimensional results tabulated in Appendix B. A summary of the results are illustrated in Section V and further discussion in Section VI for

a) Effect of Varying Neutral Pitch

b) Effect of Flapping Frequency

c) Effect of Free Stream Velocity

C. PHASE 3: TIME-DEPENDANT VELOCITY PROFILE MAPPING

The model fuselage was aligned along grid (R6,C5). Data were collected for 11 horizontal positions along the vertical C3 plane with test conditions for

S/N	Free Stream conditions	Flapping Velocity	Neutral Pitch
1.	2 m/s	10 and 15 Hz	0°, 10° and 20°
2.	3 m/s		
3.	4 m/s		

A total of 198 samples were recorded for the above test conditions using LabVIEW virtual block. Each sample consist of a minimum of 6 continuous flapping strokes and its equivalent velocities behind the flapping wings. The statistical average for 6 flapping strokes per horizontal plane per test condition along C3 is presented in Appendix C with the non-dimensional velocity plotted against time/ phase through the stroke. The statistical stroke-average of the unsteady wake velocity per horizontal plane for each testing condition are represented graphically in Section V with further discussion in Section VI for

a) Effect of Free Stream Velocity

b) Effect of Varying Neutral Pitch

c) Effect of Flapping Frequency

D. PHASE 4: DIRECT THRUST MEASUREMENT

The experiment required that the model fuselage be aligned along grid (R6,C5) and raw voltages for the thrust / drag; horizontal component were registered by a Omega LC703-10 load cell and conditioner DP41-S-A for the experimental model when tested with conditions for

S/N	Free Stream conditions	Flapping Velocity	Neutral Pitch
1.	2 m/s	10, 15, 20 and 25 Hz	0°, 10° and 20°
2.	3 m/s		
3.	4 m/s		

A total of 108 samples were recorded for the test conditions with results included in Appendix E. The statistical average of the results for respective free stream conditions are tabulated and represented graphically in Section V with further discussion in Section VI for

a) Effect of Free Stream Velocity

b) Effect of Varying Neutral Pitch

c) Effect of Flapping Frequency

V. RESULTS AND DISCUSSIONS

A. PHASE 1 SUMMARY: FLOW VISUALIZATION OF THE EFFECT OF VARYING NEUTRAL ANGLE OF ATTACK AND AERO-ELASTIC PITCHING OF FLAPPING WINGS

1. 0° Neutral; Flapping Frequency: 10, 15, 20 and 25 Hz

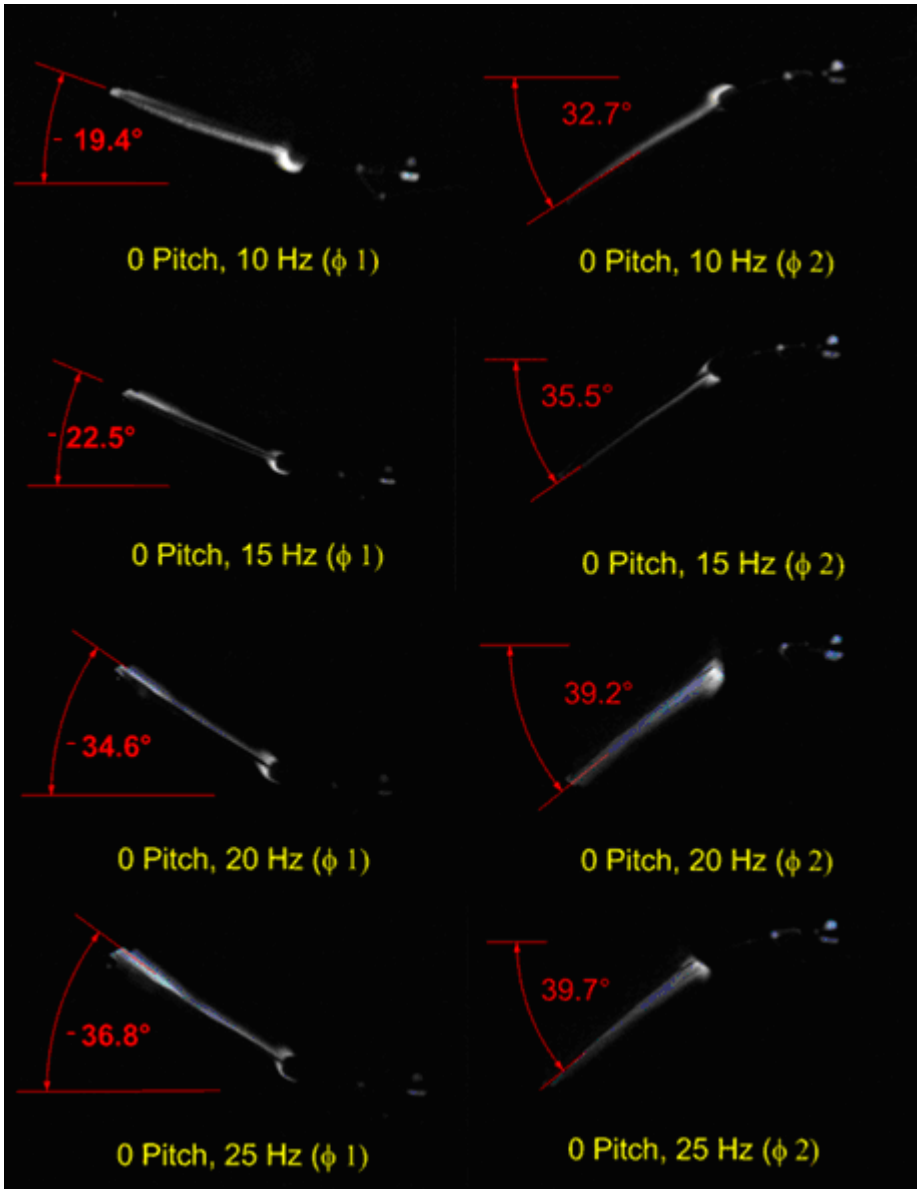

Figure 5- 1 Effect of 0° Neutral and Aero-Elastic Pitching

2. 10° Neutral; Flapping Frequency: 10, 15, 20 and 25 Hz

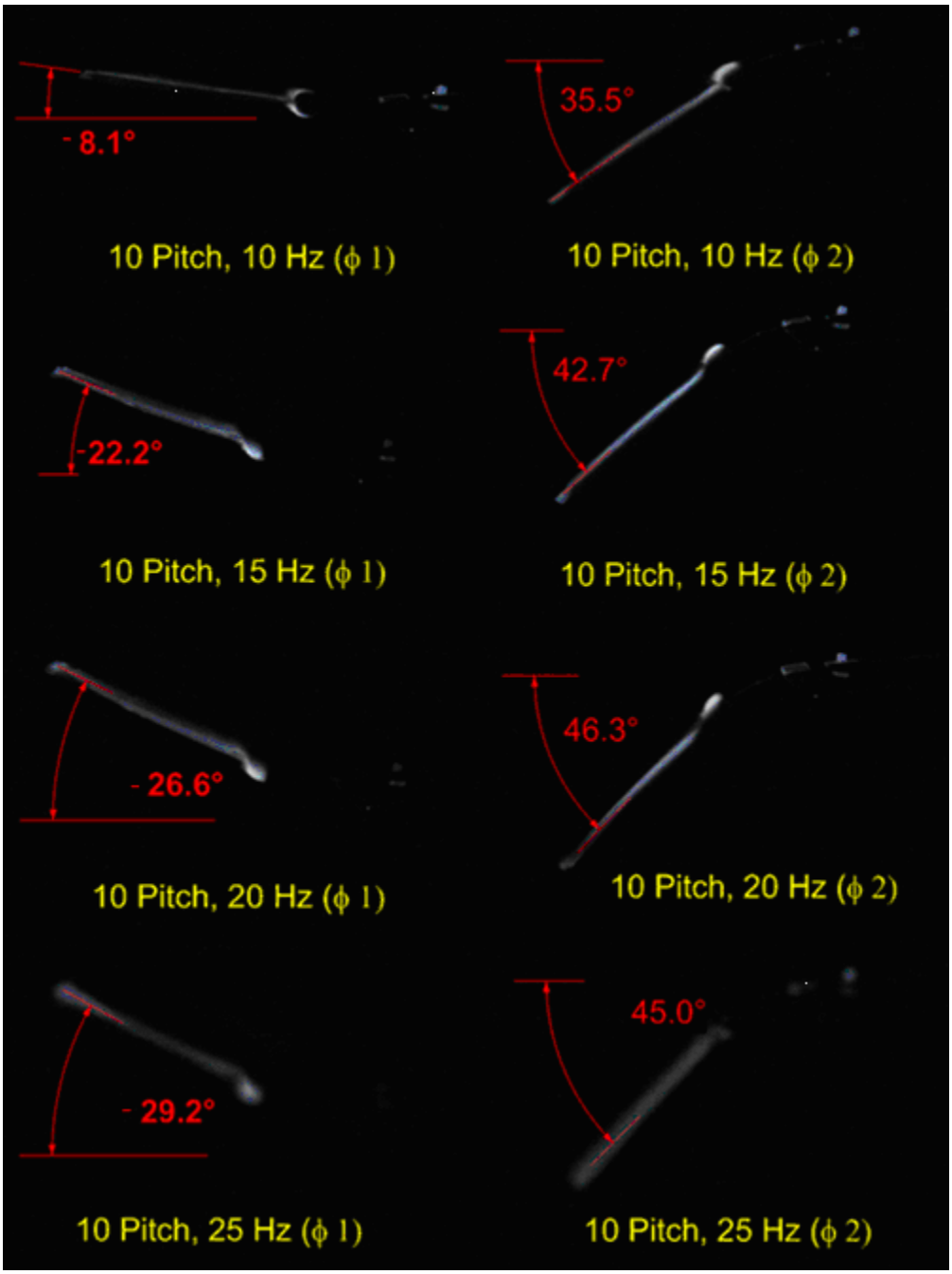

Figure 5- 2 Effect of 10° Neutral and Aero-Elastic Pitching

3. 20° Neutral; Flapping Frequency: 10, 15, 20 and 25 Hz

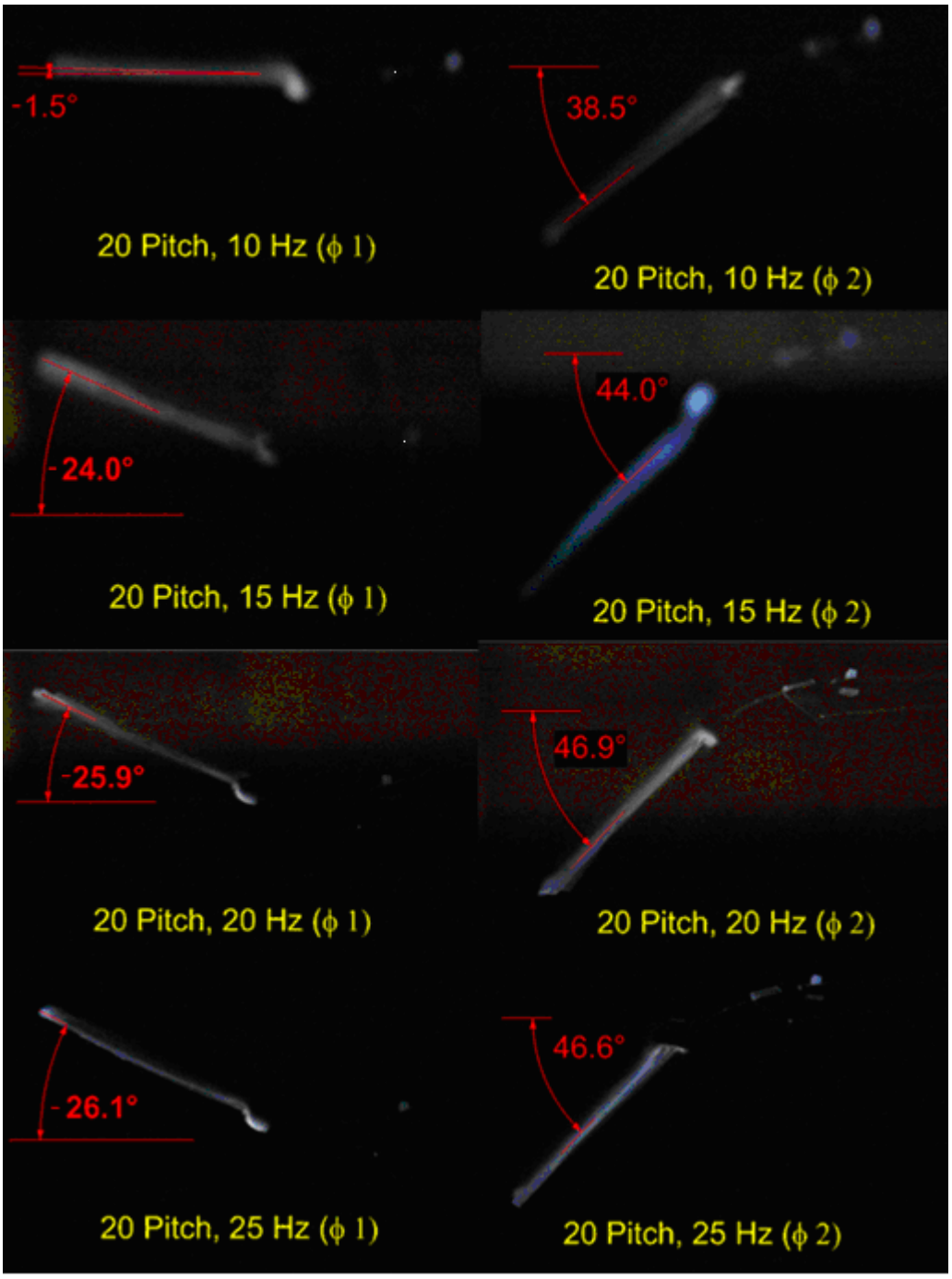

Figure 5- 3 Effect of 20° Neutral and Aero-Elastic Pitching

Effect of Aero-Elastic Pitching

It should be noted that the results illustrated are tested at static condition; and the effect of varying neutral angle of attack on aero-elastic properties of the flapping model is summarized as follows

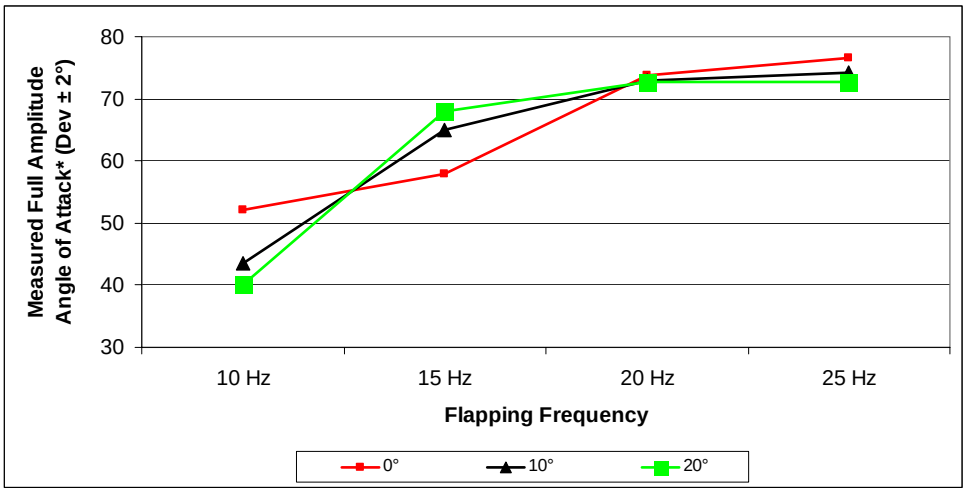

Figure 5- 4 Measured Full Amplitude Angle of Attack

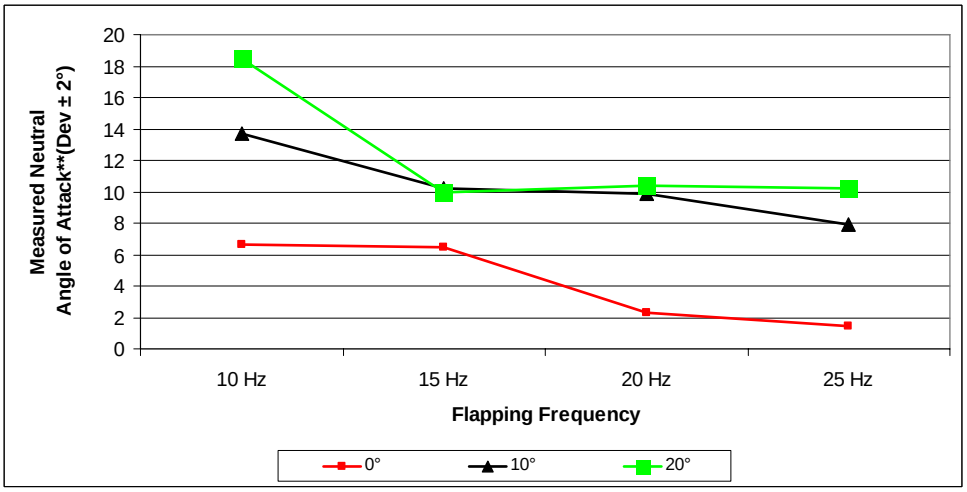

Figure 5- 5 Measured Neutral Angle of Attack

* Absolute angle measured between maximum outward and minimum inward pitching angle

** Median between maximum and minimum measured pitching angle

It is apparent that an increase in the spring neutral as illustrated in Figure 5-4 has weak effect on the measured full amplitude angle of attack; higher variation in amplitude is seen in the case of lower flapping frequency and the variation reduces with increasing frequency. In general, the effective angle α_{eff} seen by the airfoil is related by

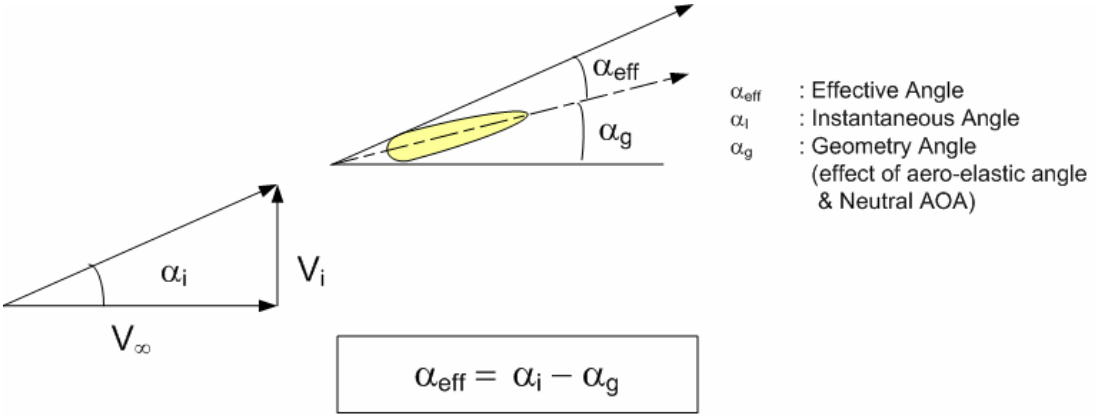

It should be noted that α_g is a representative of the aero-elastic angle and neutral angle of attack combination; where the aero-elastic angle is highly dependant on the stiffness of the carbon fiber strip that connects the flapping beams and wings; the neutral angle is the amount of mechanical pitch introduced. Contrary to findings on measured full amplitude angle of attack, increasing spring neutral as illustrated in Figure 5-5 increases the measured neutral angle of attack as seen by the airfoil.

B. PHASE 2 SUMMARY: TIME-AVERAGED VELOCITY PROFILE MAPPING

The experiment utilizes StreamWare for data acquisition and processing. The detailed computation and expanded view of the time-averaged wake profiles behind the flapping wings for free stream velocity at 2m/s, 3 m/s and 4m/s are tabulated in Appendix B. The summary of the respective velocities profiles are stipulated in the following sections as follows;

1. **Free Stream Velocity 2m/s – Non-Dimensional Velocity (Normalized 2m/s) for 0°, 10° and 20° pitch; 10 Hz and 15 Hz flapping frequency.**

   a) Figure 5-6: 0° pitch, 10 Hz
   b) Figure 5-7: 0° pitch, 15 Hz
   c) Figure 5-8: 10° pitch, 10 Hz
   d) Figure 5.9: 10° pitch, 15 Hz
   e) Figure 5-10: 20° pitch, 10 Hz
   f) Figure 5-11: 20° pitch, 15 Hz

2. **Free Stream Velocity 3m/s – Non-Dimensional Velocity (Normalized 3m/s) for 0°, 10° and 20° pitch; 10 Hz and 15 Hz flapping frequency.**

   a) Figure 5-12: 0° pitch, 10 Hz
   b) Figure 5-13: 0° pitch, 15 Hz
   c) Figure 5-14: 10° pitch, 10 Hz
   d) Figure 5-15: 10° pitch, 15 Hz
   e) Figure 5-16: 20° pitch, 10 Hz
   f) Figure 5-17: 20° pitch, 15 Hz

3. **Free Stream Velocity 4m/s – Non-Dimensional Velocity (Normalized 4m/s) for 0°, 10° and 20° pitch; 10 Hz and 15 Hz flapping frequency.**

   a) Figure 5-18: 0° pitch, 10 Hz
   b) Figure 5-19: 0° pitch, 15 Hz
   c) Figure 5-20: 10° pitch, 10 Hz
   d) Figure 5-21: 10° pitch, 15 Hz
   e) Figure 5-22: 20° pitch, 10 Hz
   f) Figure 5-23: 20° pitch, 15 Hz

1. Free Stream Velocity 2m/s

Non-Dimensional Velocity (Normalized 2m/s) for 0°, 10° and 20° pitch

10 Hz Flapping Frequency | **15 Hz flapping frequency**

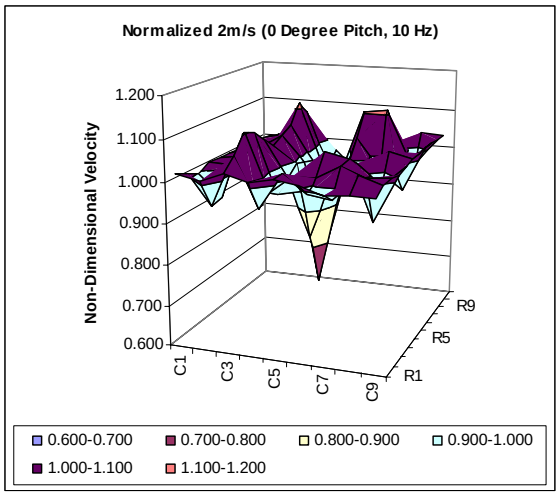

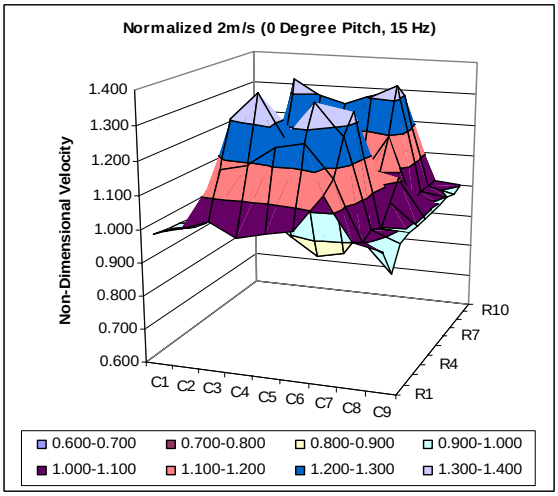

Figure 5- 6 **0° pitch, 10 Hz**

Figure 5- 7 **0° pitch, 15 Hz**

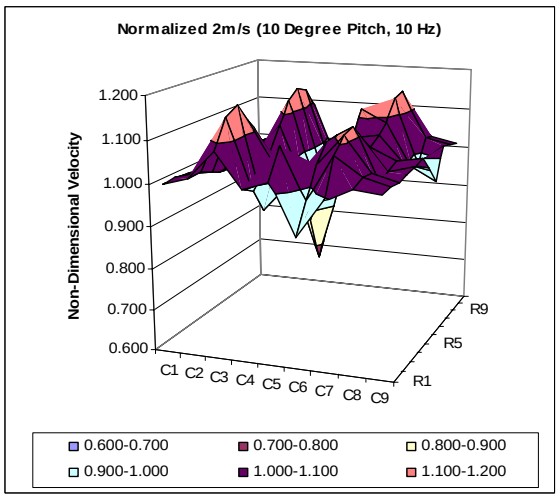

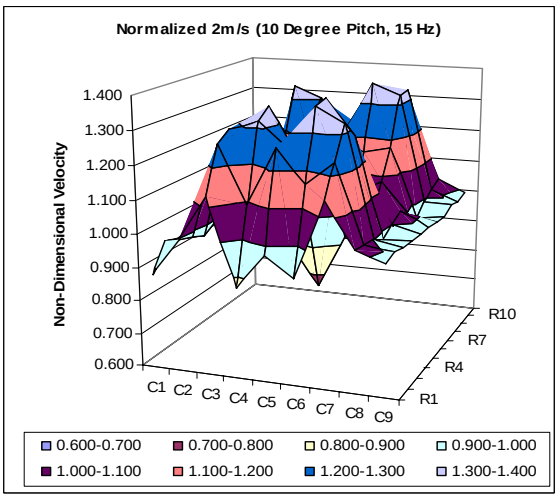

Figure 5- 8 **10° pitch, 10 Hz**

Figure 5- 9 **10° pitch, 15 Hz**

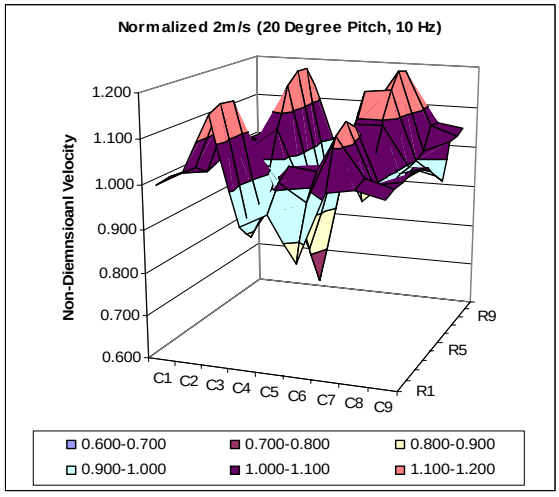

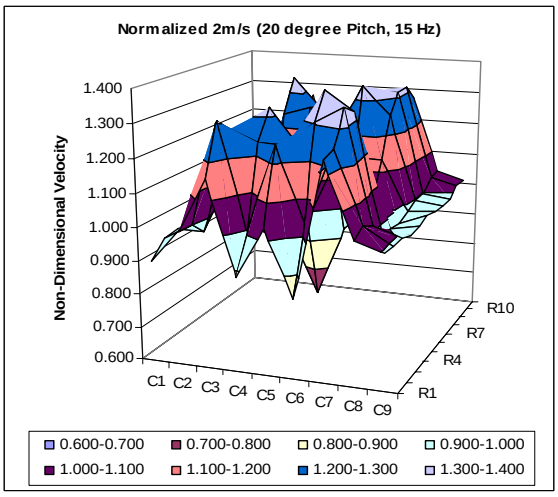

Figure 5- 10 **20° pitch, 10 Hz**

Figure 5- 11 **20° pitch, 15 Hz**

2. Free Stream Velocity 3m/s

Non-Dimensional Velocity (Normalized 3m/s) for 0°, 10° and 20° pitch

10 Hz Flapping Frequency **15 Hz flapping frequency**

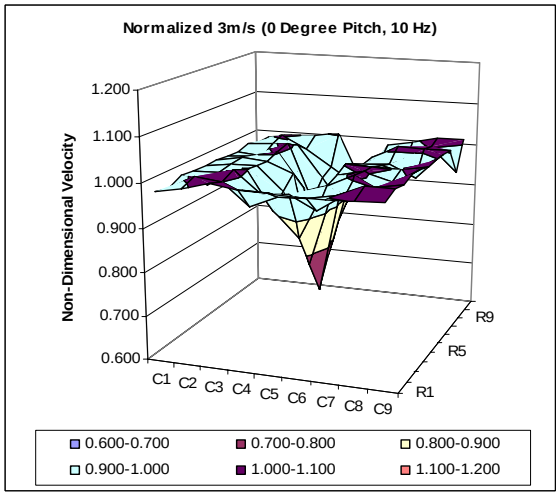

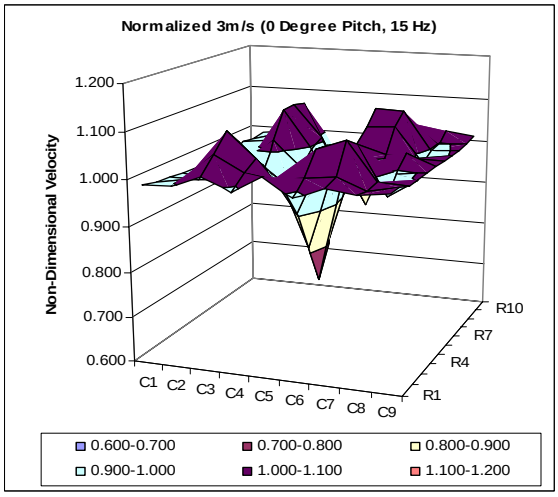

Figure 5- 12 **0° pitch, 10 Hz**

Figure 5- 13 **0° pitch, 15 Hz**

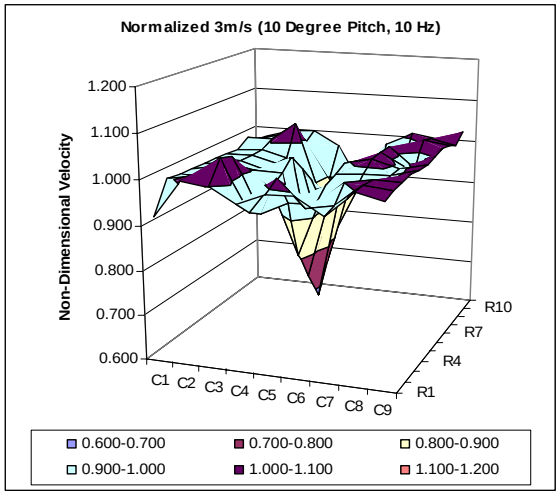

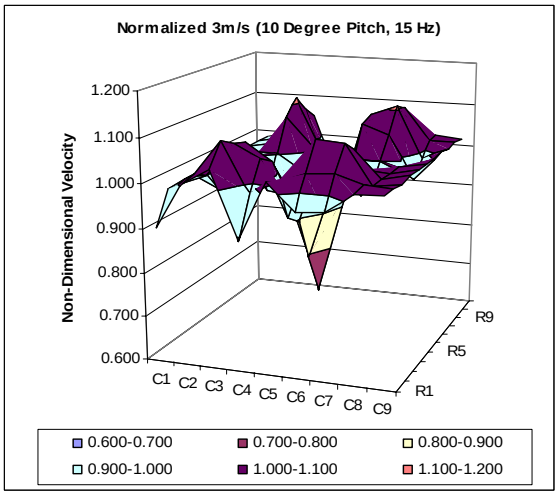

Figure 5- 14 **10° pitch, 10 Hz**

Figure 5- 15 **10° pitch, 15 Hz**

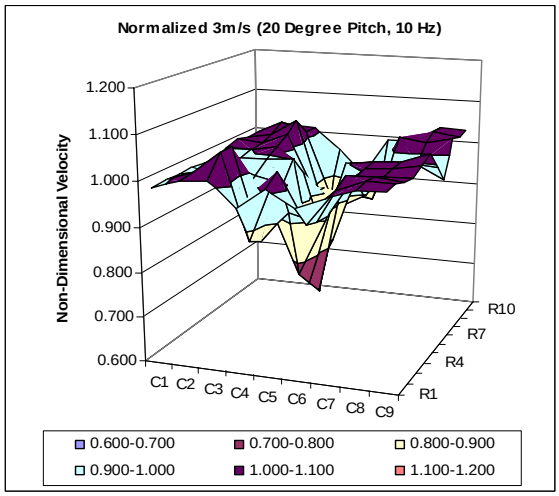

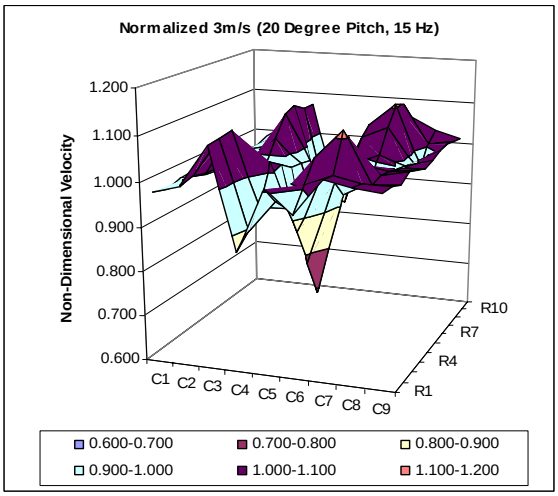

Figure 5- 16 **20° pitch, 10 Hz**

Figure 5- 17 **20° pitch, 15 Hz**

3. Free Stream Velocity 4m/s

Non-Dimensional Velocity (Normalized 4m/s) for 0°, 10° and 20° pitch

10 Hz Flapping Frequency | **15 Hz flapping frequency**

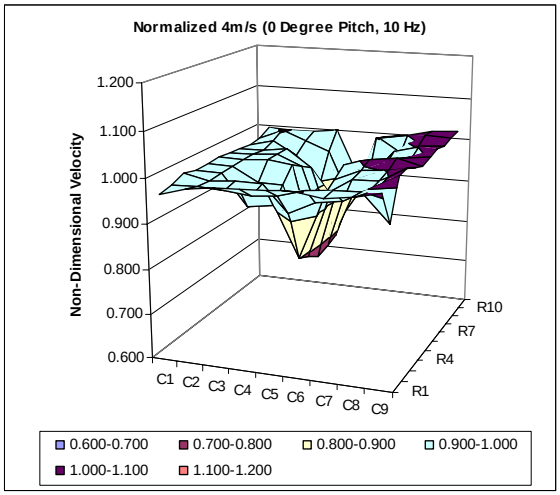

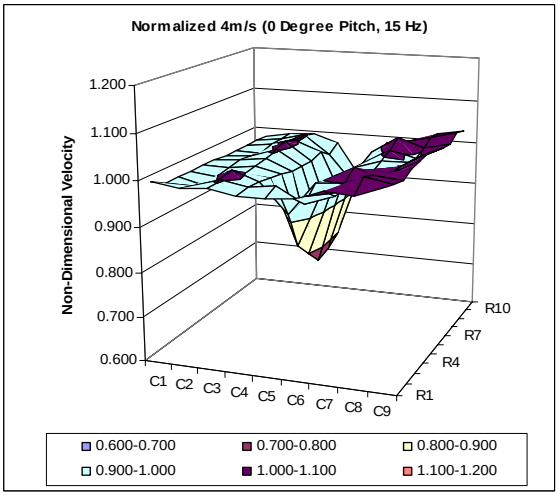

Figure 5- 18 0° pitch, 10 Hz

Figure 5- 19 0° pitch, 15 Hz

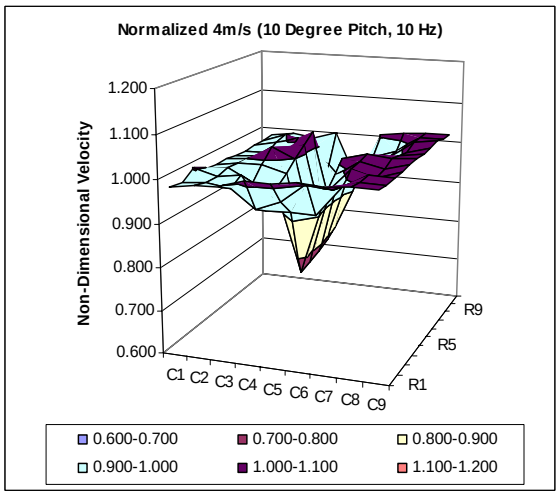

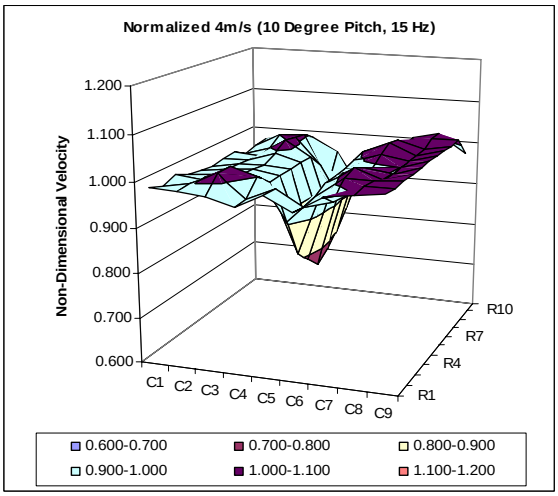

Figure 5- 20 10° pitch, 10 Hz

Figure 5- 21 10° pitch, 15 Hz

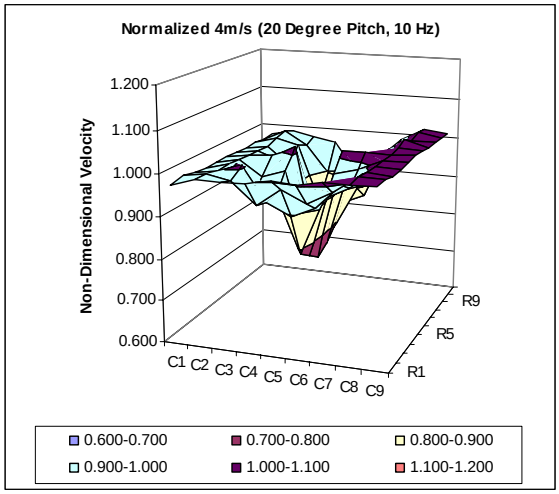

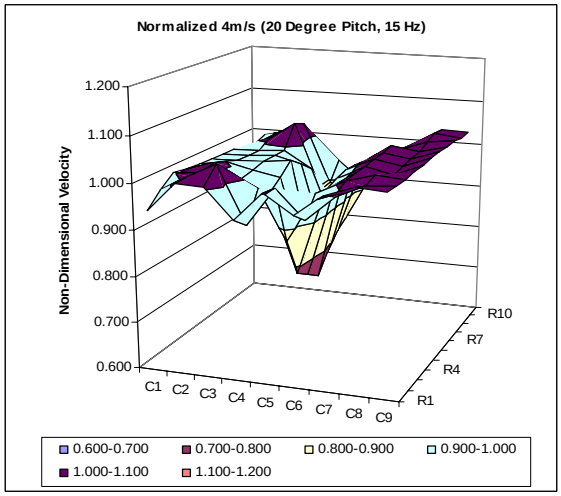

Figure 5- 22 **20° pitch, 10 Hz**

Figure 5- 23 **20° pitch, 15 Hz**

General observations on the time-averaged data from Figure 5-6 to Figure 5-23 indicated that peak velocity behind the flapping wings increases with increasing neutral angle of attack and flapping frequency, and decreases with increasing free stream condition. It is also noted that measurements recorded along the C3 plane located midway between the centerline and the outer most vertical plane C1, represented a velocity profile closest to two-dimensional flow with recurrent peak velocities for the varying test conditions. A summary of the peak (non-dimensional) velocity magnitude for the C3 plane obtained from Figure 5-6 to Figure 5-23 normalized by the free stream velocity are illustrated in Figure 5-24 and detailed computation illustrated in Appendix B.

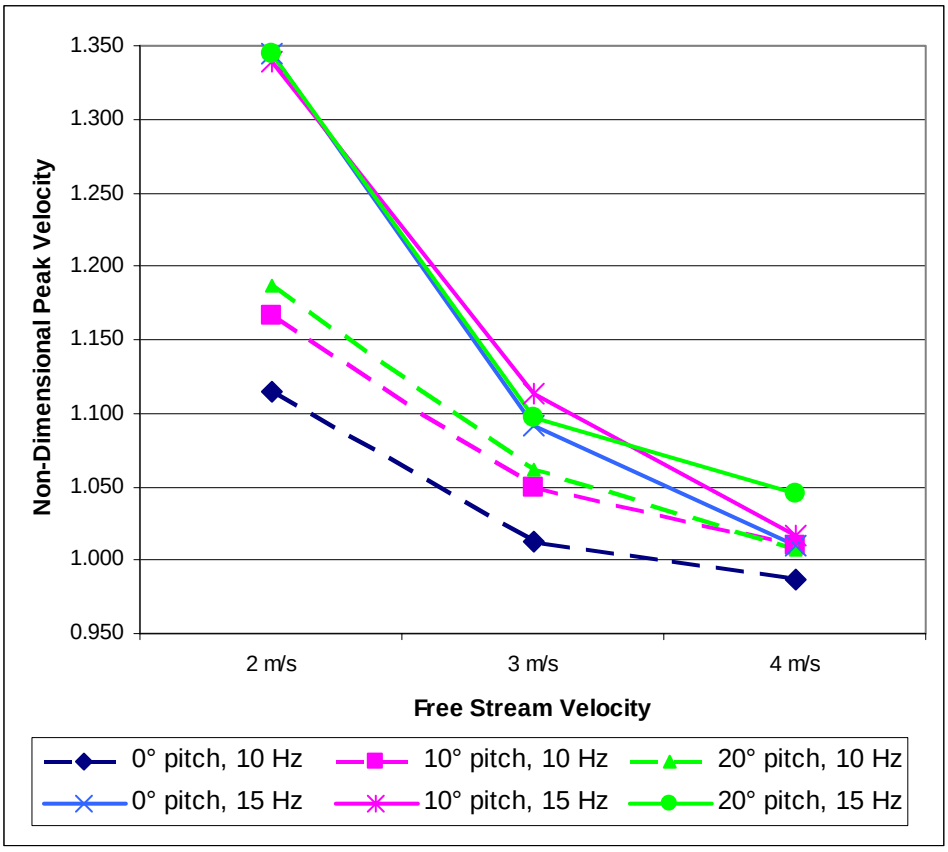

Figure 5- 24 Peak Velocity (ND) magnitude along C3 Plane

1. Effect of Flapping Frequency

It is noticed that flapping at higher frequency does provide better velocity performance. The average peak velocity gained for flapping at 10 Hz ranges from approximately 0.2% at 4m/s free stream to 15.6% at 2m/s free steam; while the velocity gained for flapping at 15 Hz ranges from approximately 2.4% at 4m/s free stream to 34.2% at 2m/s free steam

2. Effect of Varying Neutral Pitch

At low flapping frequency, it is noted that the absolute velocity gain with every 10° increase in neutral angle is approximated at an average of 1.0% at 4m/s free stream to 3.7% at 2m/s free stream. At higher flapping frequency, the

effect of varying neutral angle has little influence on absolute velocity gained; for every 10° increase in neutral angle, an absolute gain of approximately 0.3% at 3m/s free stream to 1.8% at 4m/s free stream are registered.

3. Effect of Free Stream Velocity

Peak velocity decreases with increasing free stream conditions and this may be due to the fact that the model spring was tuned for better performance during low free stream flight. For high free stream conditions, the model spring stiffness will need to increase in order to reduce effect of aero-elastic pitching.

C. PHASE 3 SUMMARY: TIME-DEPENDANT VELOCITY PROFILE MAPPING DURING A FLAPPING STROKE ALONG PLANE C3

The experiment utilizes National Instrument software LABVIEW 7.1 for data acquisition and data conversion from binary to ASCII code. Post data processing was conducted by curve fitting a 4^{th} order polynomial with coefficient stipulated in section III: Experimental Setup and according to

$$U = C_0 + C_1 E_{corr} + C_2 E_{corr}^{\ 2} + C_3 E_{corr}^{\ 3} + C_4 E_{corr}^{\ 4}$$

. The detailed graphical illustration of the averaged non-dimensional velocity magnitude per flapping stroke (statistical average of six flapping strokes) along each horizontal plane, i.e., R1 to R11 for vertical plane C3 for varying free stream velocity and neutral angle are included in Appendix C under the respective sub-section as follows;

1. Normalized 2m/s, 10 Hz Flapping Frequency
2. Normalized 2m/s, 15 Hz Flapping Frequency
3. Normalized 3m/s, 10 Hz Flapping Frequency
4. Normalized 3m/s, 15 Hz Flapping Frequency
5. Normalized 4m/s, 10 Hz Flapping Frequency
6. Normalized 4m/s, 15 Hz Flapping Frequency

A summary demonstrating the relationship between the averaged non-dimensional velocity magnitude for each averaged flapping stroke along the measured planes and the effect of varying free stream velocity, neutral angle of attack and flapping frequency are further illustrated as follows;

1. Effect of Free Stream Velocity

a) Figure 5-25: 0° pitch, 10 Hz
b) Figure 5-26: 10° pitch, 10 Hz
c) Figure 5-27: 20° pitch, 10 Hz
d) Figure 5-28: 0° pitch, 15 Hz
e) Figure 5-29: 10° pitch, 15 Hz
f) Figure 5-30: 20° pitch, 15 Hz

2. Effect of Varying Neutral Pitch

a) Figure 5-31: Normalized 2 m/s, 10 Hz
b) Figure 5-32: Normalized 3 m/s, 10 Hz
c) Figure 5-33: Normalized 4 m/s, 10 Hz
d) Figure 5-34: Normalized 2 m/s, 15 Hz
e) Figure 5-35: Normalized 3 m/s, 15 Hz
f) Figure 5-36: Normalized 4 m/s, 15 Hz

3. Effect of Flapping Frequency

a) Figure 5-37: Normalized 2 m/s, 0° pitch
b) Figure 5-38: Normalized 3 m/s, 0° pitch
c) Figure 5-39: Normalized 4 m/s, 0° pitch
d) Figure 5-40: Normalized 2 m/s, 10° pitch
e) Figure 5-41: Normalized 3 m/s, 10° pitch
f) Figure 5-42: Normalized 4 m/s, 10° pitch
g) Figure 5-43: Normalized 2 m/s, 20° pitch
h) Figure 5-44: Normalized 3 m/s, 20° pitch
i) Figure 5-45: Normalized 4 m/s, 20° pitch

1. Effect of Varying Neutral Pitch

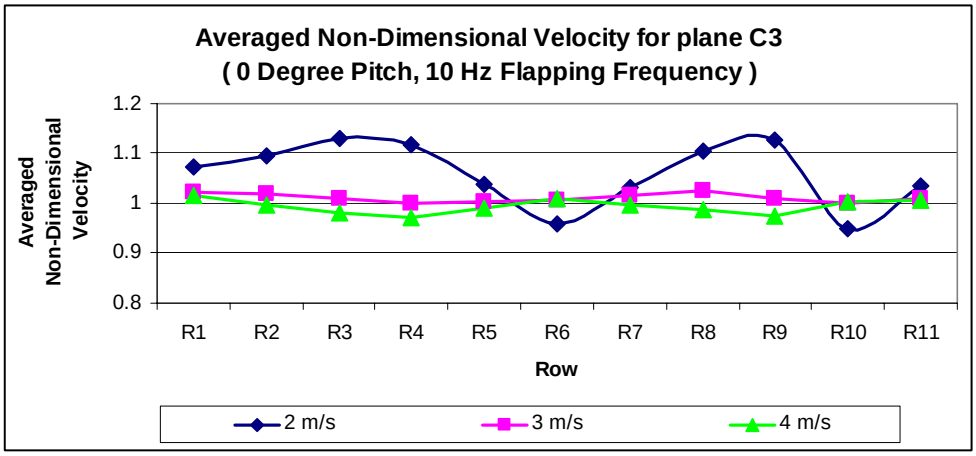

Figure 5- 25 0° pitch, 10 Hz

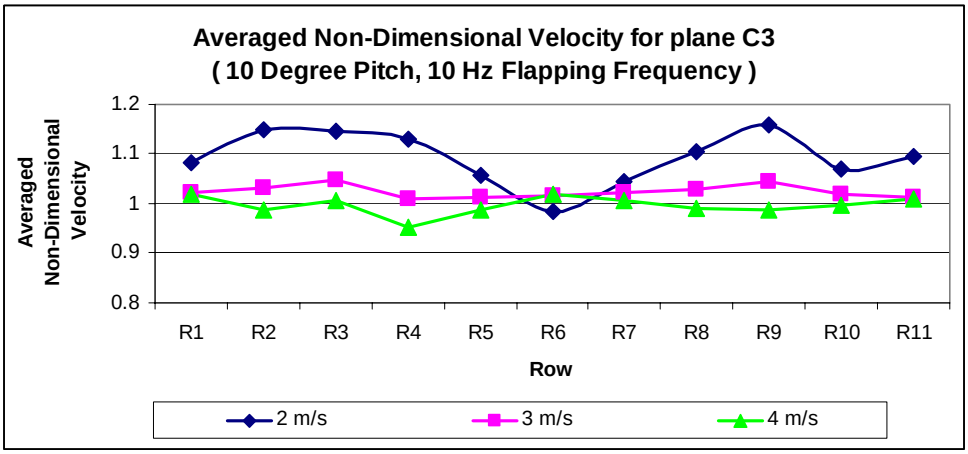

Figure 5- 26 10° pitch, 10 Hz

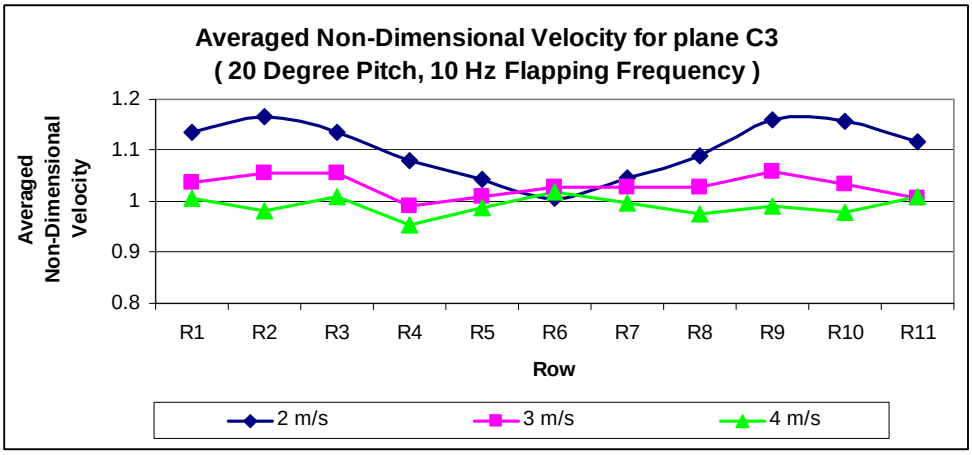

Figure 5- 27 20° pitch, 10 Hz

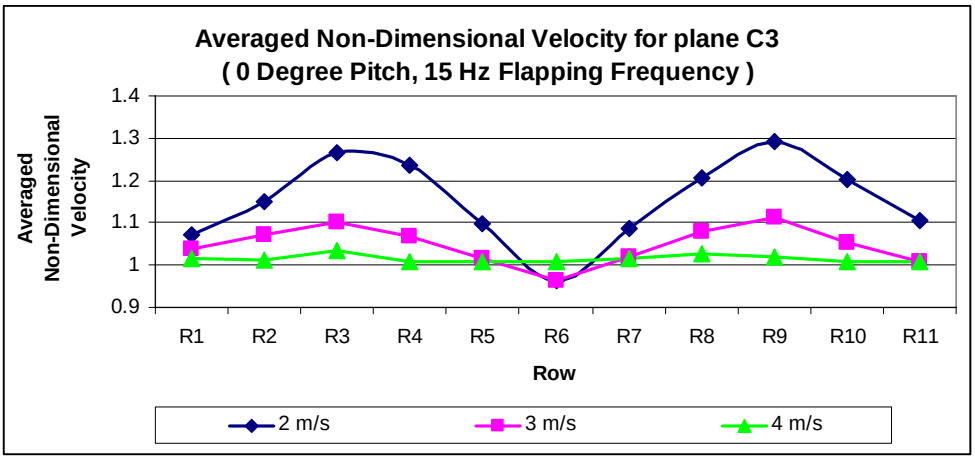

Figure 5- 28 0° pitch, 15 Hz

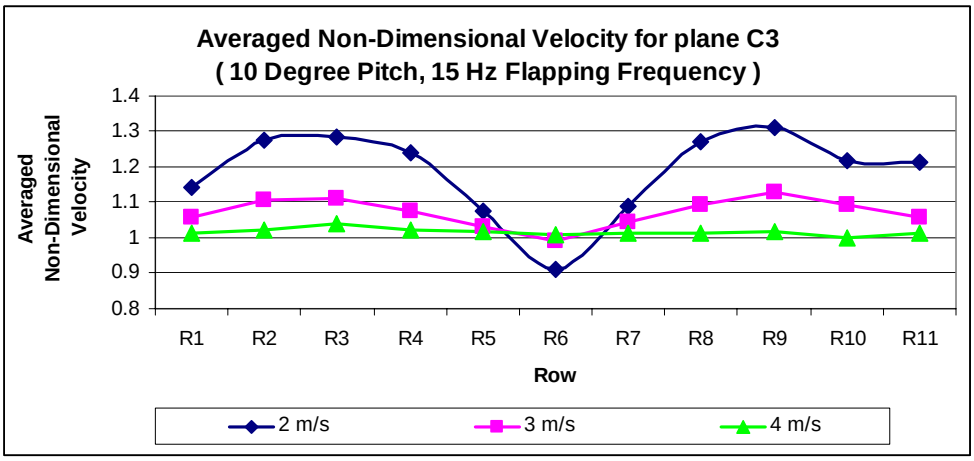

Figure 5- 29 10° pitch, 15 Hz

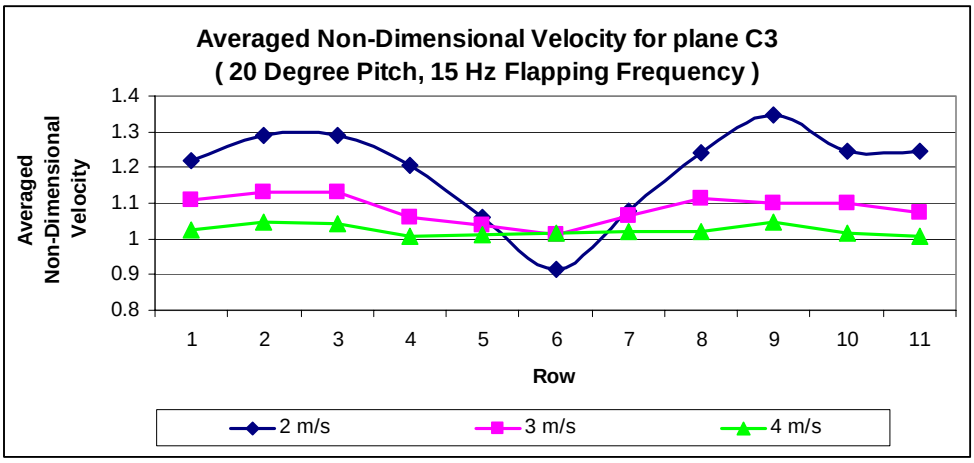

Figure 5- 30 20° pitch, 15 Hz

2. Effect of Free Stream Velocity

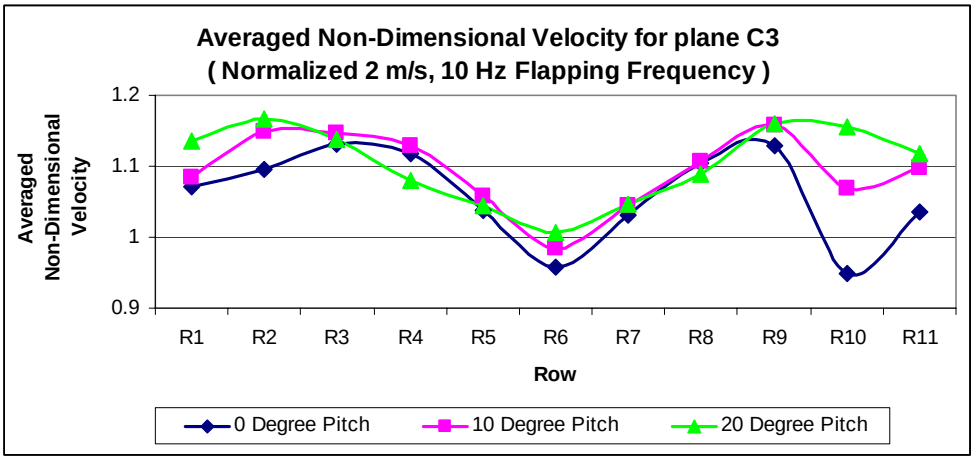

Figure 5- 31 Normalized 2 m/s, 10 Hz

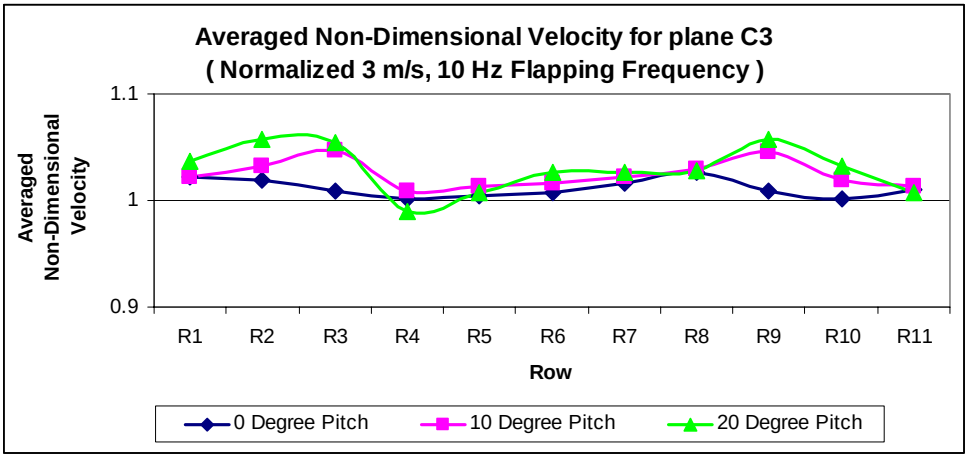

Figure 5- 32 Normalized 3 m/s, 10 Hz

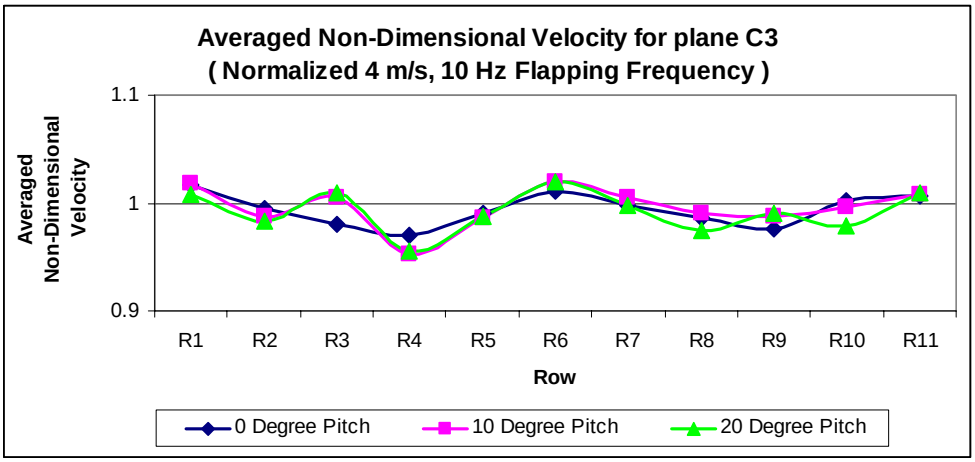

Figure 5- 33 Normalized 4 m/s, 10 Hz

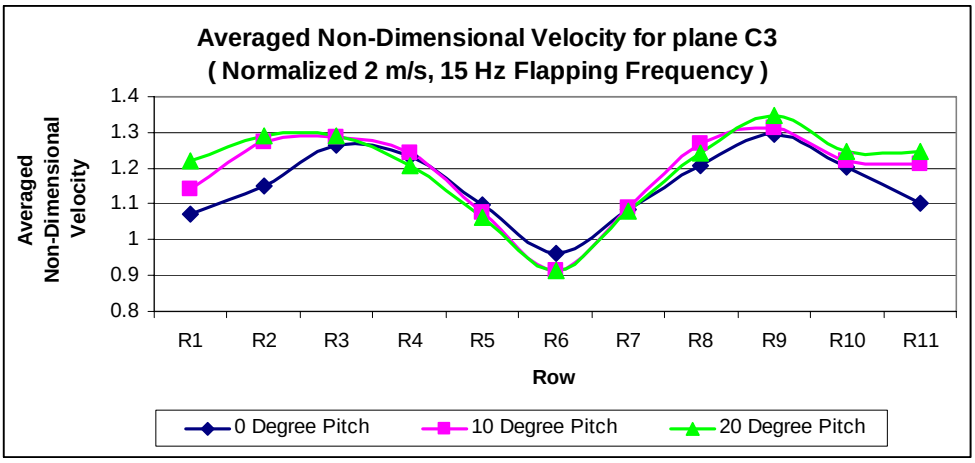

Figure 5- 34 Normalized 2 m/s, 15 Hz

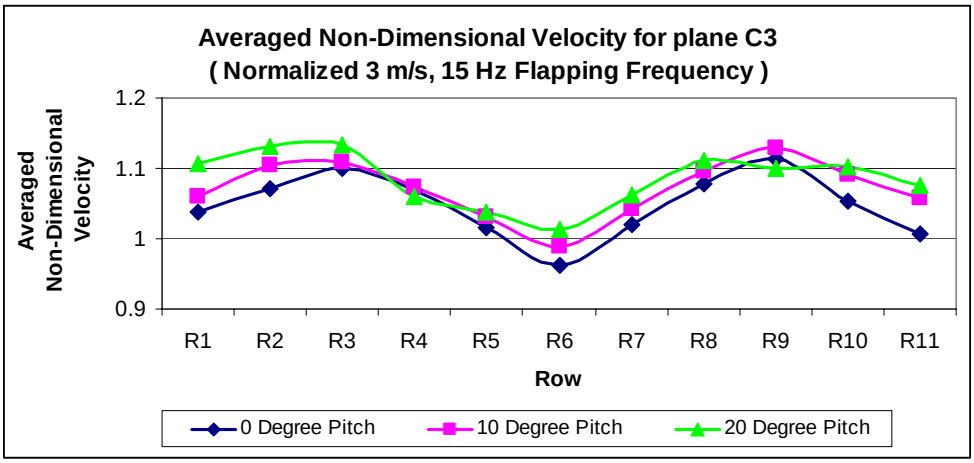

Figure 5- 35 Normalized 3 m/s, 15 Hz

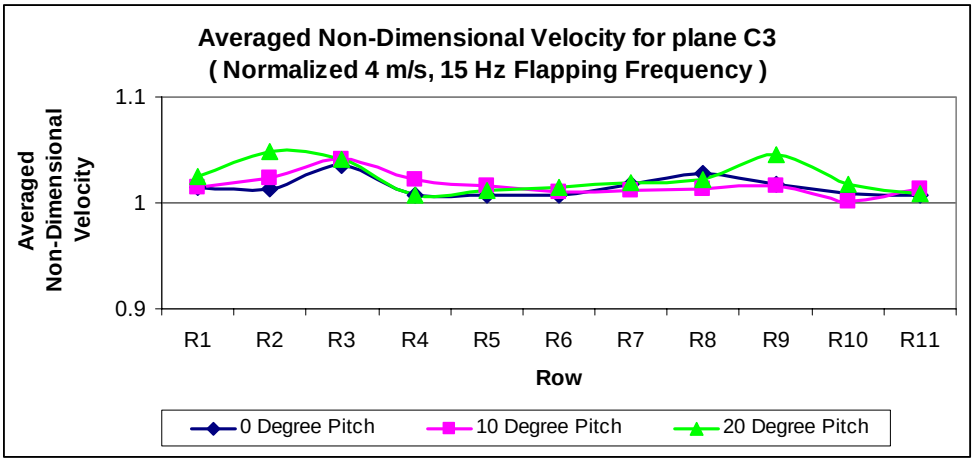

Figure 5- 36 Normalized 4 m/s, 15 Hz

3. Effect of Flapping Frequency

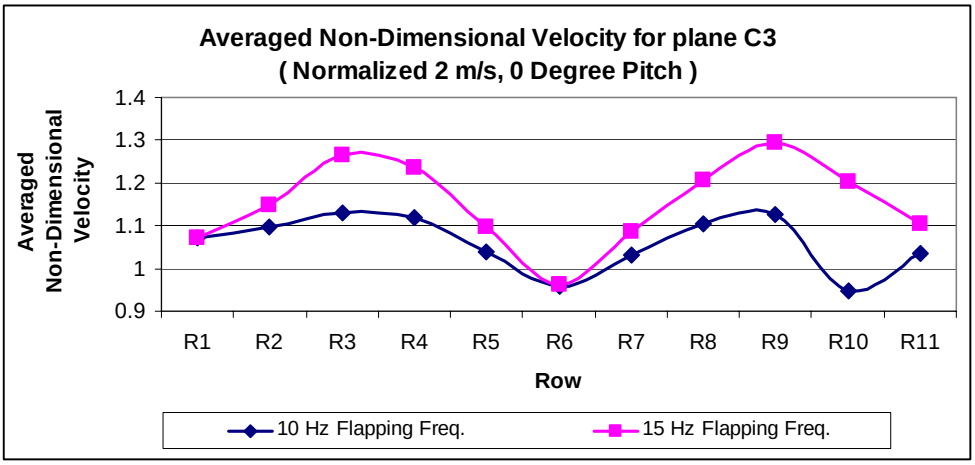

Figure 5- 37 Normalized 2 m/s, 0° pitch

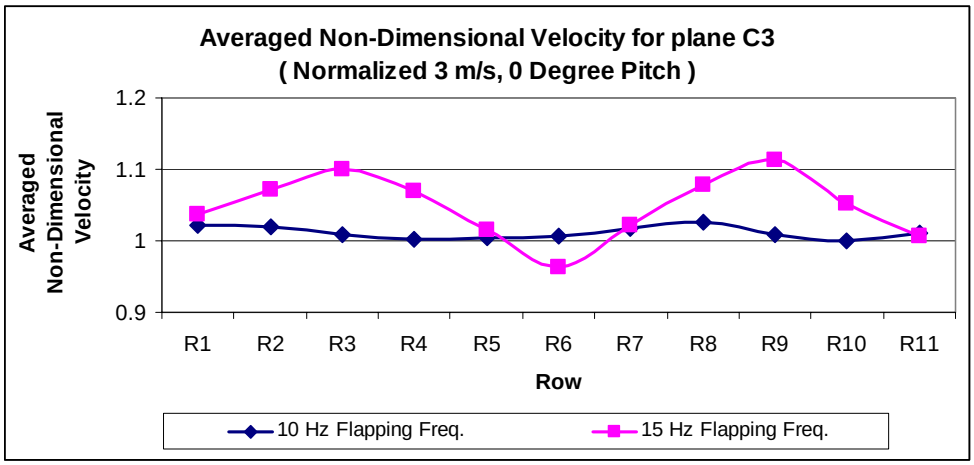

Figure 5- 38 Normalized 3 m/s, 0° pitch

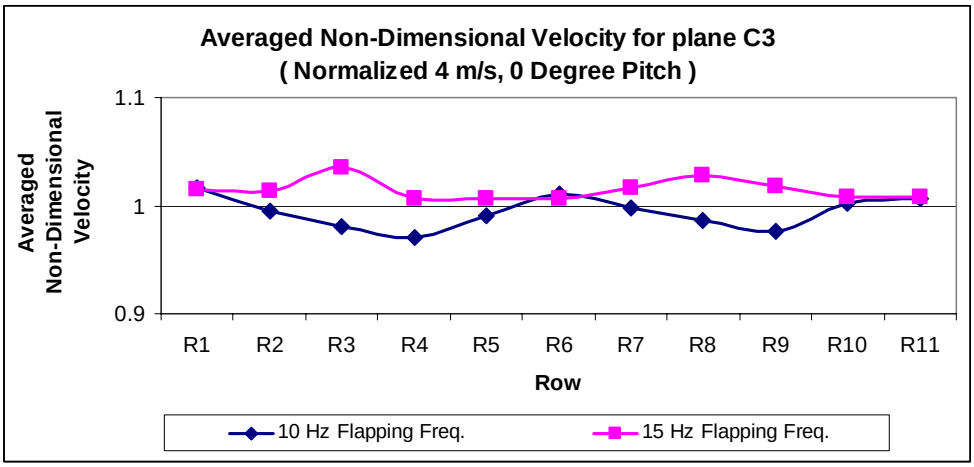

Figure 5- 39 Normalized 4 m/s, 0° pitch

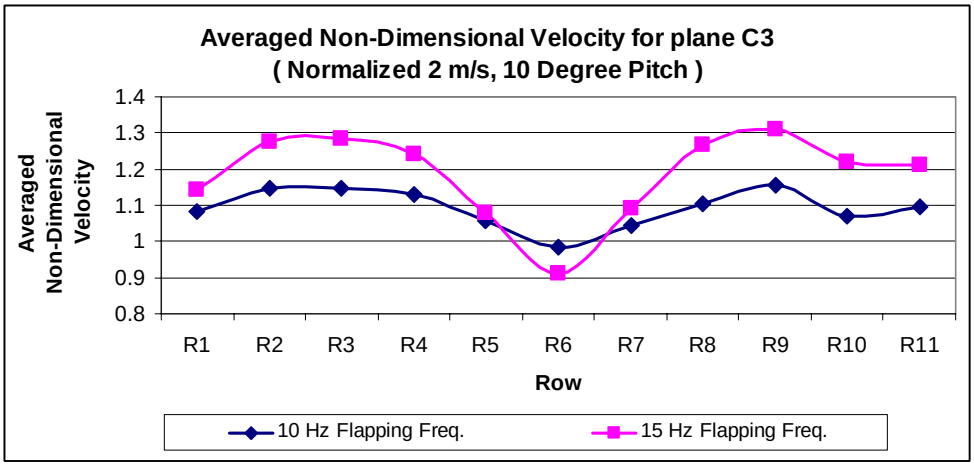

Figure 5- 40 Normalized 2 m/s, 10° pitch

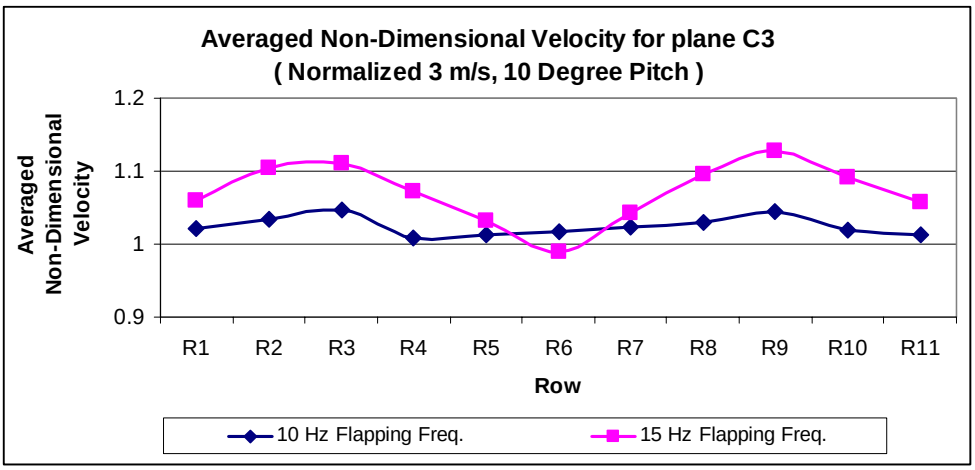

Figure 5- 41 Normalized 3 m/s, 10° pitch

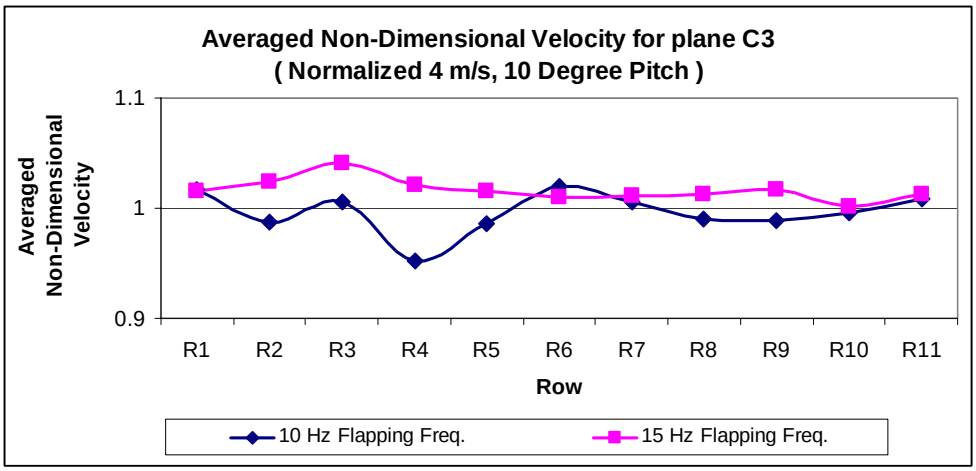

Figure 5- 42 Normalized 4 m/s, 10° pitch

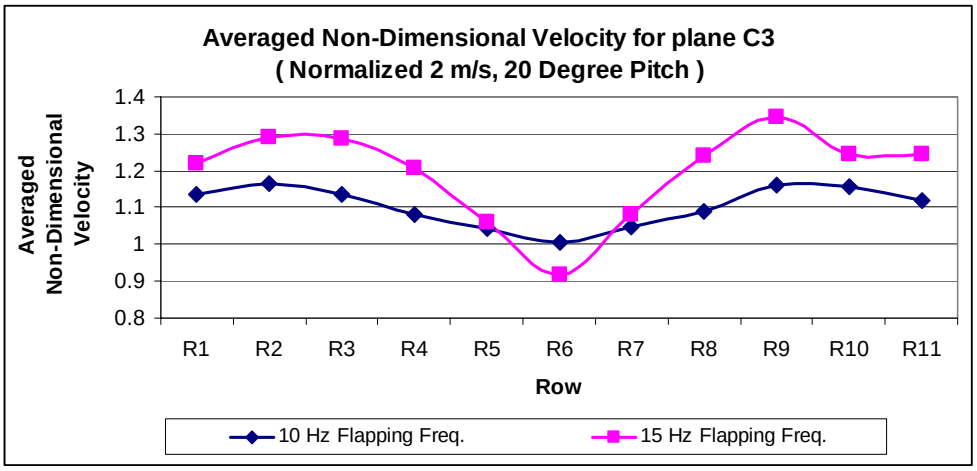

Figure 5- 43 Normalized 2 m/s, 20° pitch

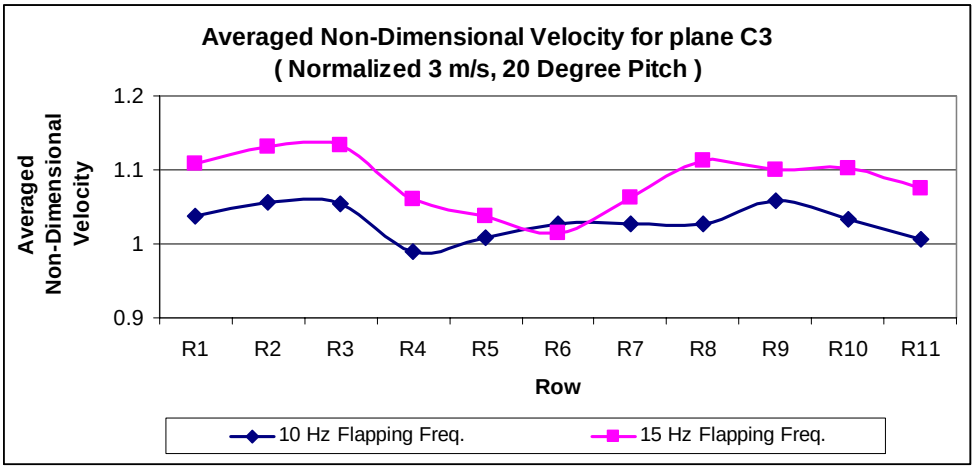

Figure 5- 44 Normalized 3 m/s, 20° pitch

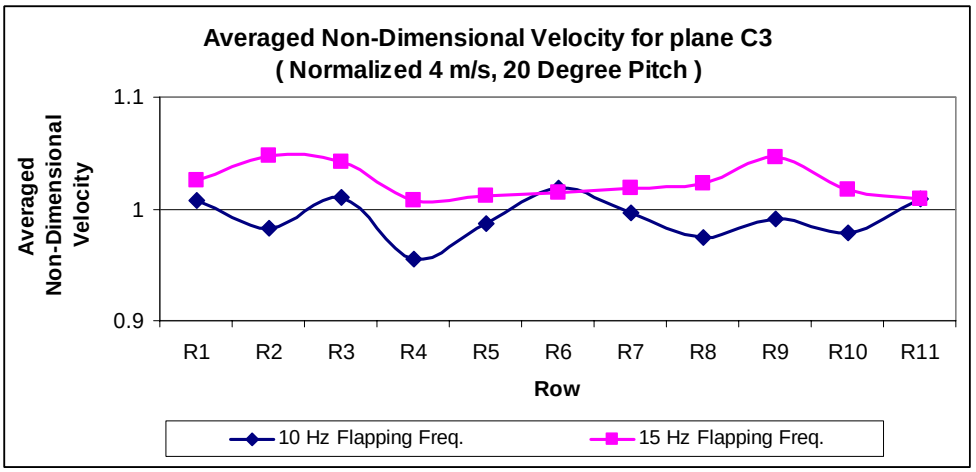

Figure 5- 45 Normalized 4 m/s, 20° pitch

PHASE 3: Time-Dependant Velocity Mapping

The statistical averaged, non-dimensional velocity profiles and its equivalent velocities magnitude at each horizontal plane recorded by LabVIEW are illustrated in Appendix C. The graphical illustrations provide an accurate representation of the statistical averaged velocity magnitude since data processing was conducted with an integer number of flapping strokes. Interestingly, recurring observations were obtained; velocity profiles recorded at each plane for a specific free stream velocity and flapping frequency are generally in phase when the neutral angle was varied. The velocity profile in general becomes “chaotic” as it moves away from the flapping dead center and this is not unexpected since interaction of vortices at planes away from the flapping dead center happens more readily.

Further discussion on the relationship between the statistical averaged time-dependant non-dimensional velocity magnitude for each flapping stroke and test conditions are illustrated as follows;

1. Effect of Varying Neutral Pitch

Higher peak velocity was recorded for increasing neutral angle and flapping frequency. The effect of varying flapping frequency will be discussed in detail in a later section. Nevertheless, findings indicated that at the lower flapping frequency, an increase of 10° (0° to 10°) increases peak velocity by an average of 5% and a further increase in neutral angle from 10° to 20° increases peak velocity by 1.7%. At the higher flapping frequency, an increase of 10° (0° to 10°) increases peak velocity approximately by 1.6% and further increase in neutral angle from 10° to 20° increases peak velocity by 2%. It was also noted that the velocity peaks began to move outward from the bottom dead center plane towards the top dead center plane as neutral angle increases. This is an

interesting phenomenon and would be a beneficial finding for a thrust vectoring study.

2. Effect of Free Stream Velocity

A higher peak velocity was recorded at lower free stream conditions. Generally, peak velocity increases by approximately 10% for every 1m/s reduction in free stream condition when flapping at 10 Hz and 15% for flapping at 15 Hz. This is probably due to the fact that the model spring was tuned for better performance at low free stream flight.

3. Effect of Flapping Frequency

Increasing flapping frequency produces higher peak velocity. The approximate percentage increase in peak velocity for flapping at 10 Hz and 15 Hz is summarized as follows;

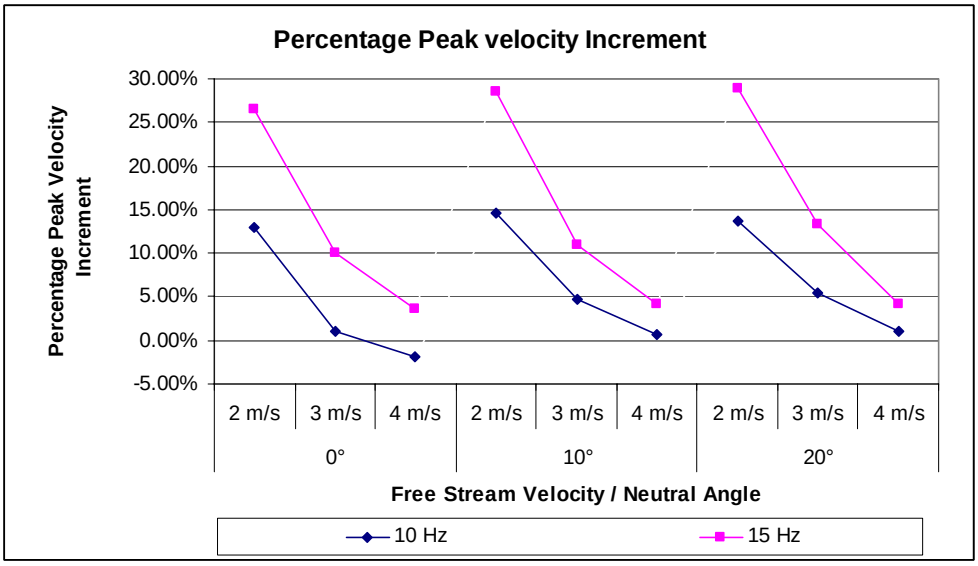

Figure 5- 46 Percentage Increment in Peak Velocity

Generally, a higher velocity gain is recorded for increasing flapping frequency at lower free-stream condition and neutral angle up to 10°.

D. PHASE 4: DIRECT THRUST MEASUREMENT

The summary of force balance results obtained for respective test conditions are tabulated graphically in Figure 5-47 to Figure 5-50. Details of measurement are tabulated in Appendix E

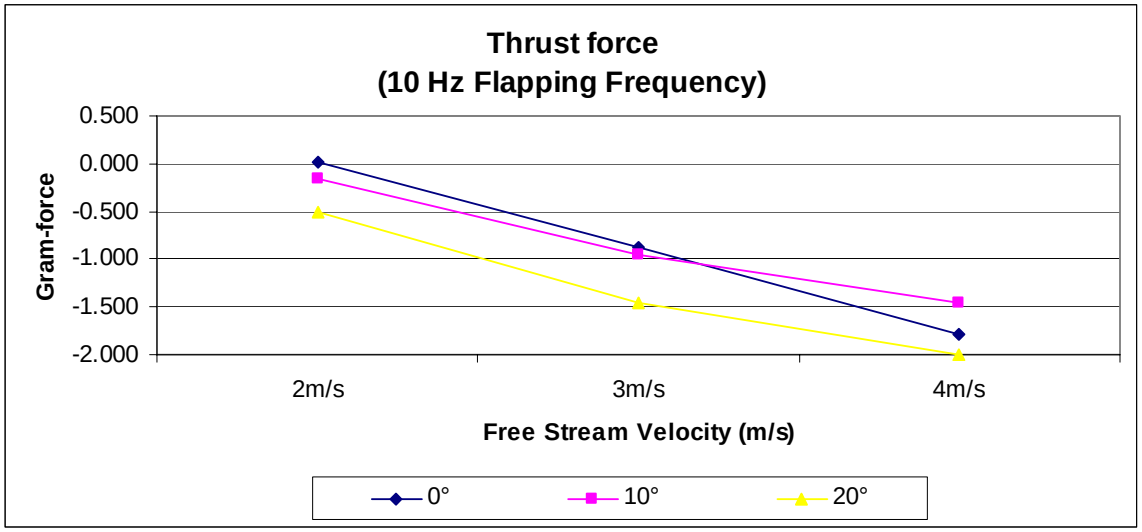

Figure 5- 47 Force Balance Summary for flapping at 10 Hz

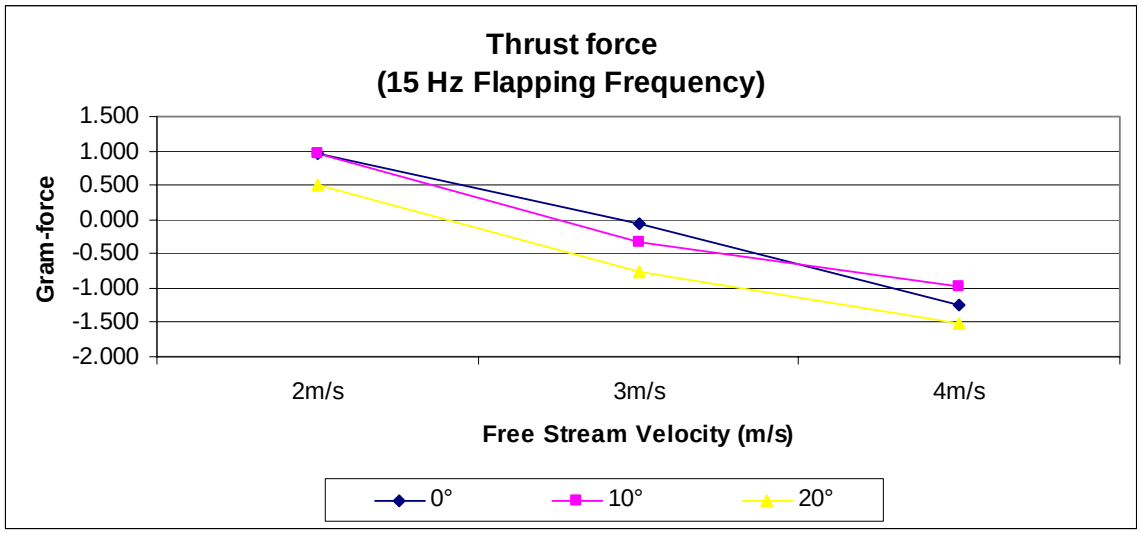

Figure 5- 48 Force Balance Summary for flapping at 15 Hz

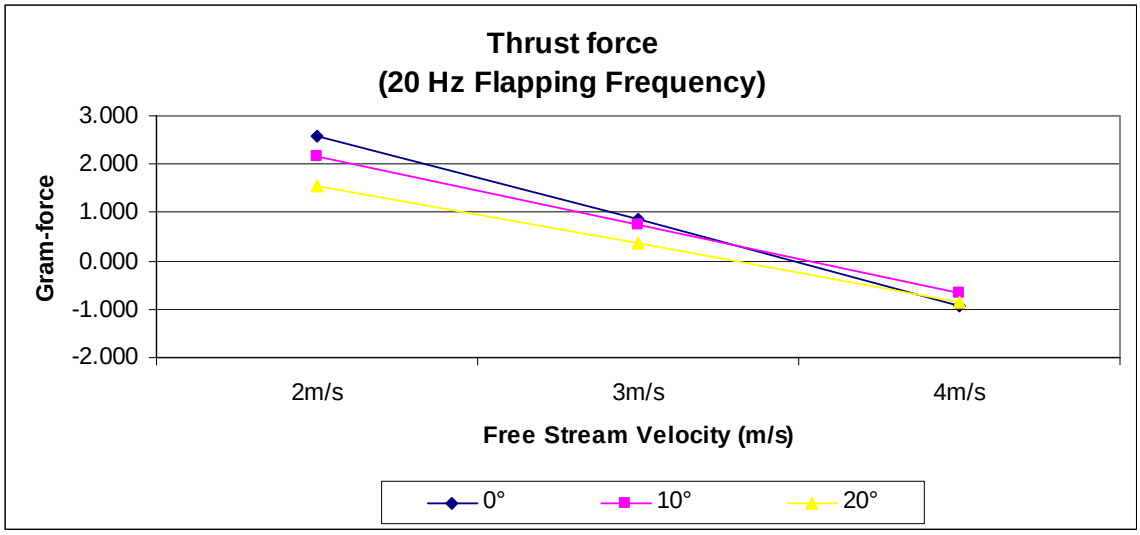

Figure 5- 49 Force Balance Summary for flapping at 20 Hz

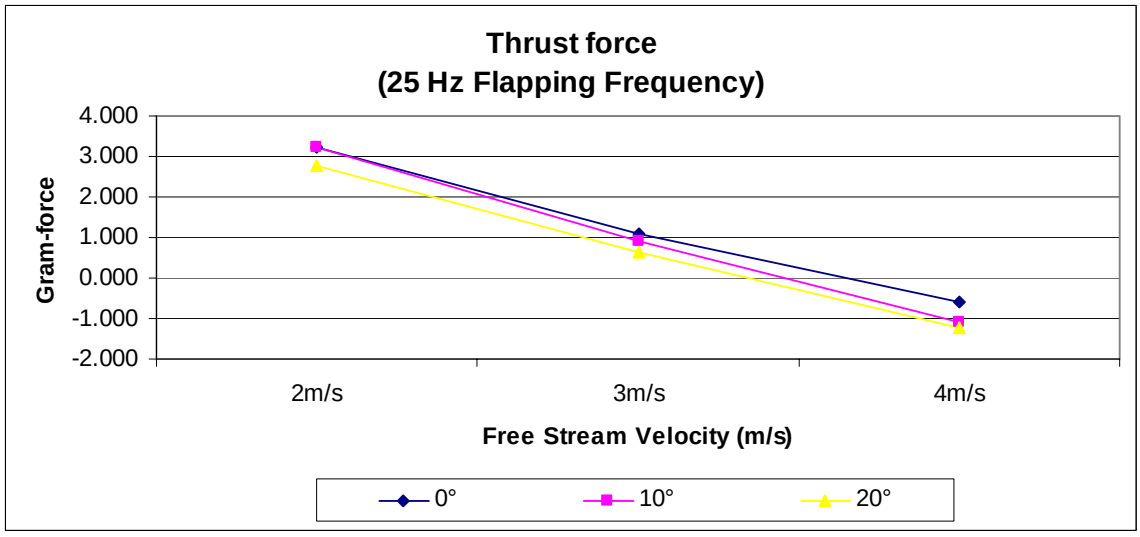

Figure 5- 50 Force Balance Summary for flapping at 25 Hz

General observation for free stream conditions at 2m/s and 3m/s indicated that thrust is reduced when the flapping wing are pitched. Positive thrust are obtained from model when tested at

a) free stream velocity at 2m/s, flapping at 15 Hz, 20 Hz and 25 Hz.

b) free stream velocity at 3m/s, flapping at 20 Hz and 25 Hz.

and negative thrust was obtained for other testing conditions where thrust generated was insufficient to overcome parasite drag.

A summary of measured thrust at varying test conditions are illustrated in Figure 5-51. The thrust indicated is biased with parasite drag inclusive of drag on model fuselage, model support and miscellaneous control, power cables.

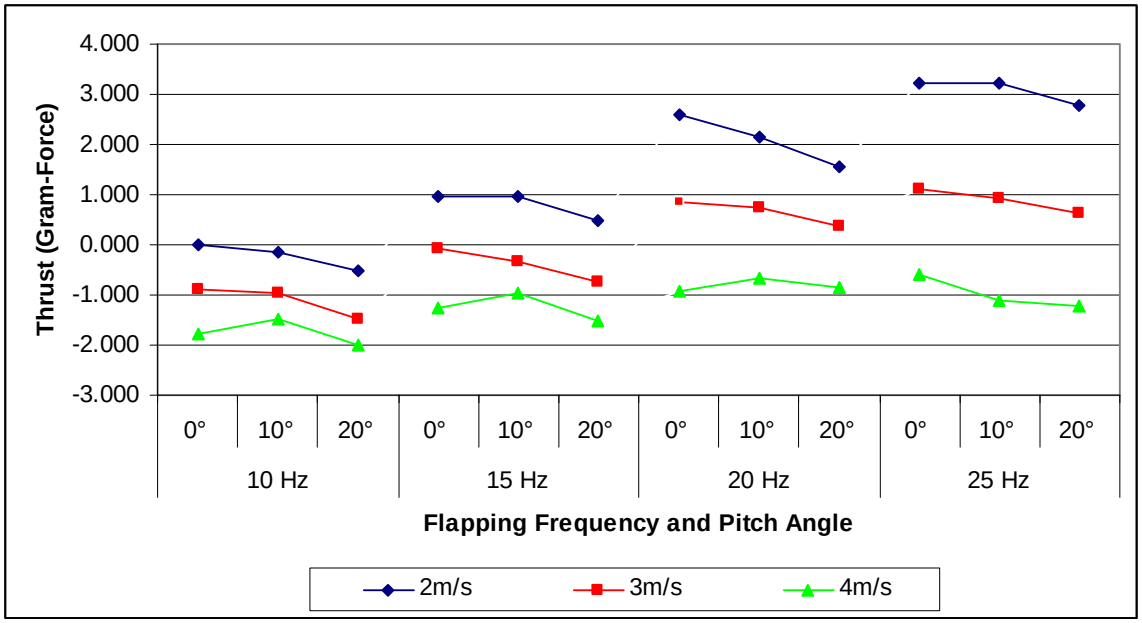

Figure 5- 51 Summary of Thrust Magnitude at Varying Neutral Angle and Flapping Frequency

1. Effect of Varying Neutral Pitch

Detailed analysis concluded that there is no clear correlation between thrust and neutral angle; varying the neutral angle for a specific free stream velocity has little influence over thrust, and thrust remains fairly constant over the tested angles with only minor variations for neutral angle from 10° to 20° (Magnitude of variation was insignificant when compared with the thrust magnitude at the specific free stream condition). Though it would be incorrect to say that the thrust magnitude obtained for flapping at 10 Hz is equal to the drag component acting on the model, it is nonetheless, a good indication of drag magnitude. The consistency of thrust over the range of tested angles at a specific

free stream velocity implies that thrust vectoring via varying neutral angle is likely a solution for pitch-control of the MAV and would be a subject of interest for future work.

2. Effect of Flapping Frequency

Linear Theory [Ref 10] suggests that thrust increases with the square of the flapping frequency; while the included experimental results indicate that thrust increases almost linearly with flapping frequency. The difference was mainly driven by the fact that assumption used in linear theory are not appropriate in this case, and are incapable of predicting flow phenomena at this low Reynolds numbers. The effect of low Reynolds numbers in the experimental flow field is non-trivial and has great influence over the actual model in flight.

3. Effect of Free Stream Velocity

Results indicated that an increase in free stream velocity reduces effective thrust as drag acting on model increases. The higher the flapping frequency, the greater the variations; while neutral angle has little influence over the variation and remains fairly constant within each frequency set in this instance. It is apparent that thrust reduction occurs more readily and with a slightly higher penalty when transitioning from 2m/s to 3m/s. In conclusion, a higher free stream condition is not favorable for flapping wing propulsion.

THIS PAGE INTENTIONALLY LEFT BLANK

VI. CONCLUSIONS

Using linear theory, it is found that the addition of pitching reduces thrust and sets a maximum speed for which thrust is produced [Ref 2]. The limitation of a purely pitching airfoil has been studied. It is now the interest of this work to provide a different perspective with regards to the effect of varying neutral pitch for effective propulsion. A number of conclusions may be drawn for the findings in this report with regards to the effect of varying neutral angle of attack of the experimental flapping wing.

The stiffness of the carbon fiber strip connecting the flapping beams and wings has great influence on the overall effect of aero-elastic pitching. The model was tuned for low free stream flight and results obtained proved that the model had better performance at low free stream condition. The introduction of a mechanical pitch angle to the neutral angle of attack of the flapping wings induced a change in the mean neutral angle seen by the airfoil which represents a complex relationship resulting from a combination of the mechanical pitch angle and the aero-elastic pitching angle. It is noted that as mechanical pitch angle increases, the measured neutral angle of attack seen by the airfoil increases. In contrast, a weak correlation is observed in the case of the measured full amplitude angle of attack.

Studies on time-averaged and time-dependant velocity profiles at discrete planes over varying test conditions, i.e., flapping frequencies, neutral angles and free stream velocities, revealed that velocity varies greatly across the regime and is highly dependent on the flight conditions. Conventional hot-wire measurement has limitations in this respect, as velocity samples are digitized and only limited discrete planes could be sampled at any one time. Nonetheless, the sampled profiles provided a better understanding of the variables influencing thrust and velocity generation at various test conditions. Further studies on the time-

dependant velocity magnitude variation per flapping cycle revealed recurring peak velocity across the same regime. The indication of peak velocity variation with neutral angle and flapping frequency implied that a good combination of plunge motion with pitch may provide meaningful thrust at various free stream conditions which has been demonstrated in the experiments. The findings on peak velocity vectoring towards the outer plane from the bottom dead center plane of the flapping stoke indicates an interesting phenomena beneficial for future thrust vectoring studies.

The test parameters evaluated show strong influence on the ability to affect thrust generation. Contrary to linear theory [Ref 10] which suggested that thrust increases with the square of flapping frequency, the experimental flapping airfoil experiences a linear relationship between thrust and flapping frequency; nevertheless, this becomes insignificant when free stream conditions increase. Graphical representation of velocity profile behind flapping wings in flow visualization leads to believe that overall propulsive performance has improved with low neutral angle of attack, nevertheless, the increase in neutral angle beyond 20° for low free steam condition is observed to lead to severe leading-edge separation with associated loss in the propulsive signature of the vortex array thus reducing effective propulsive thrust.

The trend from a combination of heaving motion with varying neutral angle not exceeding 20° has been shown to generate higher thrust under the tested conditions, while the need for higher flapping frequency for thrust generation to overcome drag in high free stream conditions remains an important criteria for efficient flight performance.

VII. RECOMMENDATION FOR FUTURE WORK

An interesting continuation of the experiment would be to further investigate and determine a set of optimum combination of flapping frequencies, pitch angles and carbon fiber stiffness for varying free stream conditions. It would also be of interest to map the velocity profile of the wake behind the flapping wings at multiple downstream planes to provide a better picture of the wake structures downstream of the flapping wings. In addition, since thrust remains fairly constant with little variations over the tested pitch angles, the findings could be useful to investigate varying neutral angle for thrust vectoring as in the cases as listed;

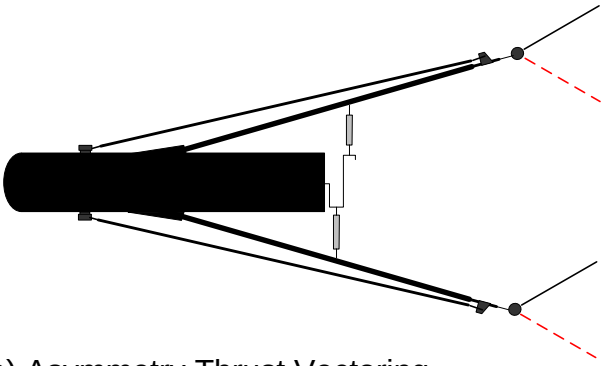

a) Asymmetry Thrust Vectoring

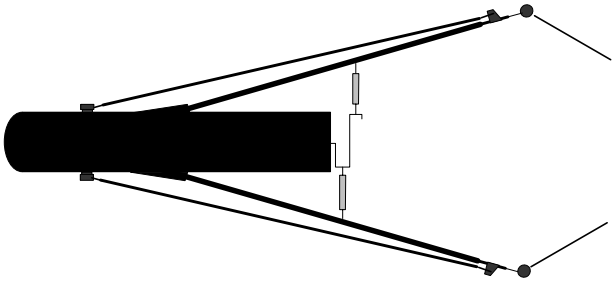

b) Inward Thrust Vectoring

THIS PAGE INTENTIONALLY LEFT BLANK

APPENDIX A. HOT WIRE CALIBRATION

Fourth Order Polynomial Curve fit

$$U = C_0 + C_1 E_{corr} + C_2 E_{corr}^{\ 2} + C_3 E_{corr}^{\ 3} + C_4 E_{corr}^{\ 4}$$

U	E1	T(C)	P(kPa)	E1corr	U1calc
1.003	0.815	20.095	101.771	0.815	0.992
1.298	0.857	20.063	101.777	0.857	1.321
1.677	0.887	20.034	101.779	0.887	1.67
2.165	0.921	20.018	101.788	0.921	2.207
2.792	0.949	20.015	101.793	0.949	2.746
3.61	0.985	20.017	101.802	0.985	3.579
4.673	1.022	20.026	101.807	1.022	4.607
6.039	1.069	20.035	101.799	1.069	6.127
7.764	1.114	20.039	101.799	1.114	7.856
10.032	1.161	20.048	101.799	1.161	9.943

THIS PAGE INTENTIONALLY LEFT BLANK

APPENDIX B. TIME-AVERAGED VELOCITY PROFILE MAPPING

TABULATION OF TIME-AVERAGED VELOCITY MAPPING

1. FREE STREAM VELOCITY 2M/S

a) Non-Dimensional Velocity for 0° pitch and 10 Hz flapping frequency (Normalized 2m/s)

	C1	C2	C3	C4	C5	C6	C7	C8	C9
R1	1.024	1.011	1.032	1.017	1.029	1.022	1.004	1.007	1.007
R2	1.010	0.938	1.062	0.943	1.029	0.987	0.978	1.040	1.024
R3	0.998	0.942	1.105	0.965	1.008	1.010	1.042	1.021	1.025
R4	1.011	1.008	1.092	0.947	0.959	1.059	1.049	0.901	1.020
R5	1.009	1.018	1.064	0.971	0.830	1.005	1.023	0.972	1.026
R6	1.008	1.028	1.036	0.996	0.701	0.951	0.998	1.044	1.032
R7	1.010	1.015	1.052	0.987	0.784	0.998	0.982	0.983	1.033
R8	1.012	1.002	1.068	0.978	0.867	1.044	0.967	0.922	1.034
R9	1.007	0.948	1.114	0.970	0.945	1.103	1.109	0.984	1.034
R10	1.003	1.018	1.079	0.940	0.939	1.073	1.012	0.963	1.032
R11	0.998	1.010	0.990	0.970	0.916	0.986	0.985	1.036	1.029

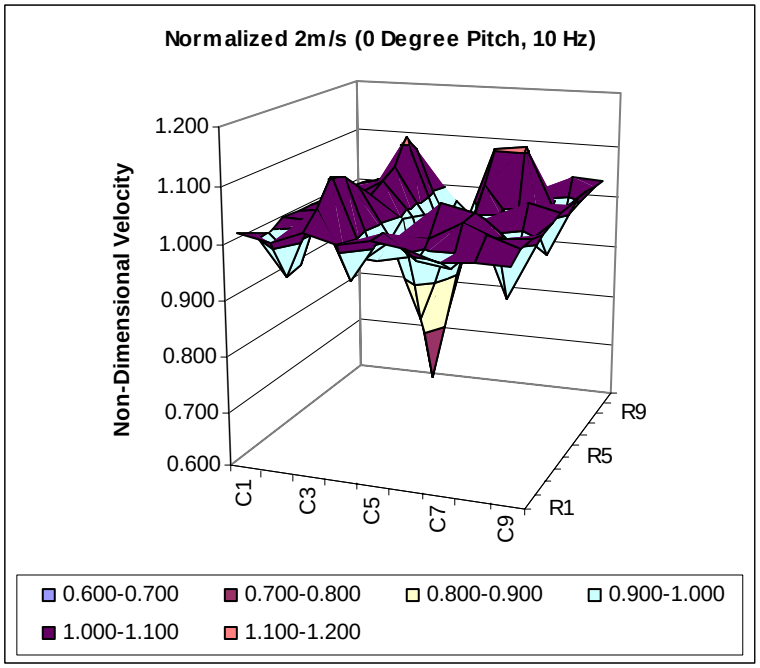

b) Non-Dimensional Velocity for 10° pitch and 10 Hz flapping frequency (Normalized 2m/s)

	C1	C2	C3	C4	C5	C6	C7	C8	C9
R1	1.000	1.020	1.086	1.005	1.026	0.909	0.995	1.025	1.019
R2	1.002	1.021	1.150	0.988	1.093	0.974	1.082	1.039	1.021
R3	0.998	1.007	1.167	0.927	0.997	1.042	1.114	1.035	1.018
R4	0.994	0.997	1.123	1.019	0.989	1.085	1.122	0.999	1.022
R5	0.998	0.993	1.072	0.986	0.878	1.042	1.086	1.011	1.027
R6	1.002	0.989	1.021	0.953	0.768	1.000	1.050	1.024	1.033
R7	0.999	0.994	1.075	0.948	0.844	1.059	1.069	1.003	0.992
R8	0.996	0.999	1.128	0.943	0.921	1.118	1.088	0.982	0.951
R9	0.990	0.995	1.148	0.948	0.968	1.081	1.140	0.976	1.025
R10	0.995	1.022	1.135	0.953	0.944	1.009	1.148	1.031	1.019
R11	0.988	1.013	1.086	0.928	0.927	0.899	1.079	1.024	1.010

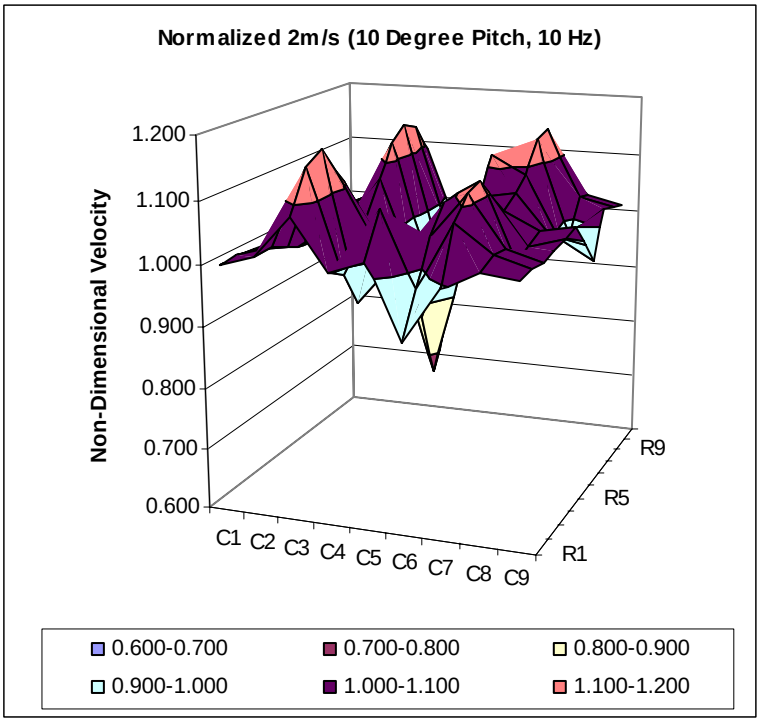

C) Non-Dimensional Velocity for 20° pitch and 10 Hz flapping frequency (Normalized 2m/s)

	C1	C2	C3	C4	C5	C6	C7	C8	C9
R1	1.001	1.033	1.164	0.925	0.957	0.858	1.014	1.027	1.012
R2	1.007	1.032	1.177	0.888	1.013	0.975	1.124	1.038	1.019
R3	1.002	1.011	1.174	0.916	1.038	1.028	1.145	1.009	1.022
R4	0.999	1.024	1.091	0.974	0.907	1.033	1.122	0.971	1.029
R5	0.998	1.018	1.030	0.951	0.815	1.026	1.070	0.982	1.020
R6	0.998	1.011	0.969	0.928	0.722	1.020	1.018	0.993	1.012
R7	1.009	1.017	1.063	0.923	0.816	1.088	1.090	0.995	0.983
R8	1.019	1.022	1.157	0.918	0.909	1.156	1.163	0.998	0.953
R9	1.013	1.005	1.187	0.901	0.967	1.102	1.200	1.008	1.037
R10	1.011	1.042	1.183	0.876	0.980	0.921	1.190	1.062	1.038
R11	1.002	1.039	1.132	0.952	0.841	0.899	1.123	1.058	1.047

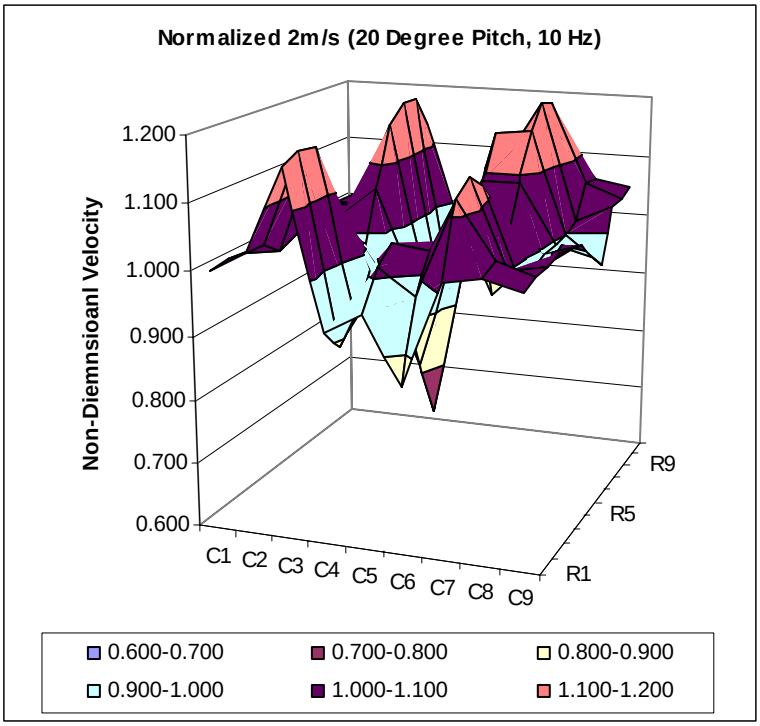

d) Non-Dimensional Velocity for 0° pitch and 15 Hz flapping frequency (Normalized 2m/s)

	C1	C2	C3	C4	C5	C6	C7	C8	C9
R1	0.991	1.016	1.042	1.004	1.024	1.037	1.147	1.024	1.004
R2	0.987	0.997	1.172	1.192	1.250	1.268	1.172	1.003	0.919
R3	0.980	0.990	1.304	1.385	1.250	1.366	1.274	1.017	0.982
R4	0.975	1.008	1.246	1.183	1.249	1.269	1.331	0.996	0.992
R5	0.975	1.061	1.103	1.039	1.045	1.065	1.155	1.053	0.992
R6	0.974	1.114	0.961	0.895	0.841	0.862	0.980	1.109	0.992
R7	0.974	1.045	1.061	0.980	1.001	0.966	1.089	1.051	0.994
R8	0.973	0.976	1.160	1.065	1.161	1.071	1.199	0.993	0.996
R9	0.974	1.008	1.344	1.297	1.274	1.304	1.341	1.011	1.000
R10	0.971	1.002	1.212	1.255	1.232	1.295	1.298	1.009	0.991
R11	0.980	1.017	1.168	0.997	0.992	1.080	1.192	1.008	1.001

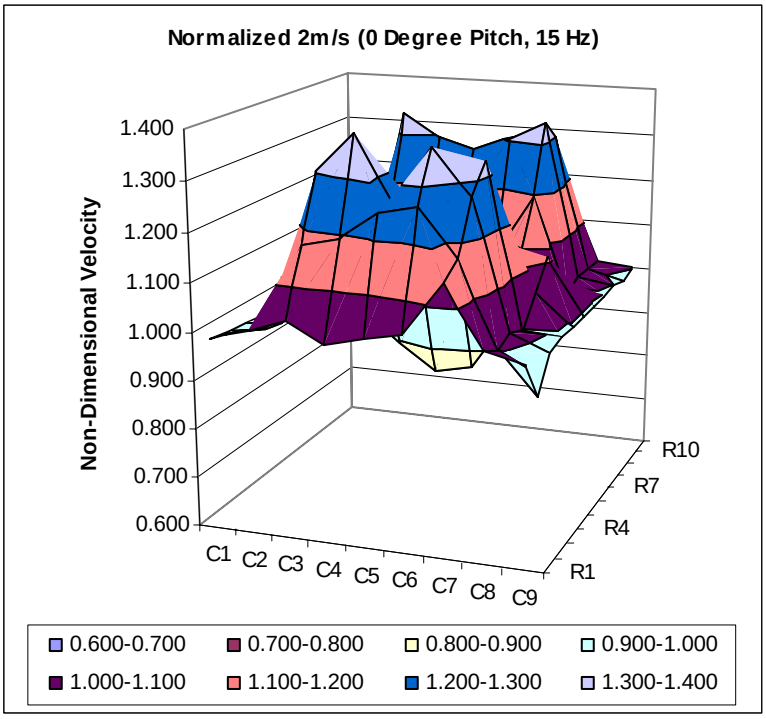

e) Non-Dimensional Velocity for 10° pitch and 15 Hz flapping frequency (Normalized 2m/s)

	C1	C2	C3	C4	C5	C6	C7	C8	C9
R1	0.884	0.997	1.128	0.872	0.972	0.916	1.147	1.014	0.986
R2	0.962	0.983	1.260	1.090	1.261	1.166	1.232	1.006	0.995
R3	0.949	0.966	1.287	1.318	1.248	1.369	1.325	1.000	0.986
R4	0.959	0.988	1.210	1.347	1.201	1.378	1.276	0.978	0.981
R5	0.954	0.963	1.061	1.113	0.981	1.153	1.136	1.001	0.981
R6	0.949	0.938	0.912	0.880	0.761	0.927	0.997	1.024	0.981
R7	0.955	0.943	1.061	1.028	0.972	1.043	1.087	0.991	0.977
R8	0.962	0.948	1.210	1.176	1.183	1.159	1.177	0.958	0.974
R9	0.957	0.963	1.339	1.304	1.216	1.360	1.328	0.991	0.990
R10	0.953	0.990	1.207	1.096	1.216	1.211	1.331	1.014	0.981
R11	0.948	0.920	1.258	0.915	0.977	0.927	1.223	1.029	0.993

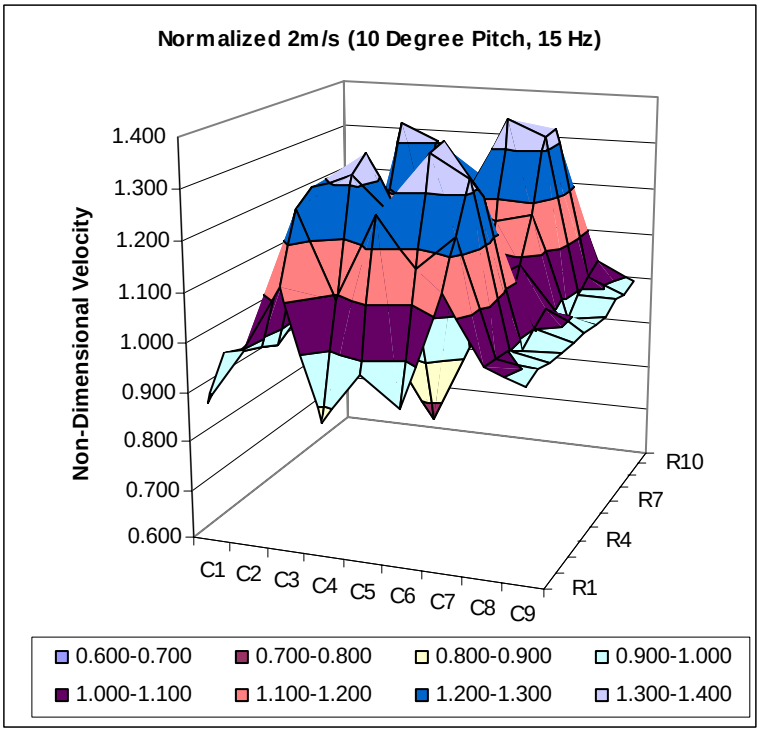

f) Non-Dimensional Velocity for 20° pitch and 15 Hz flapping frequency (Normalized 2m/s)

	C1	C2	C3	C4	C5	C6	C7	C8	C9
R1	0.904	0.999	1.159	0.885	1.033	0.837	1.237	1.022	0.998
R2	0.951	0.997	1.307	0.994	1.252	1.035	1.251	1.043	0.994
R3	0.957	0.955	1.269	1.237	1.232	1.303	1.351	1.019	0.992
R4	0.958	1.016	1.167	1.322	1.222	1.381	1.326	0.972	0.978
R5	0.961	0.987	1.032	1.112	0.972	1.155	1.170	0.968	0.986
R6	0.964	0.958	0.898	0.903	0.721	0.930	1.013	0.965	0.995
R7	0.956	0.958	1.070	1.085	0.959	1.136	1.135	0.979	0.989
R8	0.948	0.959	1.241	1.267	1.197	1.342	1.256	0.994	0.983
R9	0.960	0.959	1.344	1.252	1.219	1.314	1.315	0.997	0.989
R10	0.960	0.988	1.199	0.978	1.176	1.109	1.318	1.031	1.011
R11	0.964	1.008	1.261	0.862	0.935	0.901	1.271	1.035	1.010

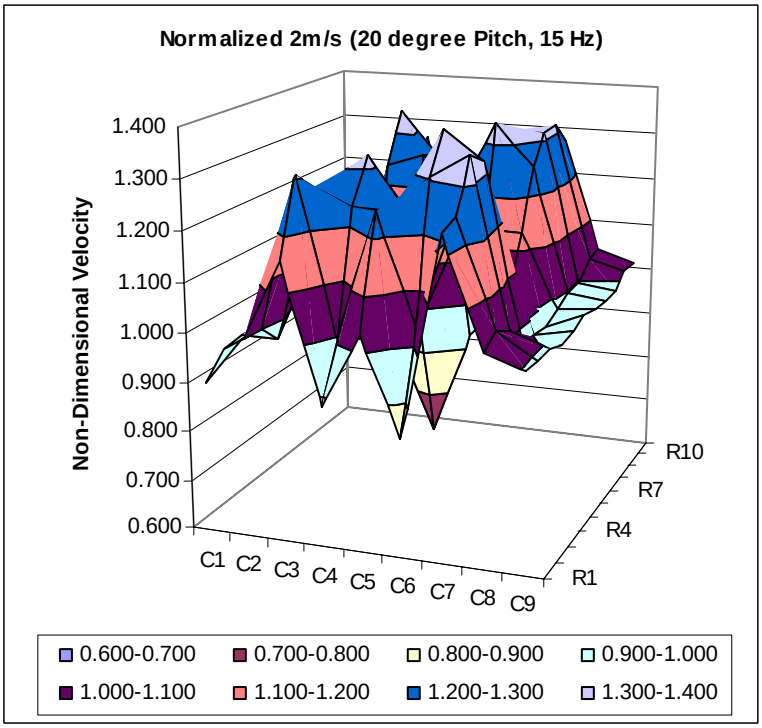

2. FREE STREAM VELOCITY 3M/S

a) Non-Dimensional Velocity for 0° pitch and 10 Hz flapping frequency (Normalized 3m/s)

	C1	C2	C3	C4	C5	C6	C7	C8	C9
R1	0.984	0.996	1.012	1.003	1.001	0.997	0.997	1.001	1.002
R2	0.977	1.006	1.000	0.951	0.979	0.981	0.993	1.017	1.018
R3	0.992	0.976	1.013	0.963	0.969	0.938	0.981	1.000	1.013
R4	0.989	0.990	1.002	0.914	0.854	0.980	1.007	0.969	1.020
R5	0.989	0.994	0.997	0.942	0.776	0.991	1.004	0.984	1.016
R6	0.989	0.998	0.993	0.970	0.698	1.003	1.000	0.999	1.011
R7	0.985	0.988	1.003	0.923	0.766	0.989	0.990	0.975	1.012
R8	0.980	0.977	1.012	0.876	0.833	0.976	0.981	0.952	1.012
R9	0.988	0.994	0.994	0.917	0.858	0.978	1.009	1.007	1.009
R10	0.981	1.003	0.972	0.934	0.892	0.952	0.960	1.002	0.944
R11	0.983	0.990	0.997	1.002	0.877	0.986	0.995	1.011	1.010

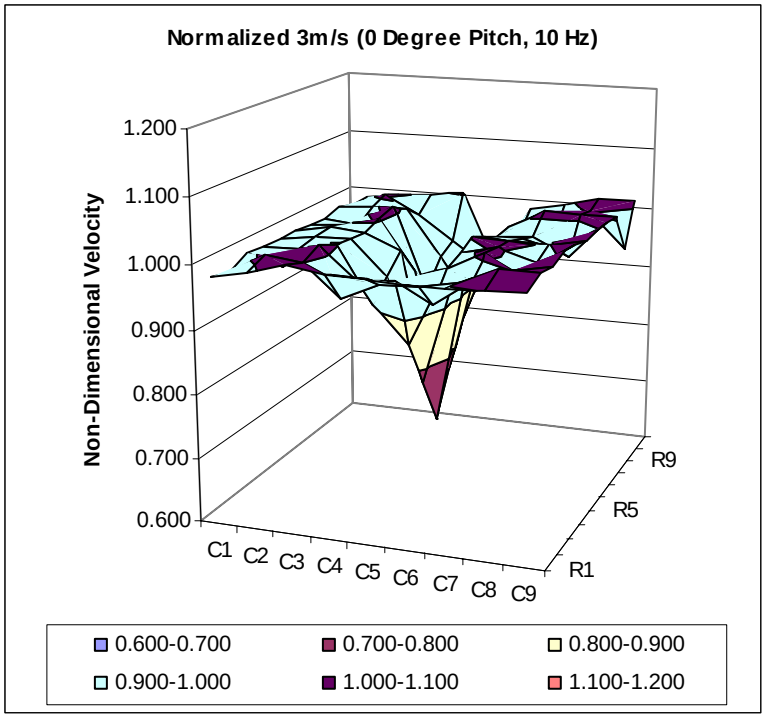

b) Non-Dimensional Velocity for 10° pitch and 10 Hz flapping frequency (Normalized 3m/s)

	C1	C2	C3	C4	C5	C6	C7	C8	C9
R1	0.923	1.006	0.999	0.966	0.993	0.996	0.958	1.013	1.001
R2	0.994	1.003	1.049	0.933	1.013	0.955	0.966	1.015	1.009
R3	0.990	0.990	1.039	0.916	0.944	0.947	1.001	1.010	1.011
R4	0.987	0.997	0.994	0.958	0.813	0.977	0.967	0.989	1.013
R5	0.987	0.990	0.980	0.980	0.746	0.987	0.990	0.992	1.011
R6	0.987	0.983	0.965	1.002	0.679	0.997	1.013	0.995	1.008
R7	0.984	0.985	0.968	0.961	0.744	0.964	1.014	0.981	1.014
R8	0.981	0.986	0.970	0.921	0.808	0.930	1.016	0.967	1.019
R9	0.997	1.000	1.042	0.865	0.851	0.941	0.996	1.023	1.015
R10	0.982	0.998	0.982	0.890	0.905	0.906	0.967	1.013	1.003
R11	0.977	0.998	1.000	0.967	0.869	0.979	1.011	1.000	1.023

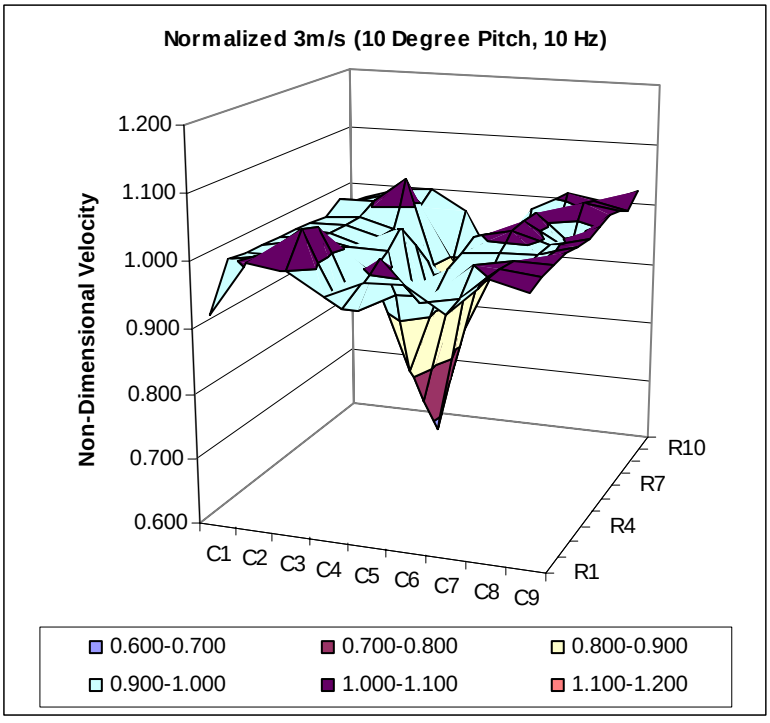

c) Non-Dimensional Velocity for 20° pitch and 10 Hz flapping frequency (Normalized 3m/s)

	C1	C2	C3	C4	C5	C6	C7	C8	C9
R1	0.990	1.010	1.015	0.963	1.008	0.973	0.998	1.021	1.022
R2	0.994	1.013	1.062	0.873	1.031	0.921	1.000	1.025	1.024
R3	0.992	1.003	1.062	0.858	0.928	0.913	1.019	1.022	1.013
R4	0.993	0.986	0.948	0.913	0.770	0.910	1.003	1.007	1.008
R5	0.991	0.990	0.972	0.957	0.732	0.954	1.006	1.010	1.021
R6	0.988	0.993	0.995	1.001	0.694	0.999	1.009	1.013	1.035
R7	0.999	0.999	1.012	0.955	0.779	0.947	0.995	0.997	0.992
R8	1.009	1.006	1.029	0.909	0.864	0.895	0.981	0.981	0.948
R9	1.001	1.012	1.050	0.862	0.881	0.872	1.027	1.021	1.033
R10	1.004	1.030	1.012	0.853	0.917	0.904	0.983	1.035	1.025
R11	0.999	1.015	1.010	0.959	0.902	0.993	0.995	1.032	1.028

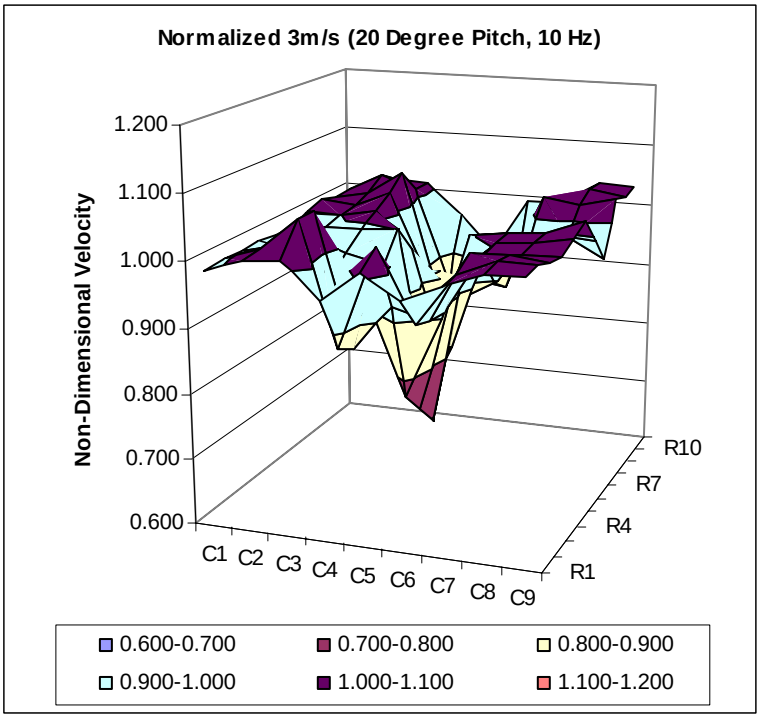

d) Non-Dimensional Velocity for 0° pitch and 15 Hz flapping frequency (Normalized 3m/s)

	C1	C2	C3	C4	C5	C6	C7	C8	C9
R1	0.992	0.995	1.021	0.991	1.029	0.992	1.016	1.007	1.016
R2	0.983	0.994	1.053	1.018	1.011	1.017	1.026	1.000	1.015
R3	0.982	0.980	1.091	1.036	0.962	1.065	1.089	1.005	1.004
R4	0.975	0.968	1.057	0.996	0.906	1.060	1.069	0.961	1.002
R5	0.976	0.969	1.009	0.964	0.814	1.031	1.012	0.995	1.003
R6	0.976	0.971	0.962	0.931	0.722	1.002	0.955	1.028	1.004
R7	0.971	0.963	1.021	0.963	0.793	1.028	1.007	1.004	1.002
R8	0.966	0.954	1.081	0.994	0.864	1.054	1.058	0.979	1.001
R9	0.985	0.993	1.085	1.008	0.897	1.086	1.083	0.996	1.002
R10	0.981	0.998	1.076	0.954	0.876	1.052	1.046	0.997	1.004
R11	0.983	0.993	1.006	0.936	0.821	0.957	0.934	1.019	1.011

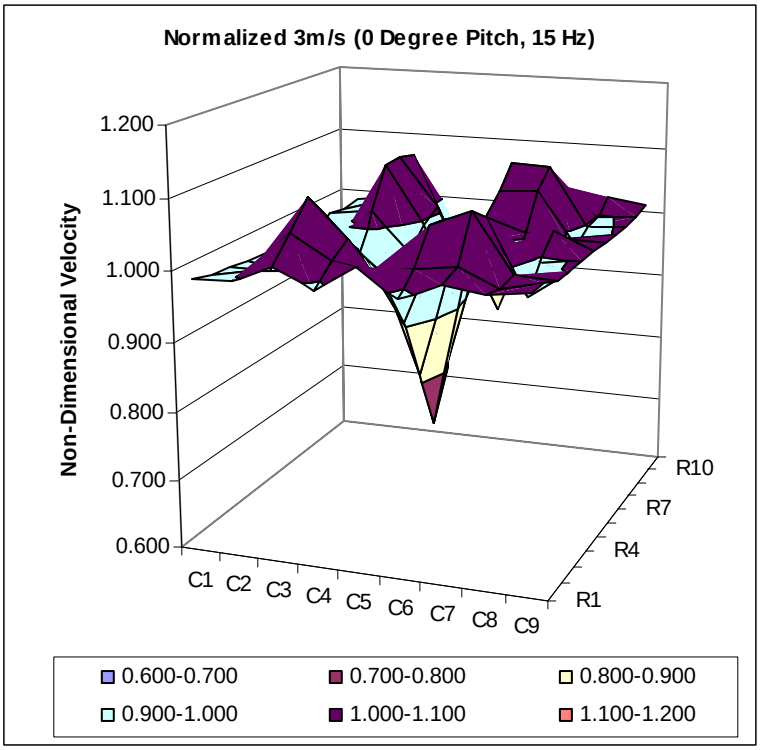

e) Non-Dimensional Velocity for 10° pitch and 15 Hz flapping frequency (Normalized 3m/s)

	C1	C2	C3	C4	C5	C6	C7	C8	C9
R1	0.904	1.008	1.042	0.892	1.026	0.966	0.972	1.014	1.018
R2	0.977	1.016	1.092	0.981	1.011	1.035	1.040	1.021	1.018
R3	0.973	0.998	1.074	1.044	0.918	1.095	1.092	1.004	1.012
R4	0.981	0.953	1.065	1.026	0.893	1.075	1.067	1.006	1.019
R5	0.986	0.977	0.996	0.971	0.795	1.000	1.009	1.005	1.018
R6	0.990	1.002	0.926	0.916	0.697	0.926	0.951	1.004	1.017
R7	0.982	0.982	1.002	0.964	0.784	1.000	1.001	0.977	1.018
R8	0.974	0.961	1.078	1.012	0.871	1.073	1.051	0.949	1.019
R9	0.986	0.996	1.113	0.989	0.869	1.084	1.107	0.987	1.015
R10	0.986	1.000	1.076	0.903	0.921	1.012	1.095	1.018	1.017
R11	0.987	1.000	1.048	0.901	0.849	0.910	0.985	1.020	1.012

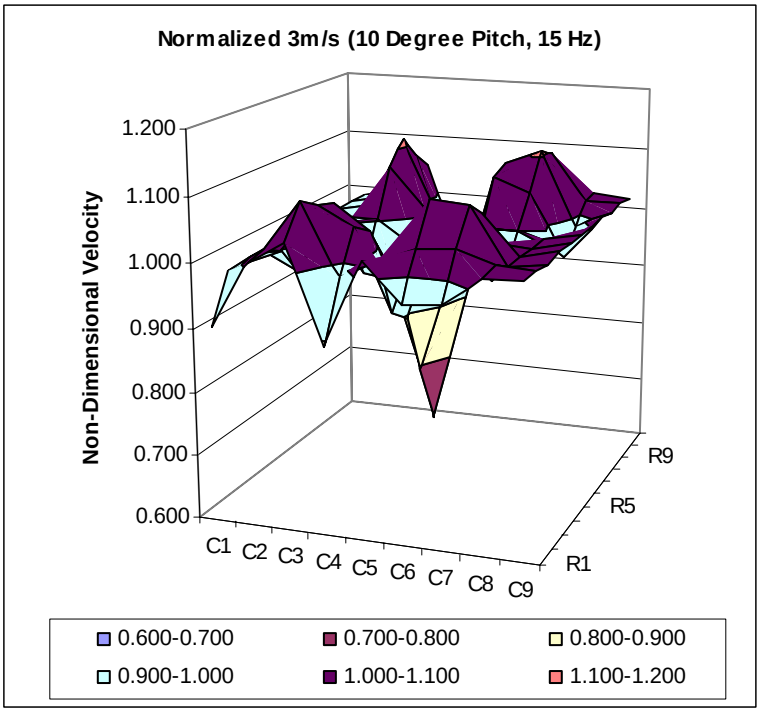

f) Non-Dimensional Velocity for 20° pitch and 15 Hz flapping frequency (Normalized 3m/s)

	C1	C2	C3	C4	C5	C6	C7	C8	C9
R1	0.981	0.998	1.089	0.866	1.009	0.958	1.038	1.025	1.020
R2	0.972	1.007	1.093	0.895	0.966	1.006	1.032	1.021	1.021
R3	0.983	0.997	1.097	0.935	0.936	1.054	1.116	1.003	1.008
R4	0.983	0.992	1.011	1.019	0.867	1.016	1.072	1.011	1.023
R5	0.980	0.985	0.996	1.001	0.778	0.972	1.016	1.004	1.012
R6	0.976	0.977	0.981	0.983	0.689	0.927	0.961	0.998	1.002
R7	0.979	0.973	1.031	0.978	0.787	0.982	1.013	0.991	1.010
R8	0.981	0.969	1.081	0.973	0.884	1.038	1.065	0.984	1.017
R9	0.973	0.989	1.089	0.872	0.861	1.056	1.106	0.965	1.020
R10	0.972	1.005	1.073	0.843	0.901	0.995	1.098	1.006	1.017
R11	0.982	1.019	1.072	0.847	0.897	0.903	1.056	1.028	1.011

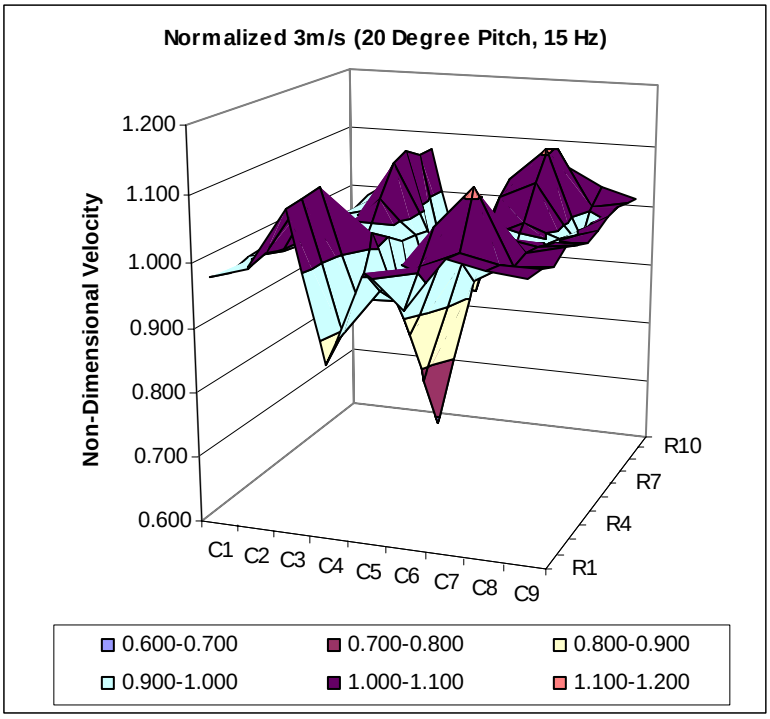

3. FREE STREAM VELOCITY 4M/S

a) Non-Dimensional Velocity for 0° pitch and 10 Hz flapping frequency (Normalized 4m/s)

	C1	C2	C3	C4	C5	C6	C7	C8	C9
R1	0.969	0.984	0.992	0.996	0.998	1.002	0.993	0.999	1.013
R2	0.975	0.975	0.974	0.968	0.972	0.988	0.993	0.996	0.935
R3	0.987	0.974	0.978	0.979	0.918	0.948	0.958	0.987	1.022
R4	0.980	0.978	0.908	0.917	0.803	0.950	0.988	0.989	1.023
R5	0.981	0.980	0.947	0.948	0.787	0.970	0.997	1.002	1.012
R6	0.982	0.983	0.986	0.979	0.771	0.990	1.006	1.014	1.000
R7	0.980	0.981	0.986	0.963	0.780	0.960	0.986	1.000	1.008
R8	0.978	0.979	0.987	0.947	0.789	0.929	0.966	0.987	1.016
R9	0.974	0.989	0.958	0.901	0.825	0.918	0.985	1.002	1.007
R10	0.981	1.003	0.981	0.959	0.842	1.003	0.970	1.016	1.015
R11	0.993	0.993	0.994	1.001	0.878	0.992	1.001	1.015	1.020

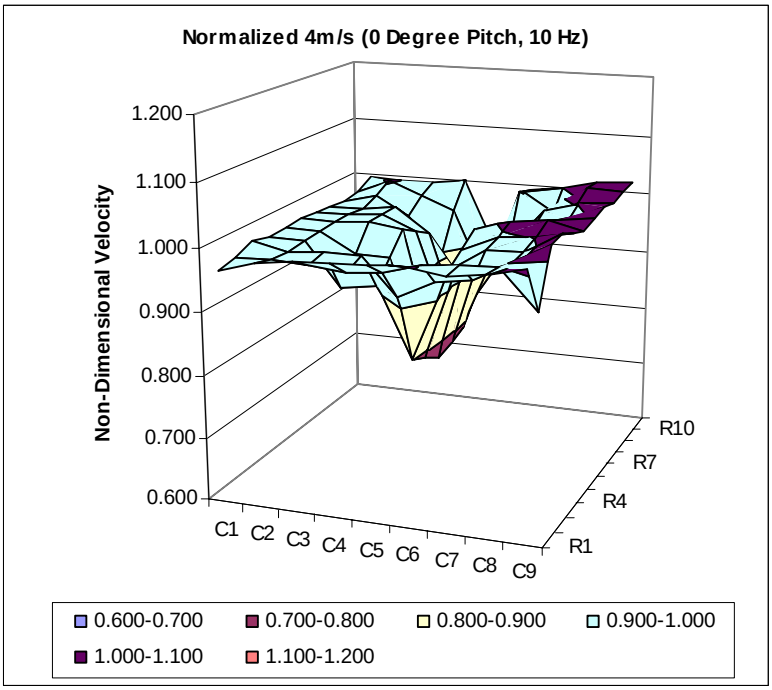

b) Non-Dimensional Velocity for 10° pitch and 10 Hz flapping frequency (Normalized 4m/s)

	C1	C2	C3	C4	C5	C6	C7	C8	C9
R1	0.987	0.997	0.998	1.017	1.014	1.024	1.018	1.023	1.024
R2	0.983	0.989	0.980	0.939	0.961	1.004	0.998	1.018	1.017
R3	1.002	0.989	0.997	0.919	0.920	0.922	0.988	1.020	1.018
R4	0.985	0.996	0.964	0.955	0.765	0.956	1.014	1.000	1.020
R5	0.984	0.992	0.993	0.977	0.771	0.983	1.019	1.009	1.022
R6	0.983	0.988	1.021	0.999	0.778	1.010	1.024	1.017	1.023
R7	0.980	0.984	0.999	1.019	0.791	0.973	0.980	1.013	1.021
R8	0.978	0.980	0.977	1.040	0.805	0.935	0.937	1.008	1.020
R9	0.981	0.991	1.010	0.894	0.858	0.932	0.977	1.019	1.028
R10	0.980	0.999	0.962	0.931	0.877	0.959	0.982	1.018	1.018
R11	0.983	0.993	0.986	1.002	0.871	1.004	1.012	1.018	1.019

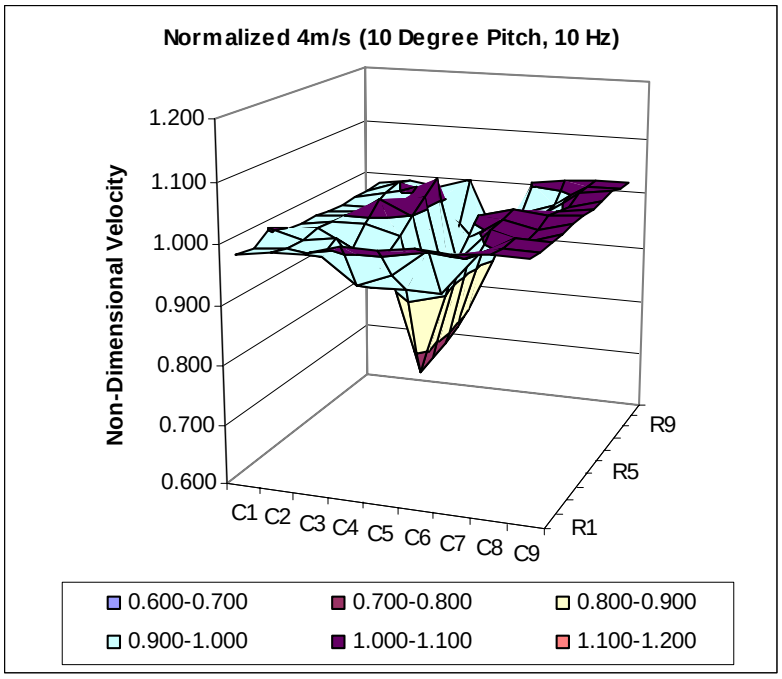

c) Non-Dimensional Velocity for 20° pitch and 10 Hz flapping frequency (Normalized 4m/s)

	C1	C2	C3	C4	C5	C6	C7	C8	C9
R1	0.978	0.995	0.994	0.996	1.007	1.003	1.016	1.014	1.016
R2	0.985	0.993	0.984	0.932	0.974	0.947	0.978	1.019	1.019
R3	0.979	0.986	1.007	0.923	0.895	0.922	0.979	1.013	1.010
R4	0.974	0.992	0.913	0.923	0.787	0.929	0.960	1.012	1.013
R5	0.976	0.988	0.951	0.969	0.765	0.971	0.988	1.013	1.015
R6	0.978	0.985	0.988	1.014	0.742	1.014	1.017	1.014	1.018
R7	0.975	0.983	0.964	0.927	0.764	0.954	0.968	1.019	1.014
R8	0.971	0.980	0.939	0.840	0.786	0.894	0.919	1.025	1.011
R9	0.974	0.993	0.976	0.835	0.837	0.861	0.984	1.009	1.013
R10	0.969	1.000	0.964	0.896	0.879	0.887	0.970	1.020	1.011
R11	0.973	0.987	0.976	0.965	0.881	0.929	0.986	1.017	1.010

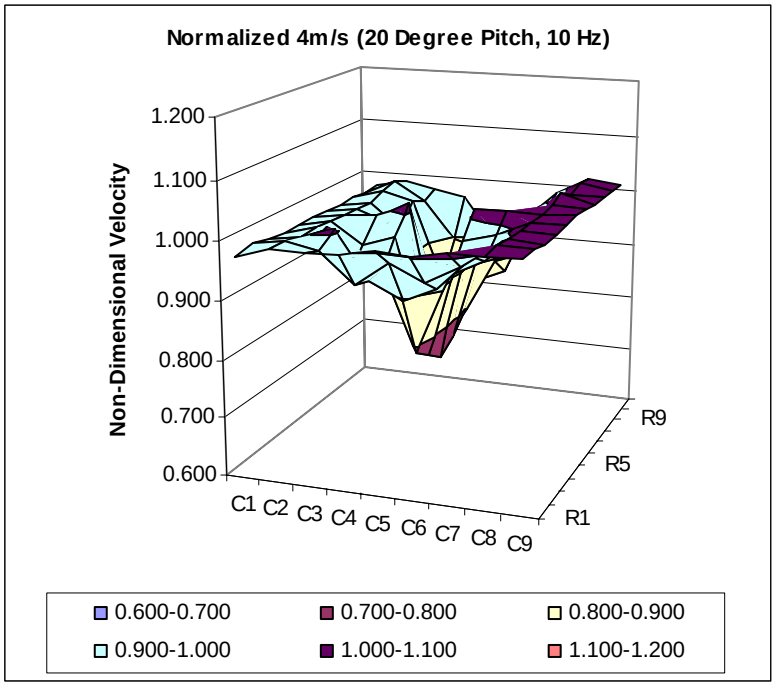

d) Non-Dimensional Velocity for 0° pitch and 15 Hz flapping frequency (Normalized 4m/s)

	C1	C2	C3	C4	C5	C6	C7	C8	C9
R1	1.000	0.992	0.997	0.988	0.986	0.992	1.013	1.007	1.033
R2	0.983	0.984	1.002	0.992	0.999	0.966	0.988	1.032	1.022
R3	0.984	0.971	1.009	0.989	0.922	0.995	1.002	1.023	1.017
R4	0.983	0.976	0.987	0.984	0.837	0.987	1.021	0.999	1.028
R5	0.983	0.982	0.991	0.977	0.802	0.983	1.002	1.000	1.032
R6	0.983	0.989	0.995	0.969	0.768	0.978	0.983	1.001	1.035
R7	0.980	0.983	1.003	0.968	0.780	0.975	0.996	0.997	1.029
R8	0.978	0.977	1.010	0.968	0.793	0.972	1.008	0.994	1.022
R9	0.979	0.988	1.003	0.979	0.847	0.986	1.024	1.004	1.020
R10	0.981	0.988	1.002	0.957	0.887	0.977	1.005	1.019	1.033
R11	0.977	0.989	0.995	0.975	0.886	0.984	0.987	1.014	1.027

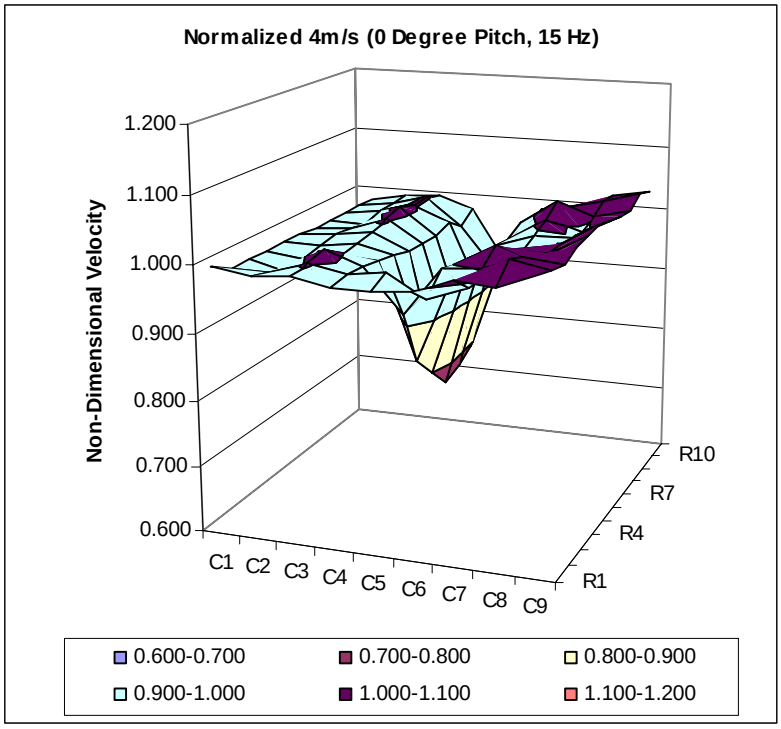

e) Non-Dimensional Velocity for 10° pitch and 15 Hz flapping frequency (Normalized 4m/s)

	C1	C2	C3	C4	C5	C6	C7	C8	C9
R1	0.990	0.987	0.980	0.963	0.995	0.964	1.002	1.012	1.020
R2	0.979	0.989	1.016	0.965	0.995	0.960	0.978	1.016	1.015
R3	0.990	0.983	1.017	1.001	0.908	0.967	1.011	1.012	1.016
R4	0.978	0.981	0.989	0.976	0.820	0.982	1.023	0.999	1.018
R5	0.974	0.980	0.985	0.977	0.789	0.985	1.008	0.999	1.018
R6	0.970	0.978	0.981	0.978	0.759	0.988	0.994	1.000	1.018
R7	0.973	0.975	0.998	0.979	0.781	0.994	1.011	1.000	1.018
R8	0.976	0.972	1.015	0.979	0.803	1.000	1.027	1.001	1.018
R9	0.962	0.980	1.011	0.946	0.845	0.993	1.022	1.003	1.013
R10	0.968	1.000	1.005	0.884	0.896	0.907	0.971	1.016	1.017
R11	0.973	0.986	0.984	0.954	0.860	0.959	1.003	1.017	0.975

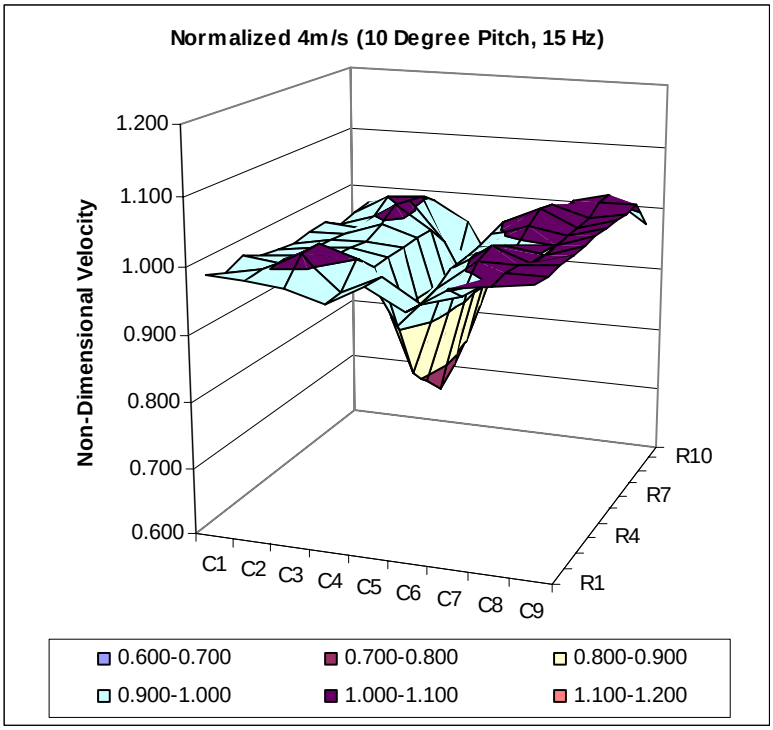

f) Non-Dimensional Velocity for 20° pitch and 15 Hz flapping frequency (Normalized 4m/s)

	C1	C2	C3	C4	C5	C6	C7	C8	C9
R1	0.945	1.008	1.004	0.942	1.003	0.965	1.009	1.031	1.027
R2	0.976	1.010	1.040	0.917	1.000	0.938	0.991	1.019	1.024
R3	0.998	1.002	1.010	0.980	0.871	0.978	1.010	1.028	1.023
R4	0.993	1.010	0.982	0.952	0.783	0.974	1.012	0.999	1.026
R5	0.991	1.000	0.987	0.976	0.763	0.981	1.014	1.002	1.028
R6	0.989	0.990	0.992	1.000	0.743	0.989	1.017	1.005	1.029
R7	0.988	0.990	0.993	0.978	0.778	0.984	1.019	1.010	1.029
R8	0.988	0.989	0.994	0.956	0.814	0.980	1.021	1.014	1.029
R9	0.972	1.005	1.045	0.892	0.828	0.949	1.001	1.024	1.029
R10	0.973	1.008	1.032	0.895	0.886	0.938	0.993	1.031	1.022
R11	0.985	1.000	0.993	0.936	0.888	0.957	0.956	1.026	1.027

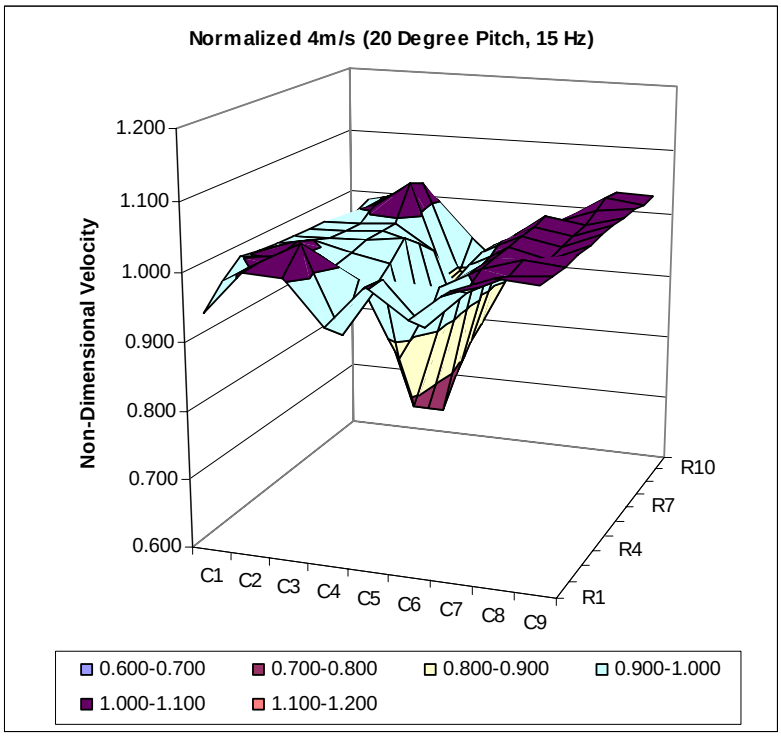

4. PEAK (NON-DIMENSIONAL) VELOCITY MAGNITUDE FOR C3 PLANE

Flapping Frequency	Pitch Angle	Free Stream Velocity		
		2 m/s	3 m/s	4 m/s
10 Hz	0°	1.114	1.013	0.987
	10°	1.167	1.049	1.010
	20°	1.187	1.062	1.007
15 Hz	0°	1.344	1.091	1.010
	10°	1.339	1.113	1.017
	20°	1.344	1.097	1.045

THIS PAGE INTENTIONALLY LEFT BLANK

APPENDIX C. TIME-DEPENDANT VELOCITY PROFILE MAPPING

TIME-DEPENDANT VELOCITY MAPPING ALONG PLANE C3 FOR VARYING FREE STREAM VELOCITY AND NEUTRAL ANGLE.

1. NORMALIZED 2M/S, 10 HZ FLAPPING FREQUENCY

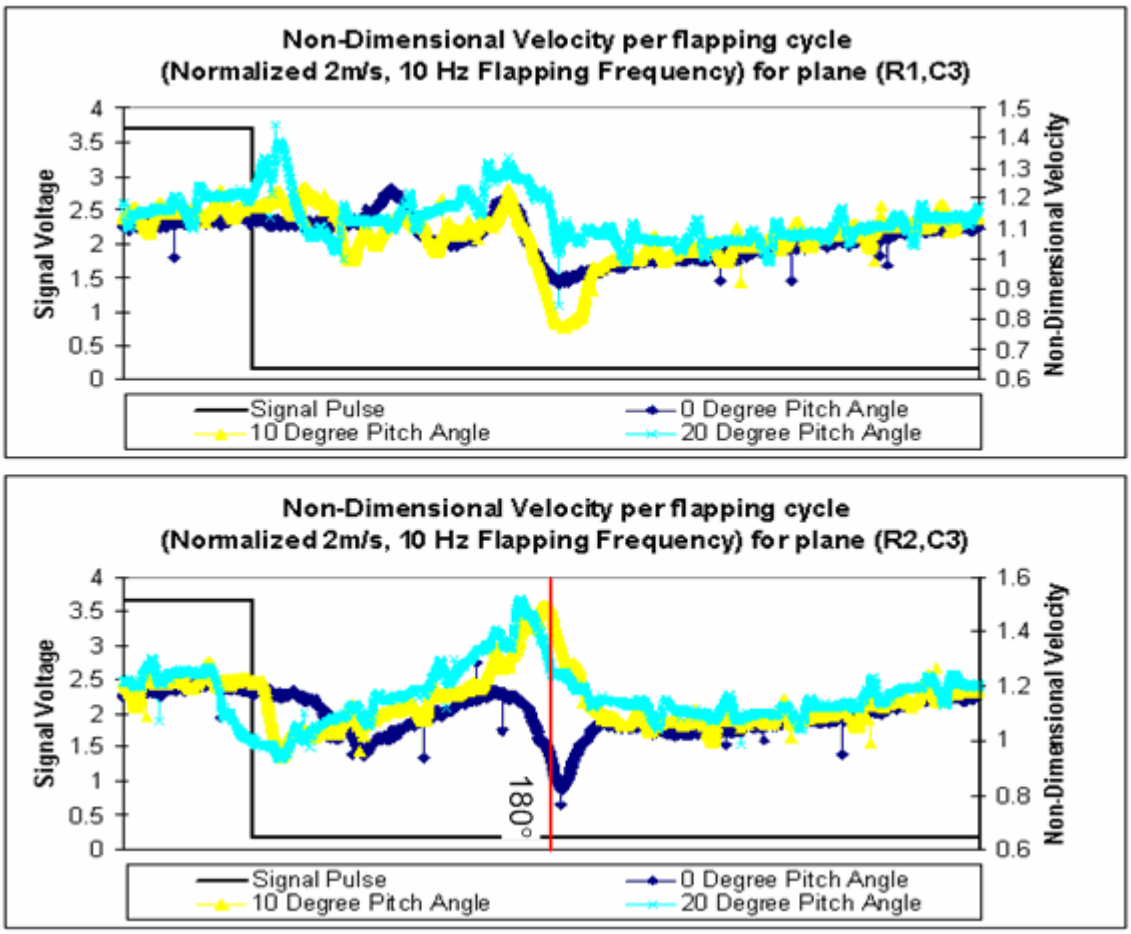

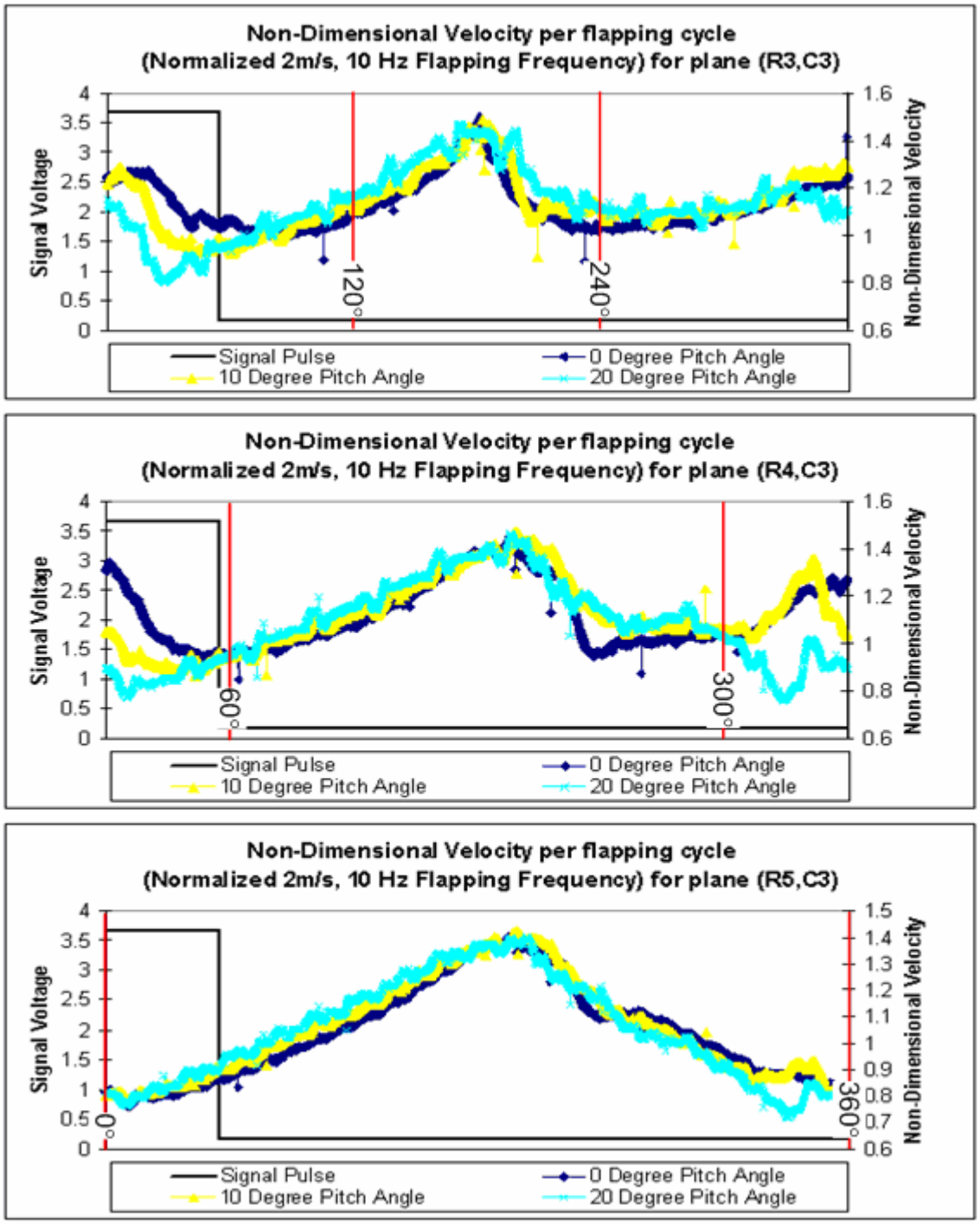
Non-Dimensional Velocity per flapping cycle
(Normalized 2m/s, 10 Hz Flapping Frequency) for plane (R3,C3)
Signal Voltage
Non-Dimensional Velocity
120°
240°
Signal Pulse
10 Degree Pitch Angle
0 Degree Pitch Angle
20 Degree Pitch Angle
Non-Dimensional Velocity per flapping cycle
(Normalized 2m/s, 10 Hz Flapping Frequency) for plane (R4,C3)
Signal Voltage
Non-Dimensional Velocity
60°
300°
Signal Pulse
10 Degree Pitch Angle
0 Degree Pitch Angle
20 Degree Pitch Angle
Non-Dimensional Velocity per flapping cycle
(Normalized 2m/s, 10 Hz Flapping Frequency) for plane (R5,C3)
Signal Voltage
Non-Dimensional Velocity
0°
360°
Signal Pulse
10 Degree Pitch Angle
0 Degree Pitch Angle
20 Degree Pitch Angle

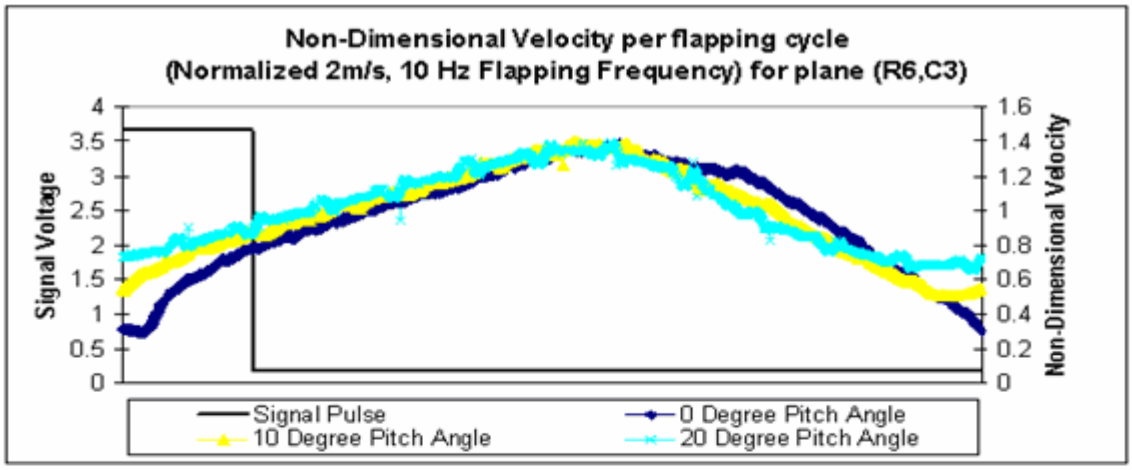
Non-Dimensional Velocity per flapping cycle
(Normalized 2m/s, 10 Hz Flapping Frequency) for plane (R6,C3)
Signal Voltage
Non-Dimensional Velocity
Signal Pulse
0 Degree Pitch Angle
10 Degree Pitch Angle
20 Degree Pitch Angle

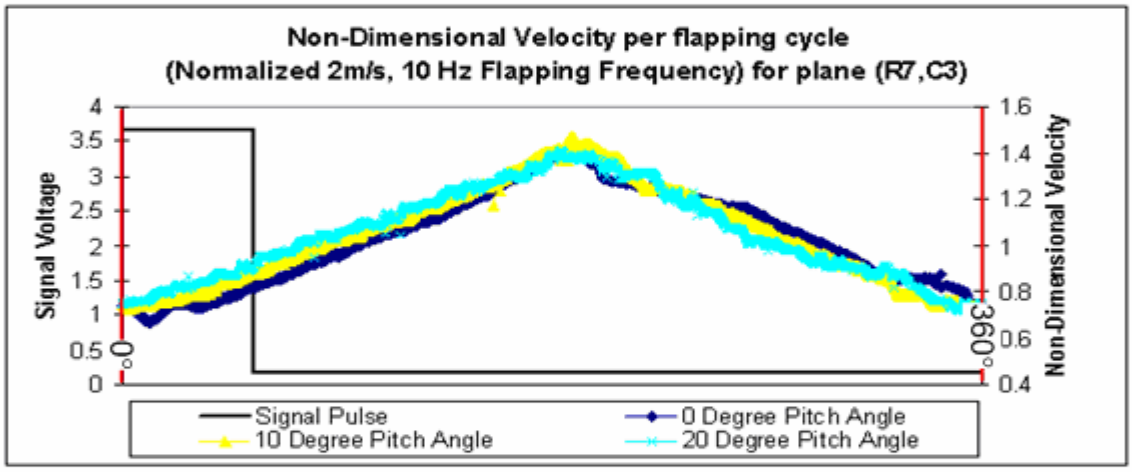
Non-Dimensional Velocity per flapping cycle
(Normalized 2m/s, 10 Hz Flapping Frequency) for plane (R7,C3)
Signal Voltage
Non-Dimensional Velocity
0°
360°
Signal Pulse
0 Degree Pitch Angle
10 Degree Pitch Angle
20 Degree Pitch Angle

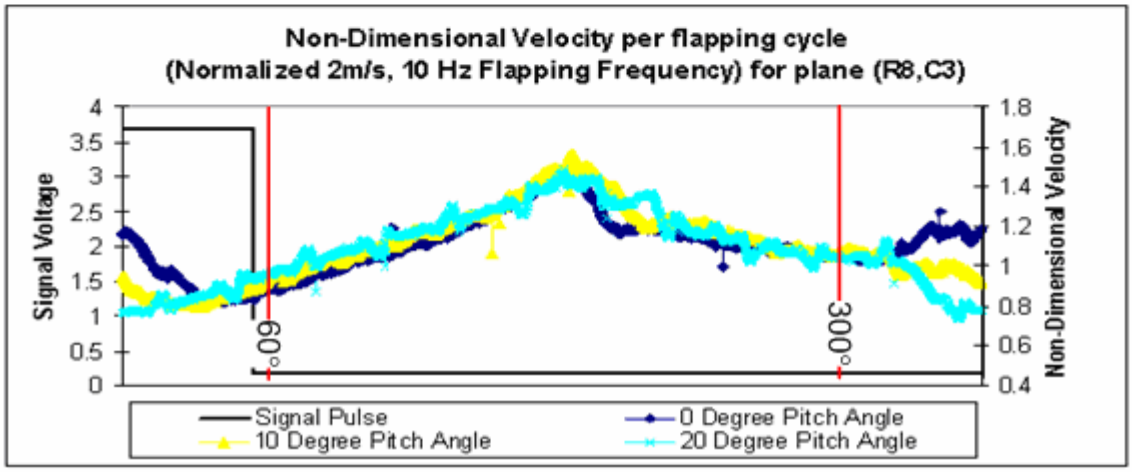
Non-Dimensional Velocity per flapping cycle
(Normalized 2m/s, 10 Hz Flapping Frequency) for plane (R8,C3)
Signal Voltage
Non-Dimensional Velocity
60°
300°
Signal Pulse
0 Degree Pitch Angle
10 Degree Pitch Angle
20 Degree Pitch Angle

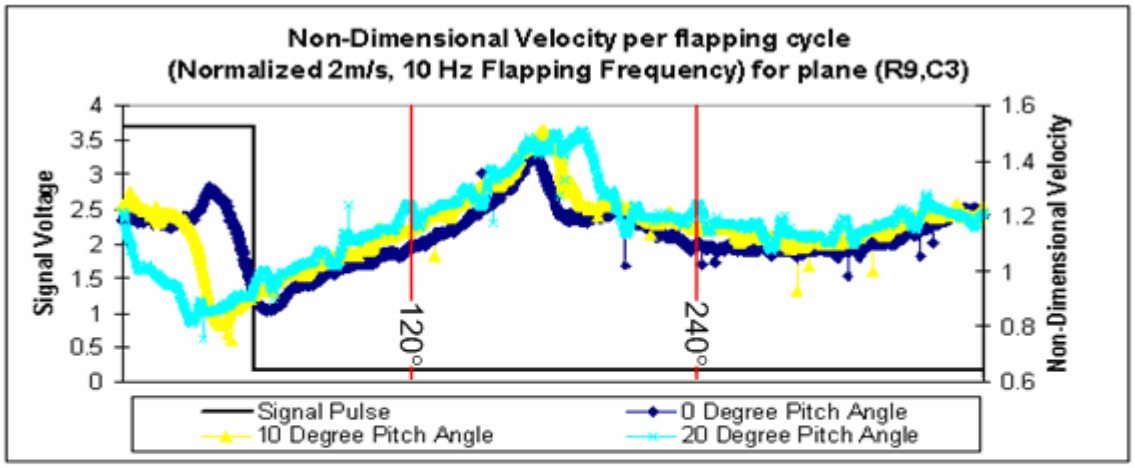
Non-Dimensional Velocity per flapping cycle
(Normalized 2m/s, 10 Hz Flapping Frequency) for plane (R9,C3)
Signal Voltage
Non-Dimensional Velocity
120°
240°
Signal Pulse
0 Degree Pitch Angle
10 Degree Pitch Angle
20 Degree Pitch Angle

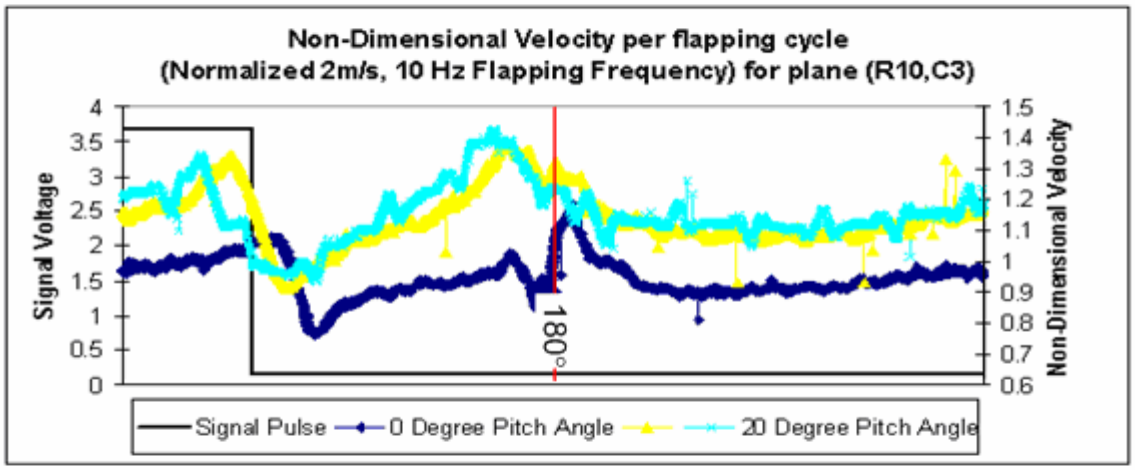
Non-Dimensional Velocity per flapping cycle
(Normalized 2m/s, 10 Hz Flapping Frequency) for plane (R10,C3)
Signal Voltage
Non-Dimensional Velocity
180°
Signal Pulse
0 Degree Pitch Angle
20 Degree Pitch Angle

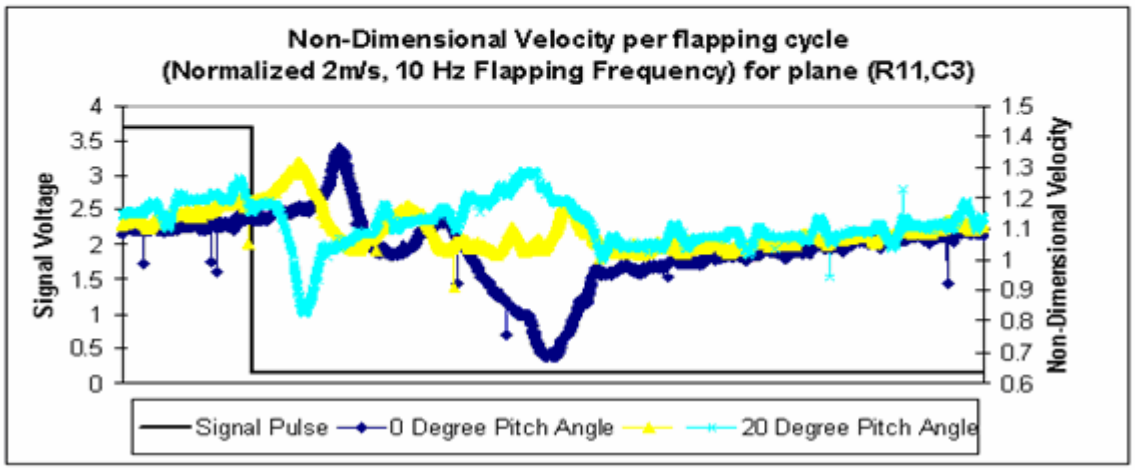
Non-Dimensional Velocity per flapping cycle
(Normalized 2m/s, 10 Hz Flapping Frequency) for plane (R11,C3)
Signal Voltage
Non-Dimensional Velocity
Signal Pulse
0 Degree Pitch Angle
20 Degree Pitch Angle

TIME-DEPENDANT VELOCITY MAPPING ALONG PLANE C3 FOR VARYING FREE STREAM VELOCITY AND NEUTRAL ANGLE.

2. NORMALIZED 2M/S, 15 HZ FLAPPING FREQUENCY

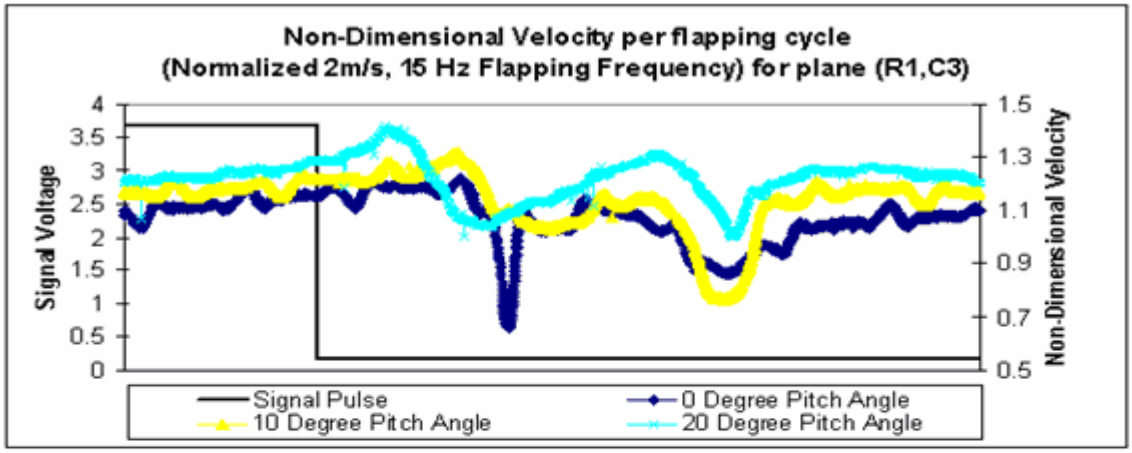

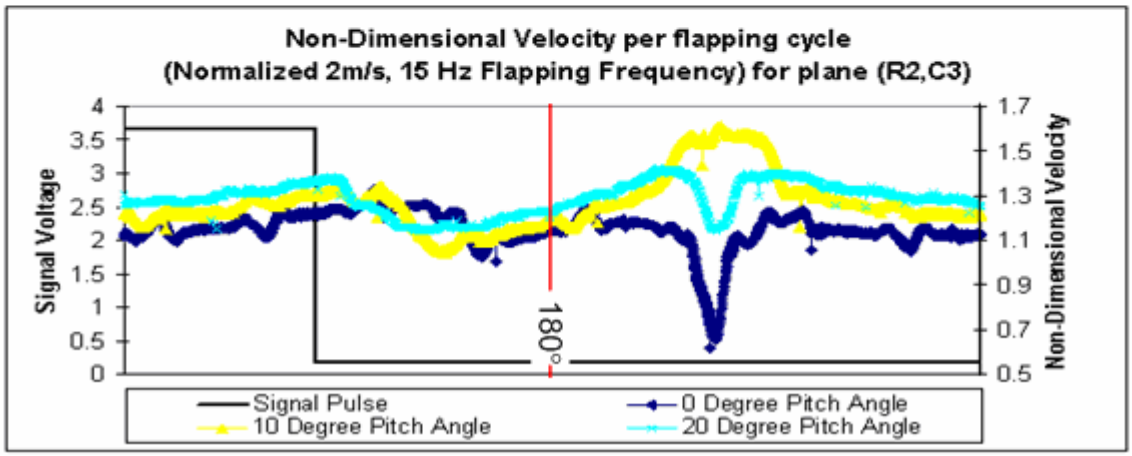

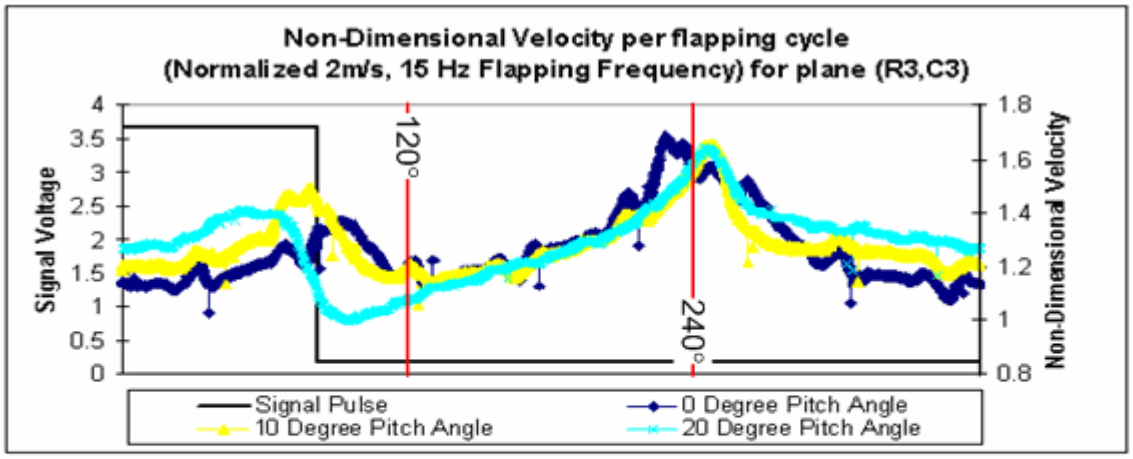
Non-Dimensional Velocity per flapping cycle
(Normalized 2m/s, 15 Hz Flapping Frequency) for plane (R3,C3)
Signal Voltage
Non-Dimensional Velocity
120°
240°
Signal Pulse
10 Degree Pitch Angle
0 Degree Pitch Angle
20 Degree Pitch Angle

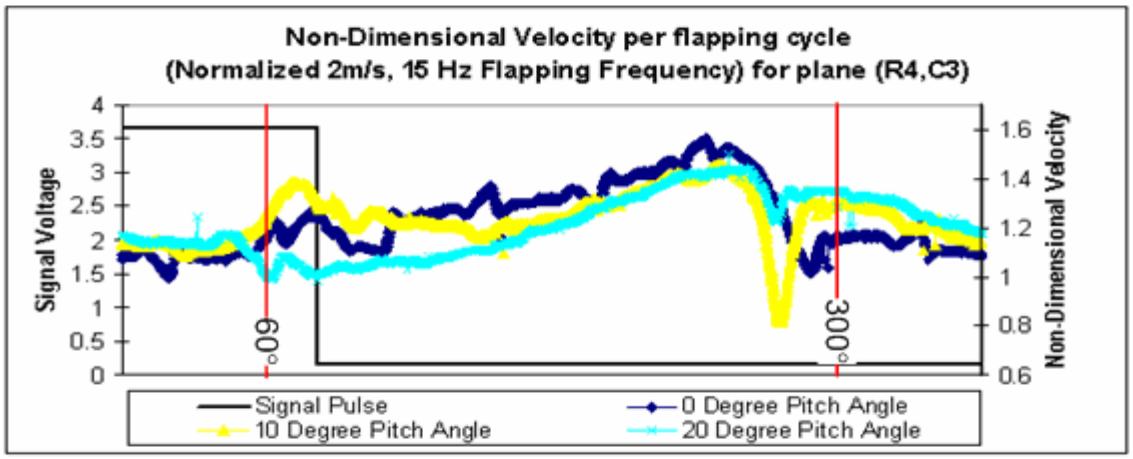
Non-Dimensional Velocity per flapping cycle
(Normalized 2m/s, 15 Hz Flapping Frequency) for plane (R4,C3)
Signal Voltage
Non-Dimensional Velocity
60°
300°
Signal Pulse
10 Degree Pitch Angle
0 Degree Pitch Angle
20 Degree Pitch Angle

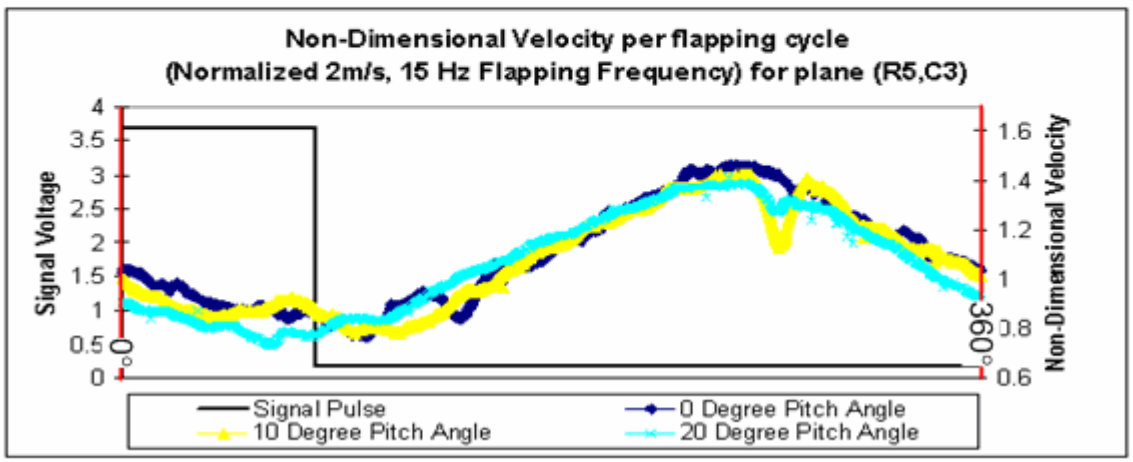
Non-Dimensional Velocity per flapping cycle
(Normalized 2m/s, 15 Hz Flapping Frequency) for plane (R5,C3)
Signal Voltage
Non-Dimensional Velocity
0°
360°
Signal Pulse
10 Degree Pitch Angle
0 Degree Pitch Angle
20 Degree Pitch Angle

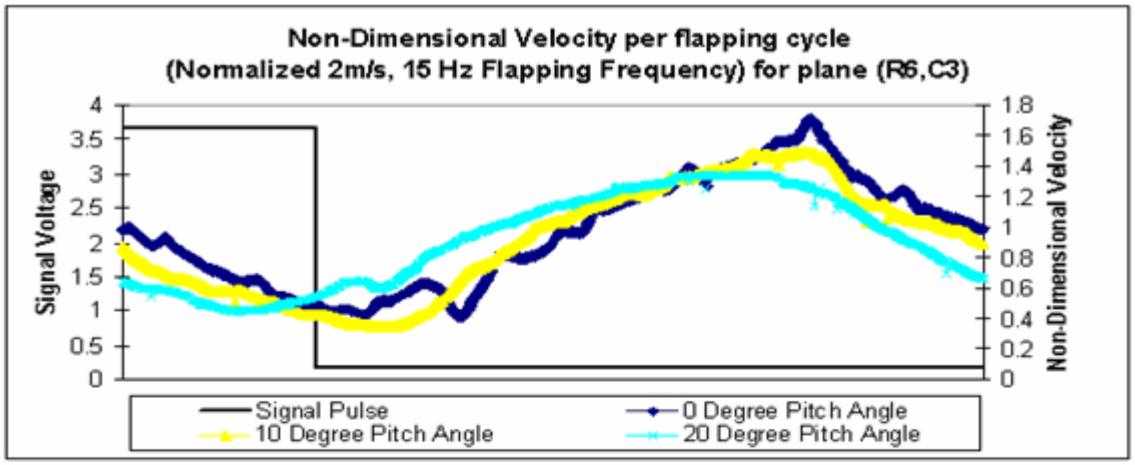
Non-Dimensional Velocity per flapping cycle
(Normalized 2m/s, 15 Hz Flapping Frequency) for plane (R6,C3)
Signal Voltage
Non-Dimensional Velocity
Signal Pulse
0 Degree Pitch Angle
10 Degree Pitch Angle
20 Degree Pitch Angle

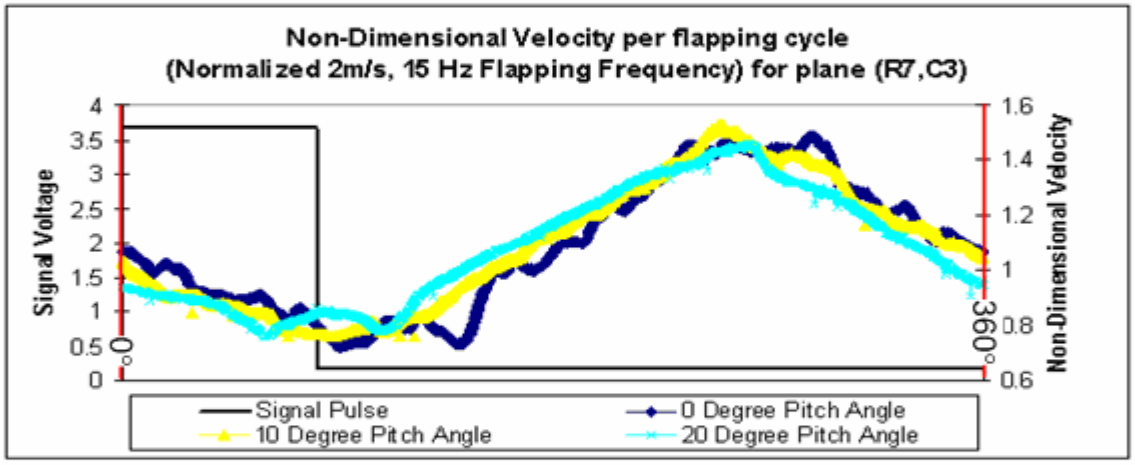
Non-Dimensional Velocity per flapping cycle
(Normalized 2m/s, 15 Hz Flapping Frequency) for plane (R7,C3)
Signal Voltage
Non-Dimensional Velocity
0°
360°
Signal Pulse
0 Degree Pitch Angle
10 Degree Pitch Angle
20 Degree Pitch Angle

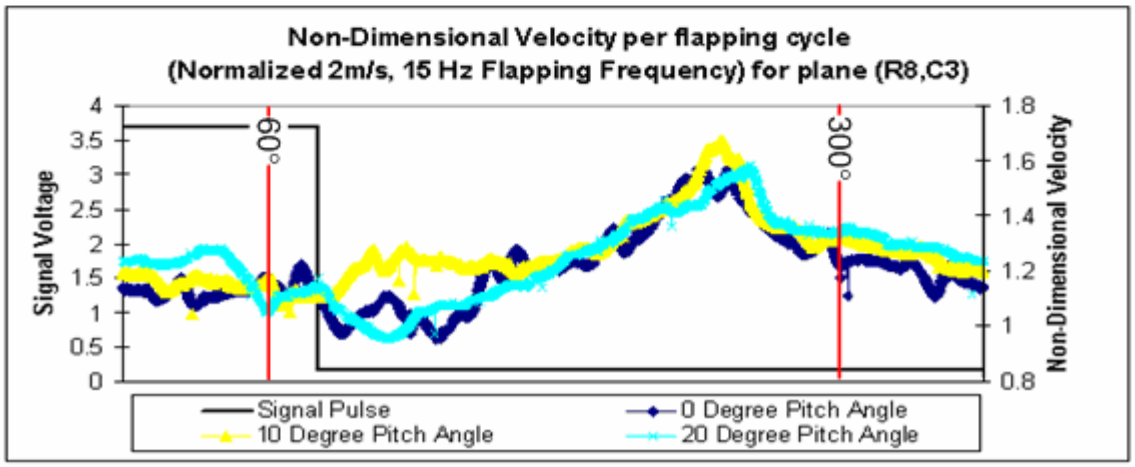
Non-Dimensional Velocity per flapping cycle
(Normalized 2m/s, 15 Hz Flapping Frequency) for plane (R8,C3)
Signal Voltage
Non-Dimensional Velocity
60°
300°
Signal Pulse
0 Degree Pitch Angle
10 Degree Pitch Angle
20 Degree Pitch Angle

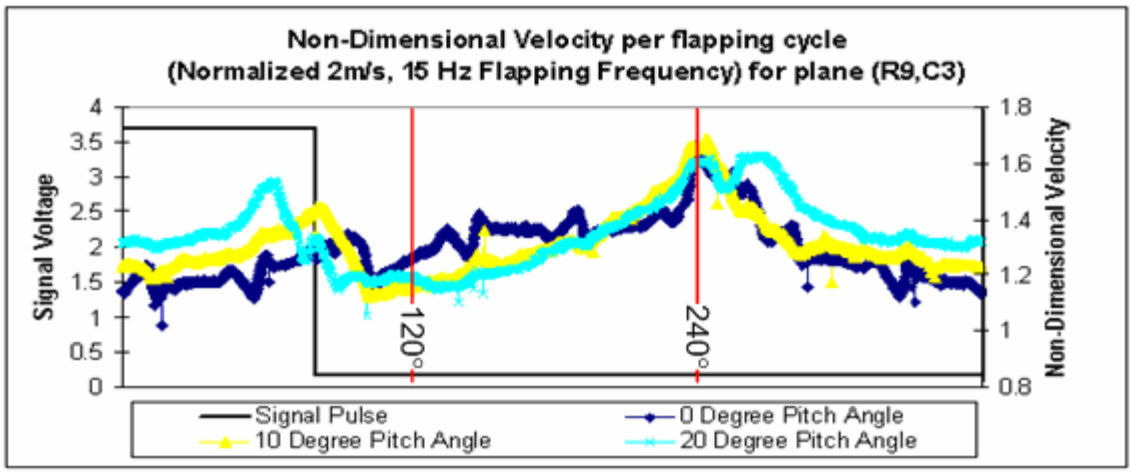
Non-Dimensional Velocity per flapping cycle
(Normalized 2m/s, 15 Hz Flapping Frequency) for plane (R9,C3)
Signal Voltage
Non-Dimensional Velocity
120°
240°
Signal Pulse
10 Degree Pitch Angle
0 Degree Pitch Angle
20 Degree Pitch Angle

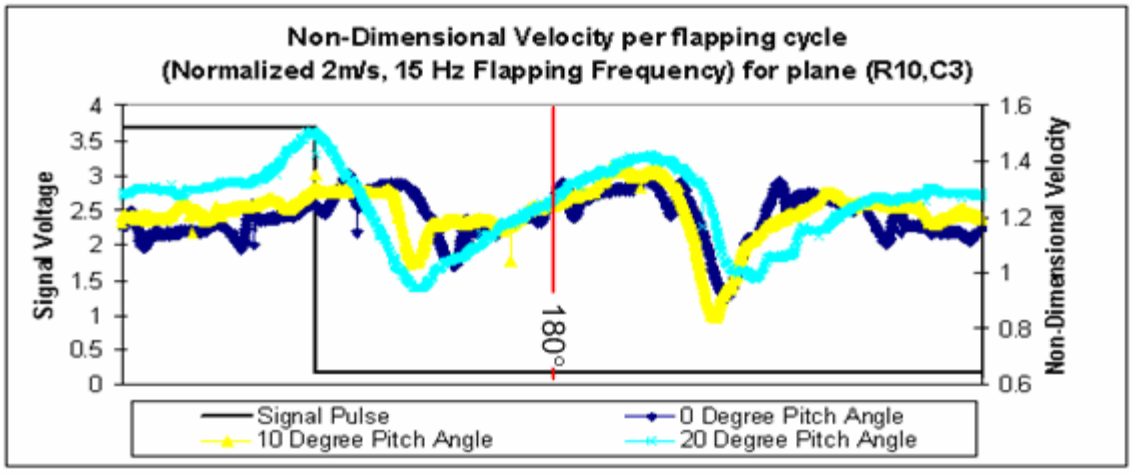
Non-Dimensional Velocity per flapping cycle
(Normalized 2m/s, 15 Hz Flapping Frequency) for plane (R10,C3)
Signal Voltage
Non-Dimensional Velocity
180°
Signal Pulse
10 Degree Pitch Angle
0 Degree Pitch Angle
20 Degree Pitch Angle

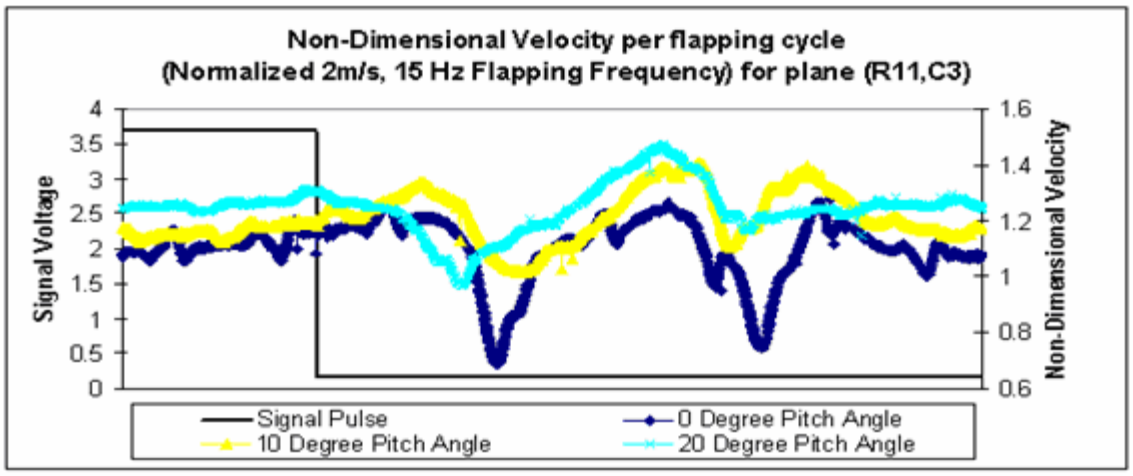
Non-Dimensional Velocity per flapping cycle
(Normalized 2m/s, 15 Hz Flapping Frequency) for plane (R11,C3)
Signal Voltage
Non-Dimensional Velocity
Signal Pulse
10 Degree Pitch Angle
0 Degree Pitch Angle
20 Degree Pitch Angle

TIME-DEPENDANT VELOCITY MAPPING ALONG PLANE C3 FOR VARYING FREE STREAM VELOCITY AND NEUTRAL ANGLE.

3. NORMALIZED 3M/S, 10 HZ FLAPPING FREQUENCY

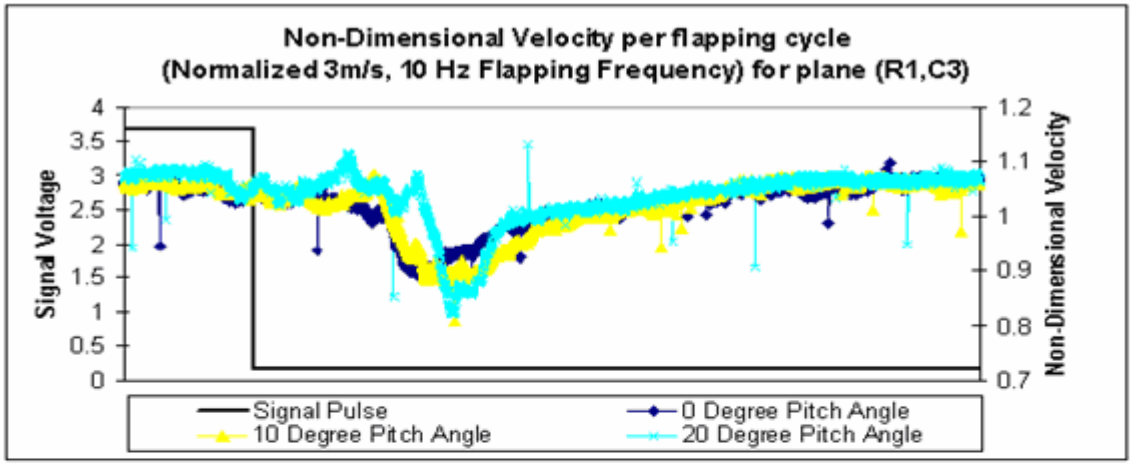

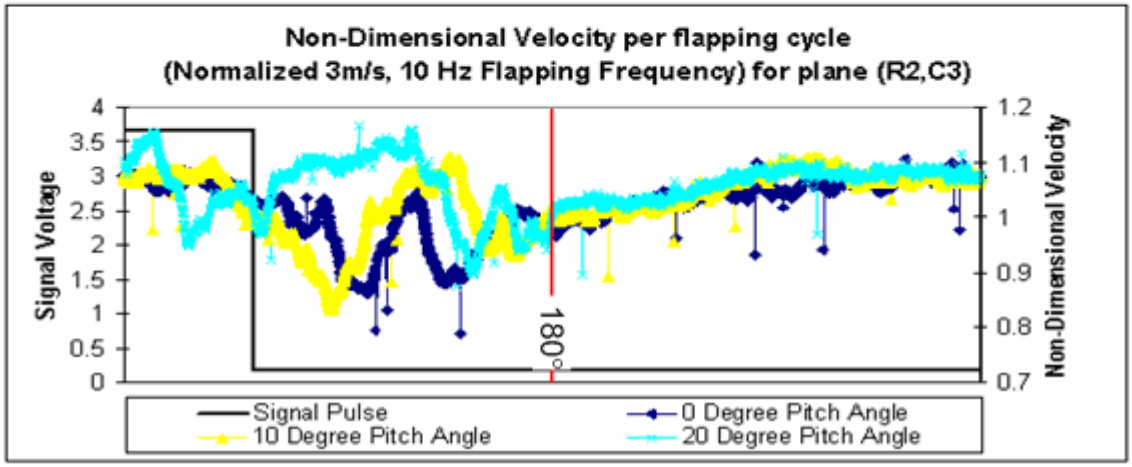

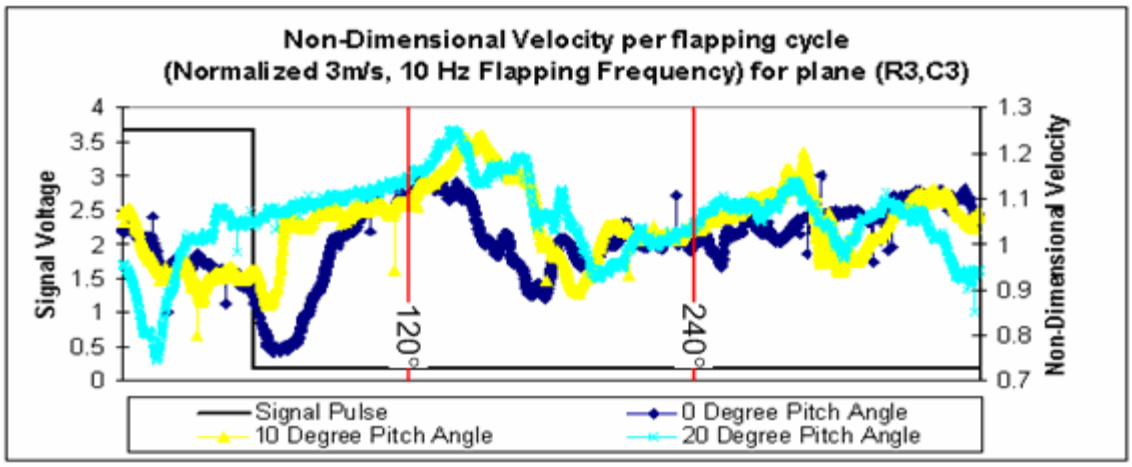
Non-Dimensional Velocity per flapping cycle
(Normalized 3m/s, 10 Hz Flapping Frequency) for plane (R3,C3)
Signal Voltage
Non-Dimensional Velocity
120°
240°
Signal Pulse
10 Degree Pitch Angle
0 Degree Pitch Angle
20 Degree Pitch Angle

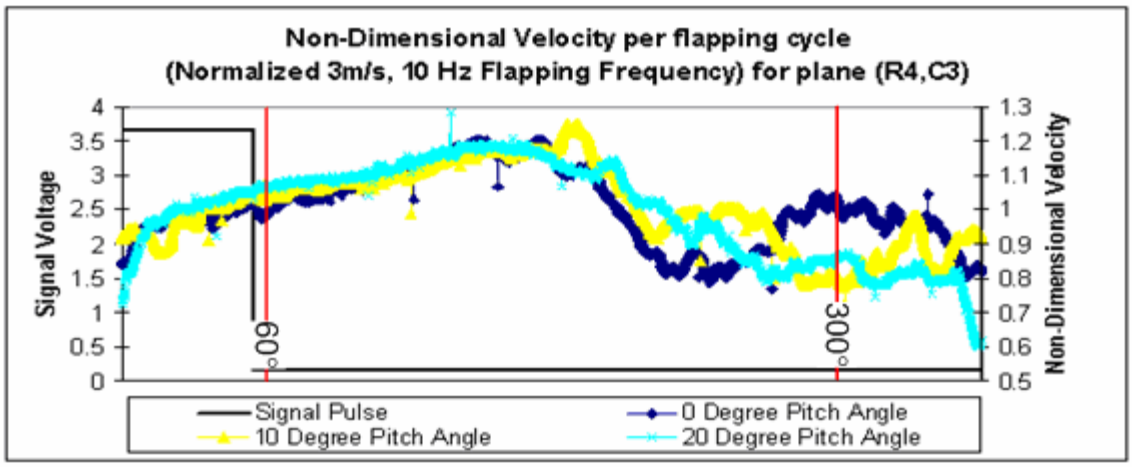
Non-Dimensional Velocity per flapping cycle
(Normalized 3m/s, 10 Hz Flapping Frequency) for plane (R4,C3)
Signal Voltage
Non-Dimensional Velocity
60°
300°
Signal Pulse
10 Degree Pitch Angle
0 Degree Pitch Angle
20 Degree Pitch Angle

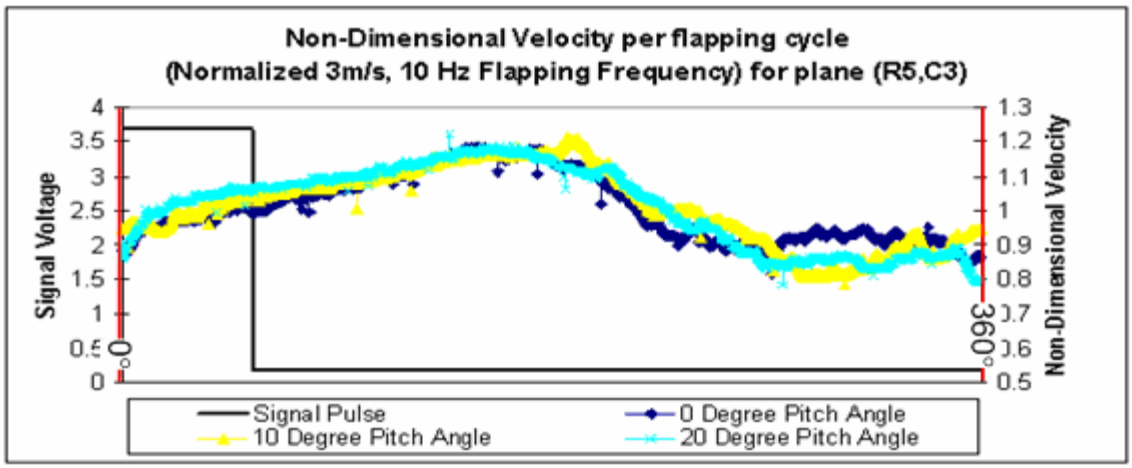
Non-Dimensional Velocity per flapping cycle
(Normalized 3m/s, 10 Hz Flapping Frequency) for plane (R5,C3)
Signal Voltage
Non-Dimensional Velocity
0°
360°
Signal Pulse
10 Degree Pitch Angle
0 Degree Pitch Angle
20 Degree Pitch Angle

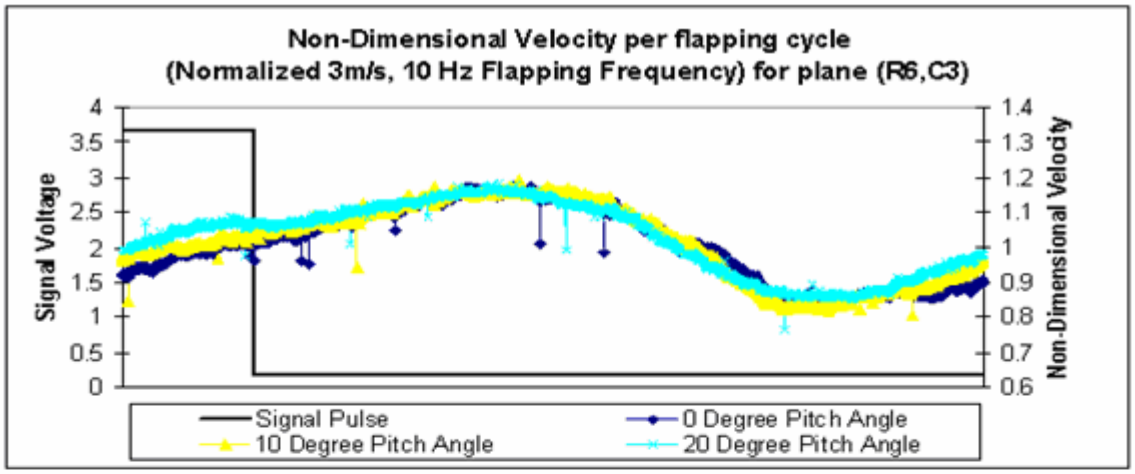
Non-Dimensional Velocity per flapping cycle
(Normalized 3m/s, 10 Hz Flapping Frequency) for plane (R6,C3)
Signal Voltage
Non-Dimensional Velocity
Signal Pulse
0 Degree Pitch Angle
10 Degree Pitch Angle
20 Degree Pitch Angle

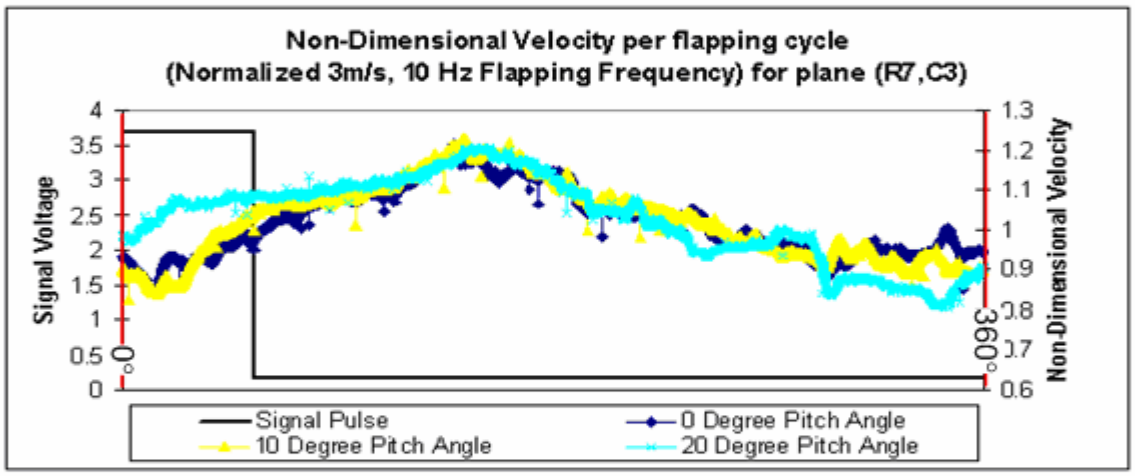
Non-Dimensional Velocity per flapping cycle
(Normalized 3m/s, 10 Hz Flapping Frequency) for plane (R7,C3)
Signal Voltage
Non-Dimensional Velocity
0°
360°
Signal Pulse
0 Degree Pitch Angle
10 Degree Pitch Angle
20 Degree Pitch Angle

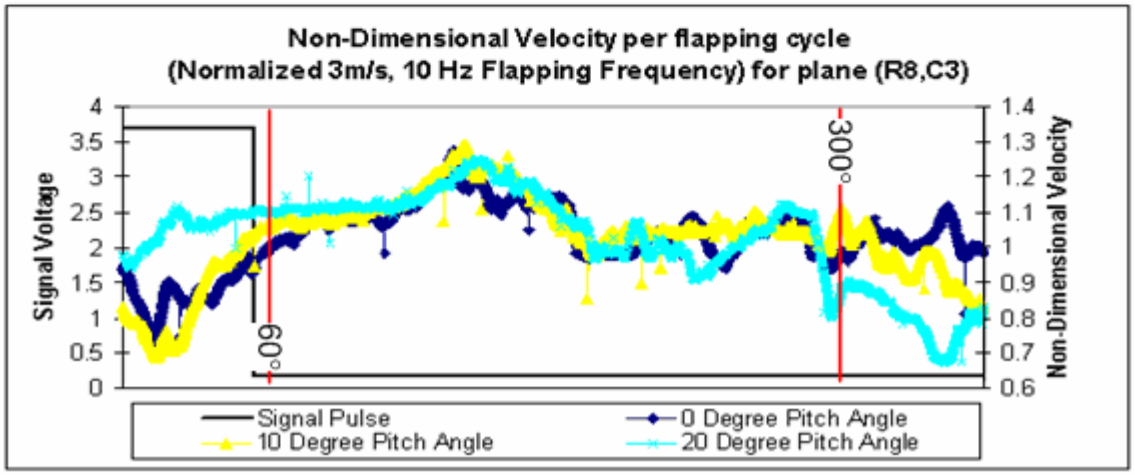
Non-Dimensional Velocity per flapping cycle
(Normalized 3m/s, 10 Hz Flapping Frequency) for plane (R8,C3)
Signal Voltage
Non-Dimensional Velocity
60°
300°
Signal Pulse
0 Degree Pitch Angle
10 Degree Pitch Angle
20 Degree Pitch Angle

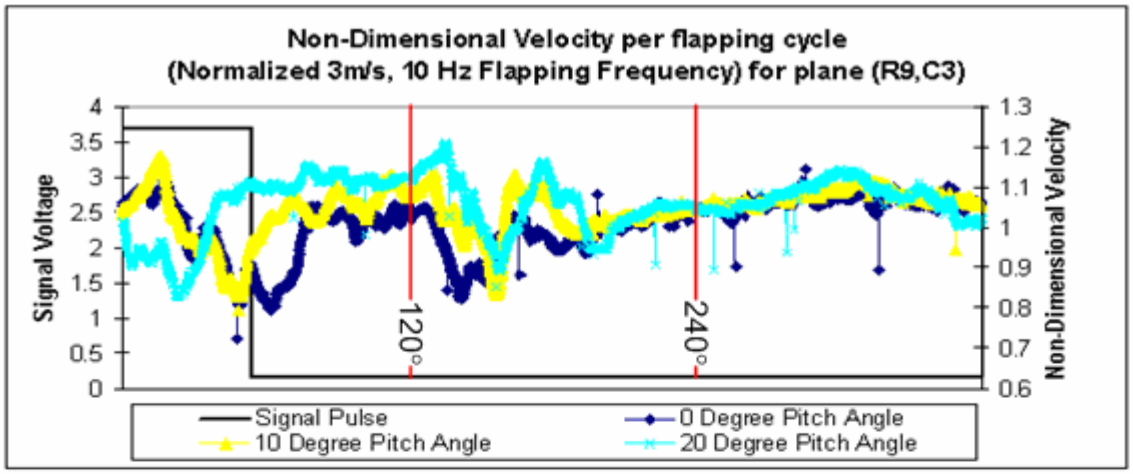
Non-Dimensional Velocity per flapping cycle
(Normalized 3m/s, 10 Hz Flapping Frequency) for plane (R9,C3)
Signal Voltage
Non-Dimensional Velocity
120°
240°
Signal Pulse
0 Degree Pitch Angle
10 Degree Pitch Angle
20 Degree Pitch Angle

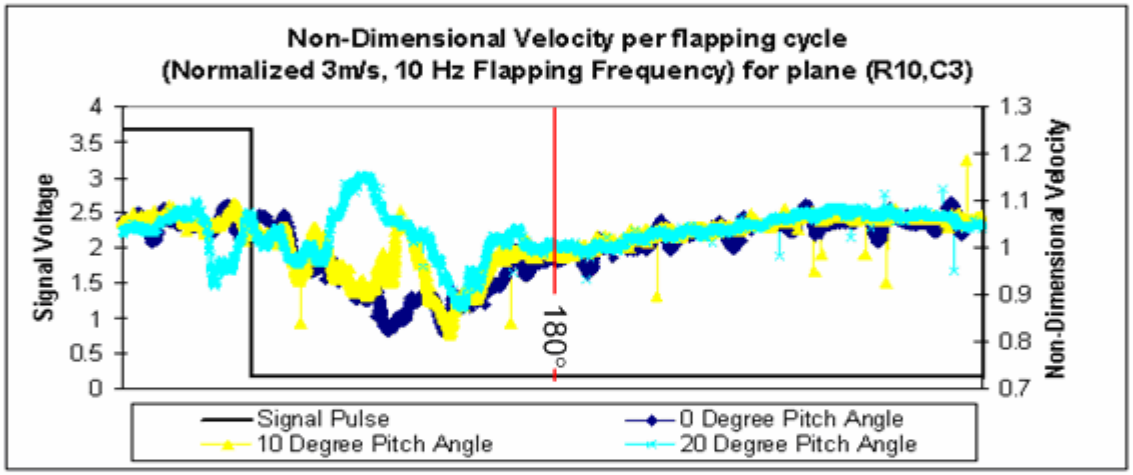
Non-Dimensional Velocity per flapping cycle
(Normalized 3m/s, 10 Hz Flapping Frequency) for plane (R10,C3)
Signal Voltage
Non-Dimensional Velocity
180°
Signal Pulse
0 Degree Pitch Angle
10 Degree Pitch Angle
20 Degree Pitch Angle

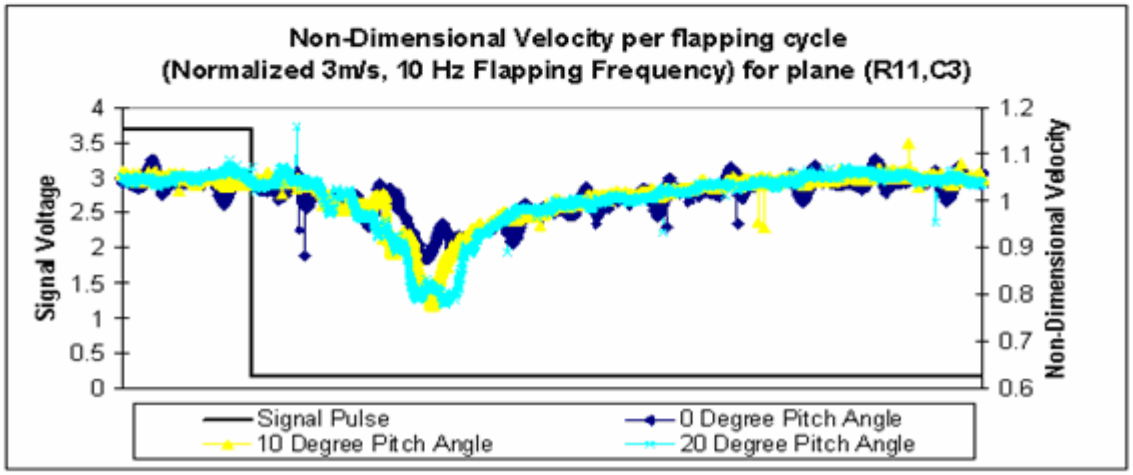
Non-Dimensional Velocity per flapping cycle
(Normalized 3m/s, 10 Hz Flapping Frequency) for plane (R11,C3)
Signal Voltage
Non-Dimensional Velocity
Signal Pulse
0 Degree Pitch Angle
10 Degree Pitch Angle
20 Degree Pitch Angle

TIME-DEPENDANT VELOCITY MAPPING ALONG PLANE C3 FOR VARYING FREE STREAM VELOCITY AND NEUTRAL ANGLE.

4. NORMALIZED 3M/S, 15 HZ FLAPPING FREQUENCY

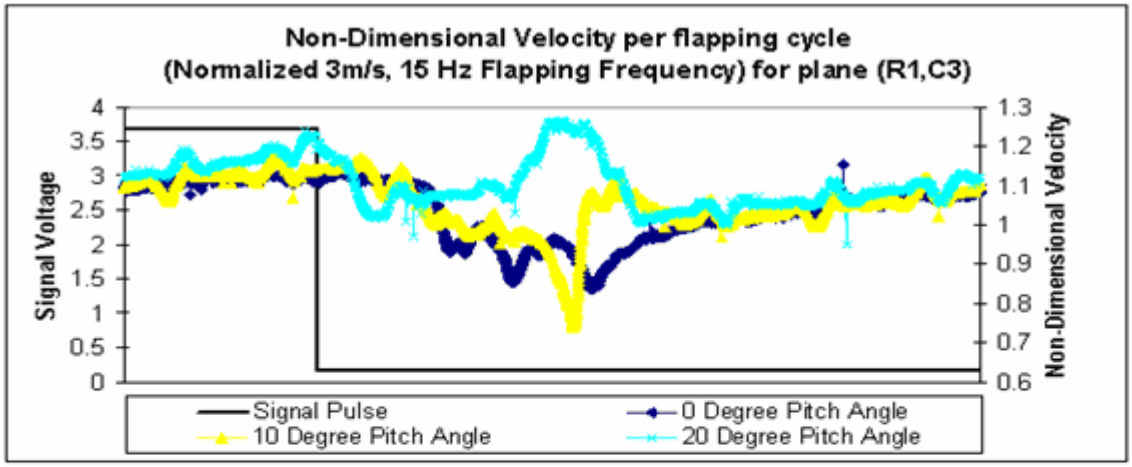

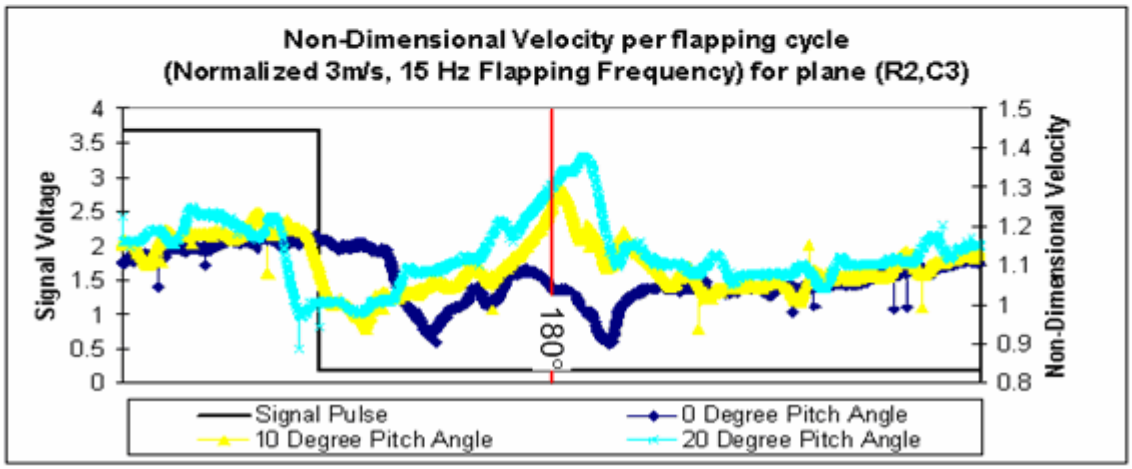

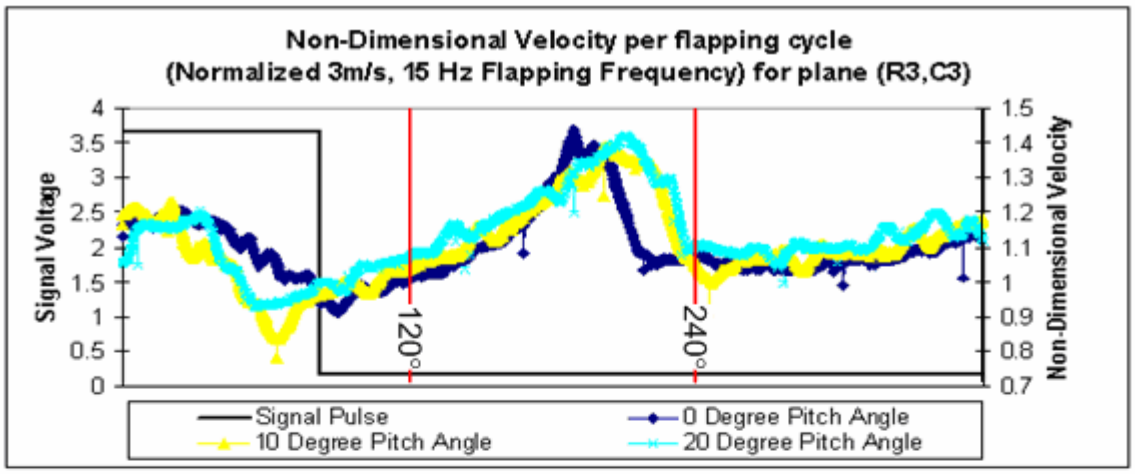
Non-Dimensional Velocity per flapping cycle
(Normalized 3m/s, 15 Hz Flapping Frequency) for plane (R3,C3)
Signal Voltage
Non-Dimensional Velocity
120°
240°
Signal Pulse
10 Degree Pitch Angle
0 Degree Pitch Angle
20 Degree Pitch Angle

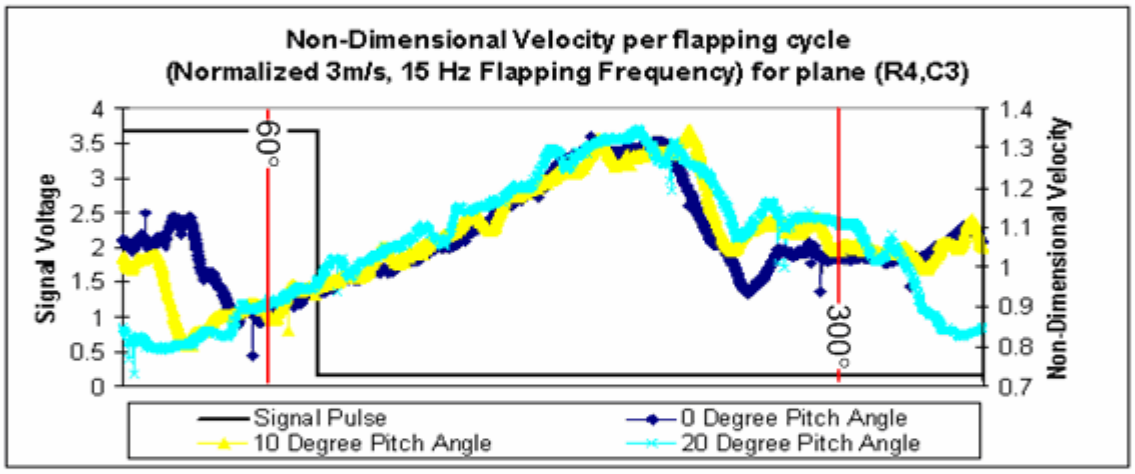
Non-Dimensional Velocity per flapping cycle
(Normalized 3m/s, 15 Hz Flapping Frequency) for plane (R4,C3)
Signal Voltage
Non-Dimensional Velocity
60°
300°
Signal Pulse
10 Degree Pitch Angle
0 Degree Pitch Angle
20 Degree Pitch Angle

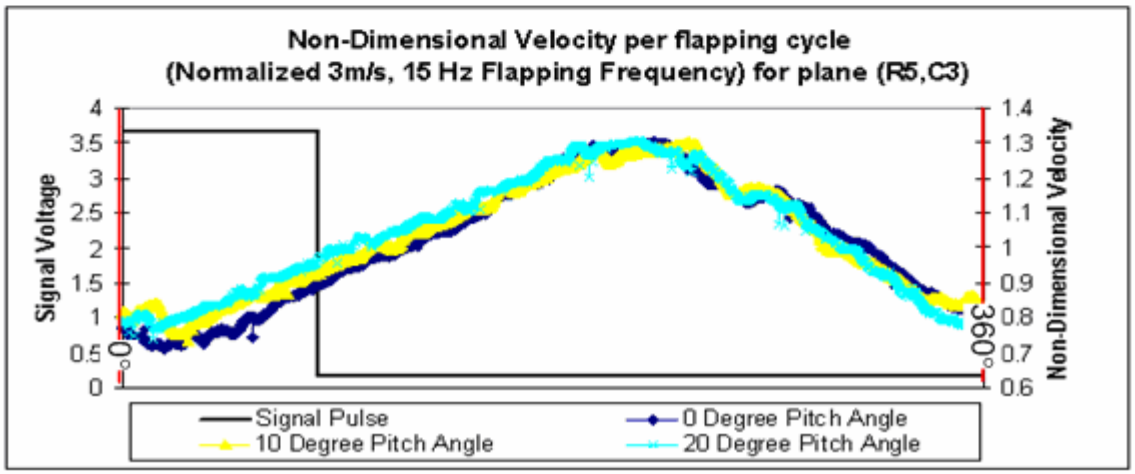
Non-Dimensional Velocity per flapping cycle
(Normalized 3m/s, 15 Hz Flapping Frequency) for plane (R5,C3)
Signal Voltage
Non-Dimensional Velocity
0°
360°
Signal Pulse
10 Degree Pitch Angle
0 Degree Pitch Angle
20 Degree Pitch Angle

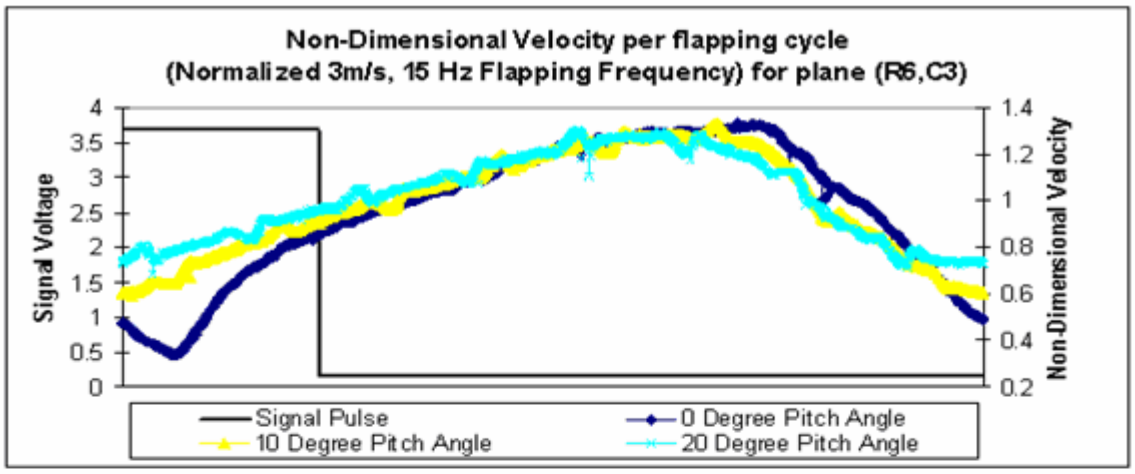
Non-Dimensional Velocity per flapping cycle
(Normalized 3m/s, 15 Hz Flapping Frequency) for plane (R6,C3)
Signal Voltage
Non-Dimensional Velocity
Signal Pulse
0 Degree Pitch Angle
10 Degree Pitch Angle
20 Degree Pitch Angle

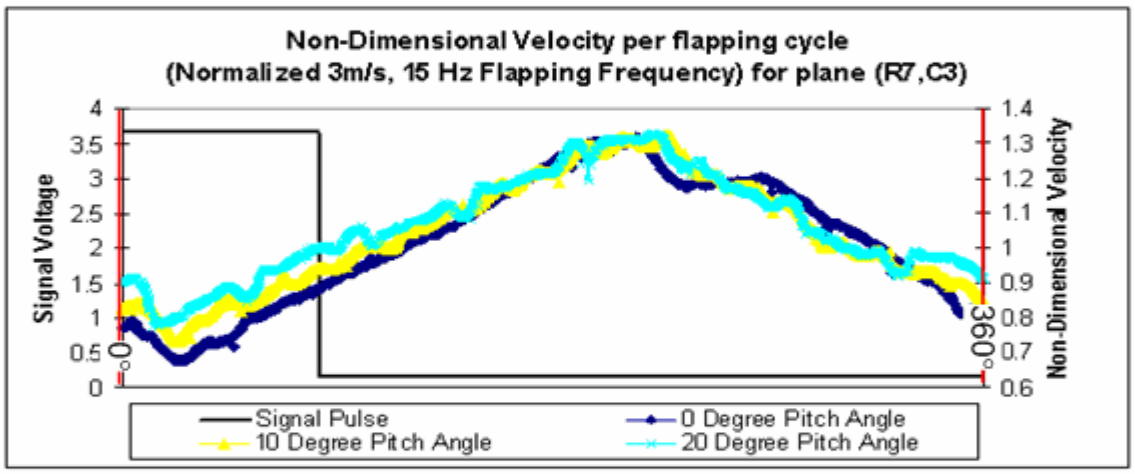
Non-Dimensional Velocity per flapping cycle
(Normalized 3m/s, 15 Hz Flapping Frequency) for plane (R7,C3)
Signal Voltage
Non-Dimensional Velocity
0°
360°
Signal Pulse
0 Degree Pitch Angle
10 Degree Pitch Angle
20 Degree Pitch Angle

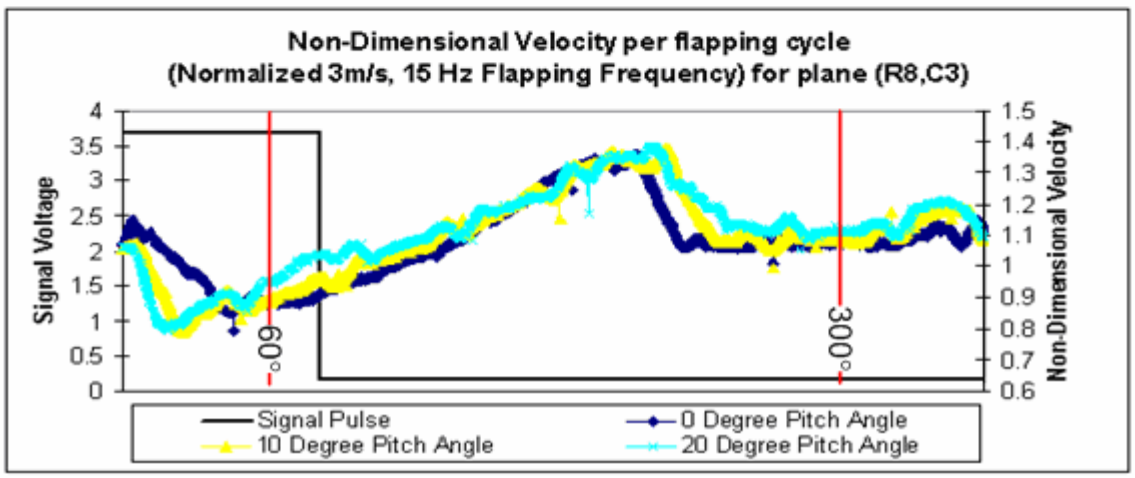
Non-Dimensional Velocity per flapping cycle
(Normalized 3m/s, 15 Hz Flapping Frequency) for plane (R8,C3)
Signal Voltage
Non-Dimensional Velocity
60°
300°
Signal Pulse
0 Degree Pitch Angle
10 Degree Pitch Angle
20 Degree Pitch Angle

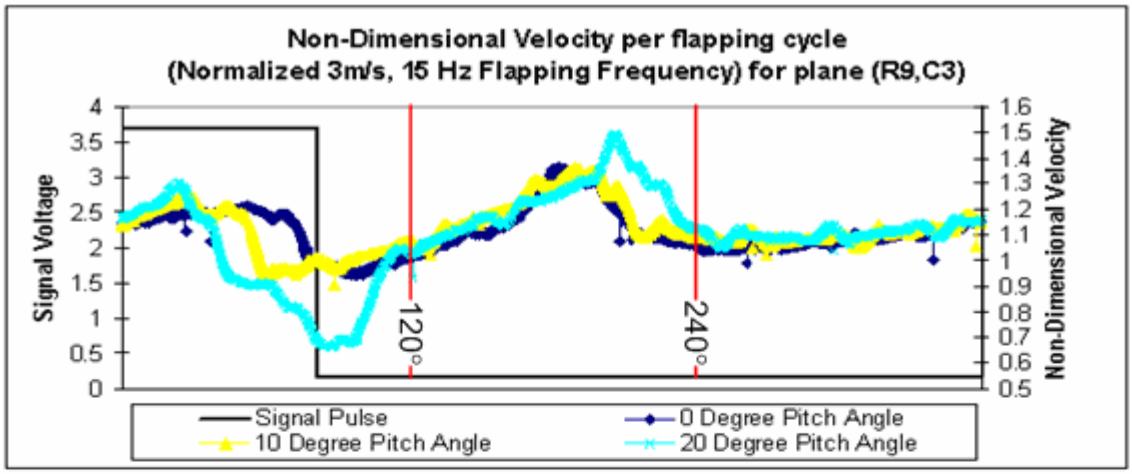
Non-Dimensional Velocity per flapping cycle
(Normalized 3m/s, 15 Hz Flapping Frequency) for plane (R9,C3)
Signal Voltage
Non-Dimensional Velocity
120°
240°
Signal Pulse
0 Degree Pitch Angle
10 Degree Pitch Angle
20 Degree Pitch Angle

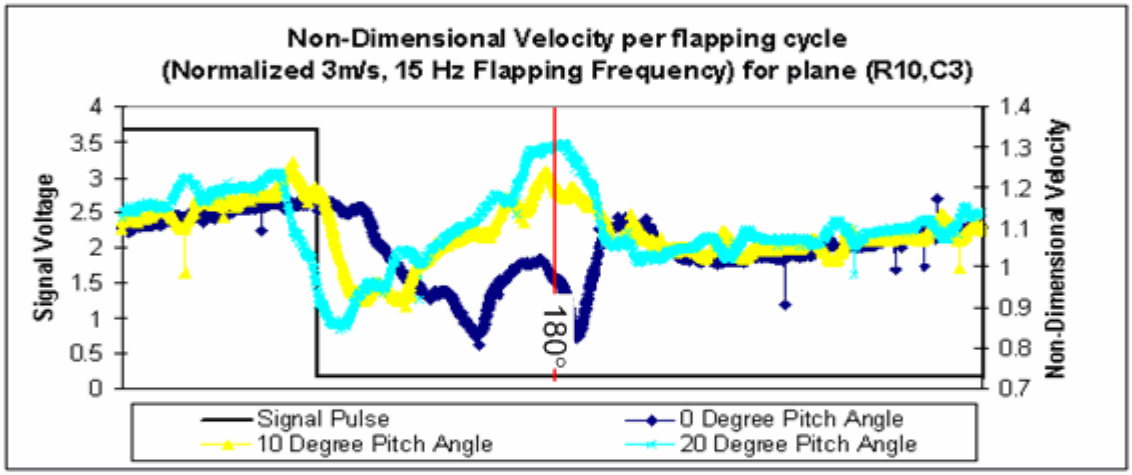
Non-Dimensional Velocity per flapping cycle
(Normalized 3m/s, 15 Hz Flapping Frequency) for plane (R10,C3)
Signal Voltage
Non-Dimensional Velocity
180°
Signal Pulse
0 Degree Pitch Angle
10 Degree Pitch Angle
20 Degree Pitch Angle

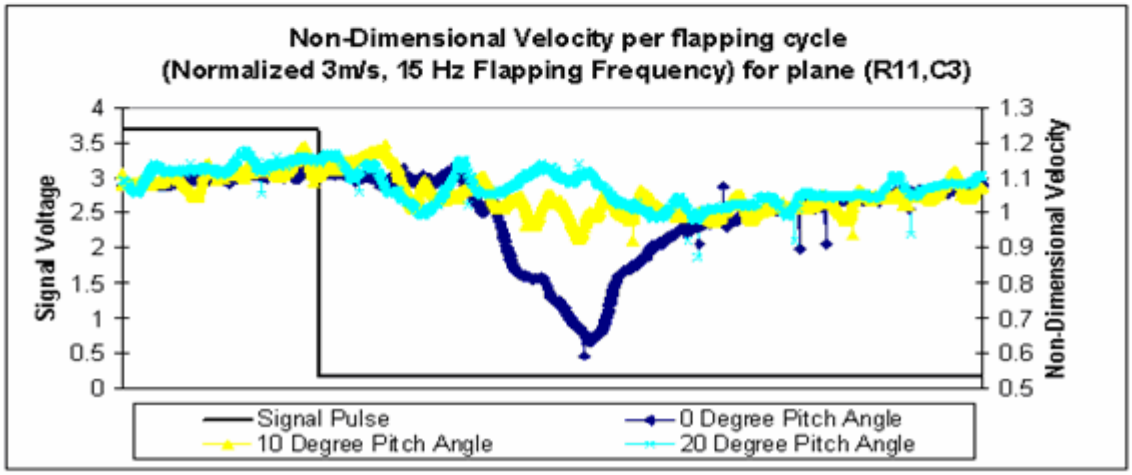
Non-Dimensional Velocity per flapping cycle
(Normalized 3m/s, 15 Hz Flapping Frequency) for plane (R11,C3)
Signal Voltage
Non-Dimensional Velocity
Signal Pulse
0 Degree Pitch Angle
10 Degree Pitch Angle
20 Degree Pitch Angle

TIME-DEPENDANT VELOCITY MAPPING ALONG PLANE C3 FOR VARYING FREE STREAM VELOCITY AND NEUTRAL ANGLE.

5. NORMALIZED 4M/S, 10 HZ FLAPPING FREQUENCY

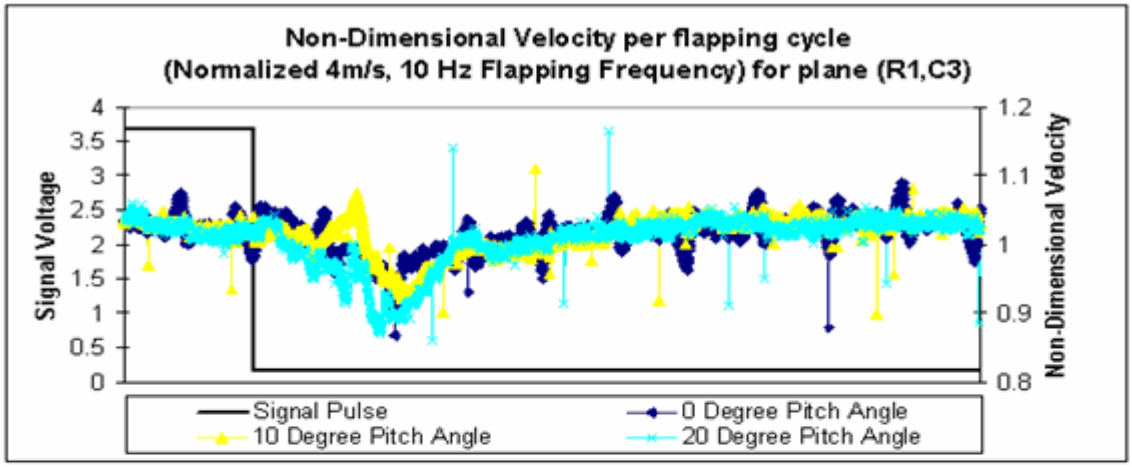

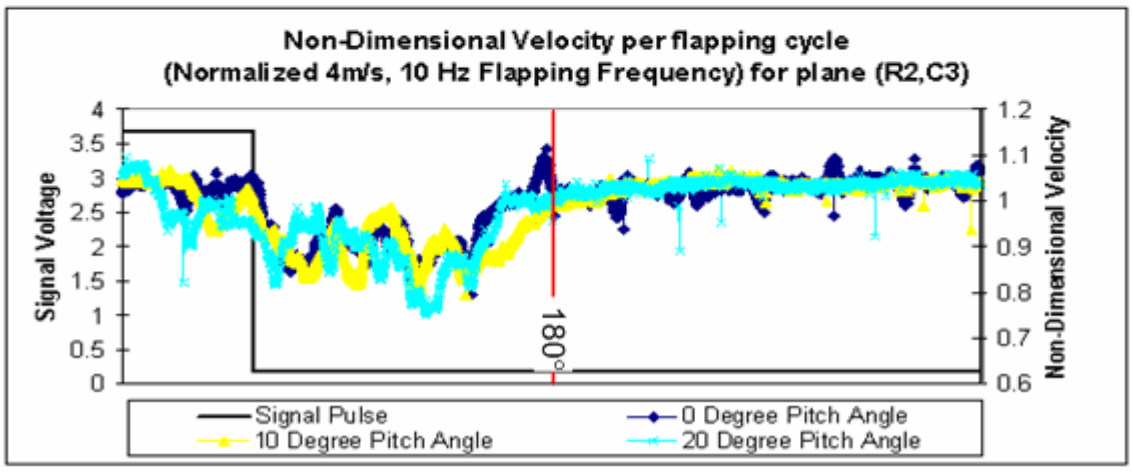

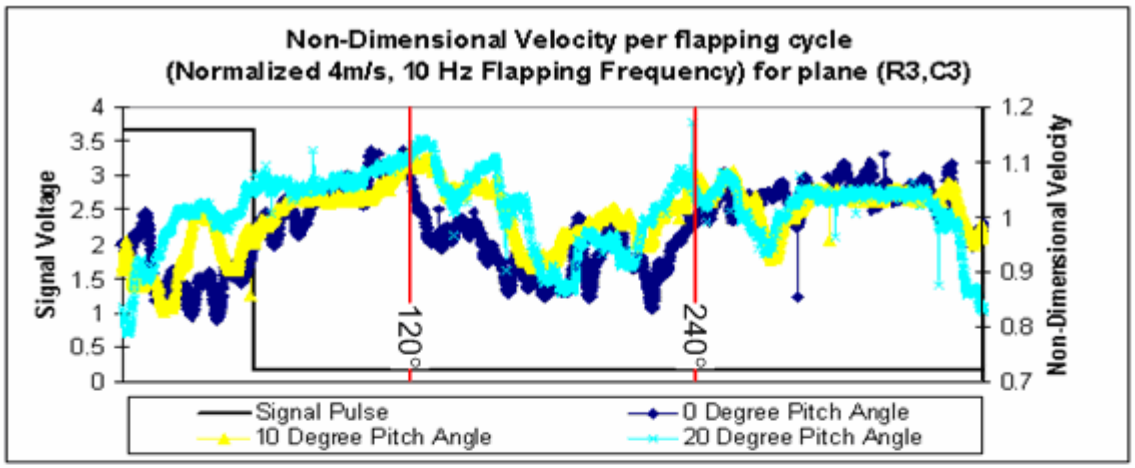
Non-Dimensional Velocity per flapping cycle
(Normalized 4m/s, 10 Hz Flapping Frequency) for plane (R3,C3)
Signal Voltage
Non-Dimensional Velocity
120°
240°
Signal Pulse
0 Degree Pitch Angle
10 Degree Pitch Angle
20 Degree Pitch Angle

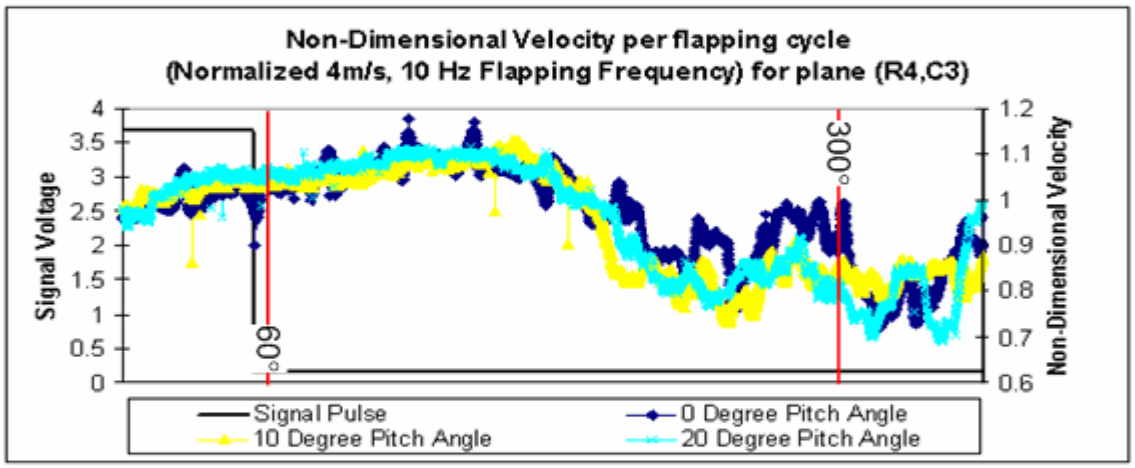
Non-Dimensional Velocity per flapping cycle
(Normalized 4m/s, 10 Hz Flapping Frequency) for plane (R4,C3)
Signal Voltage
Non-Dimensional Velocity
60°
300°
Signal Pulse
0 Degree Pitch Angle
10 Degree Pitch Angle
20 Degree Pitch Angle

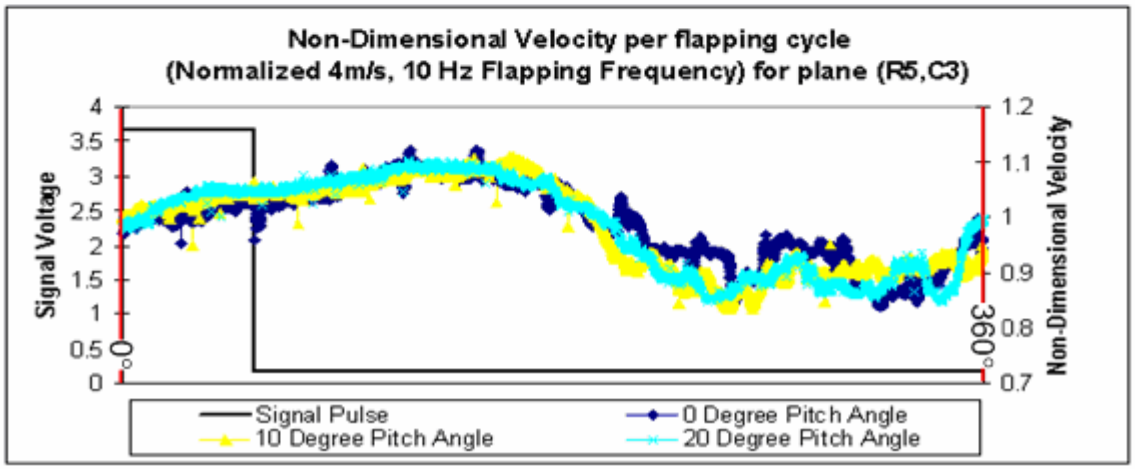
Non-Dimensional Velocity per flapping cycle
(Normalized 4m/s, 10 Hz Flapping Frequency) for plane (R5,C3)
Signal Voltage
Non-Dimensional Velocity
0°
360°
Signal Pulse
0 Degree Pitch Angle
10 Degree Pitch Angle
20 Degree Pitch Angle

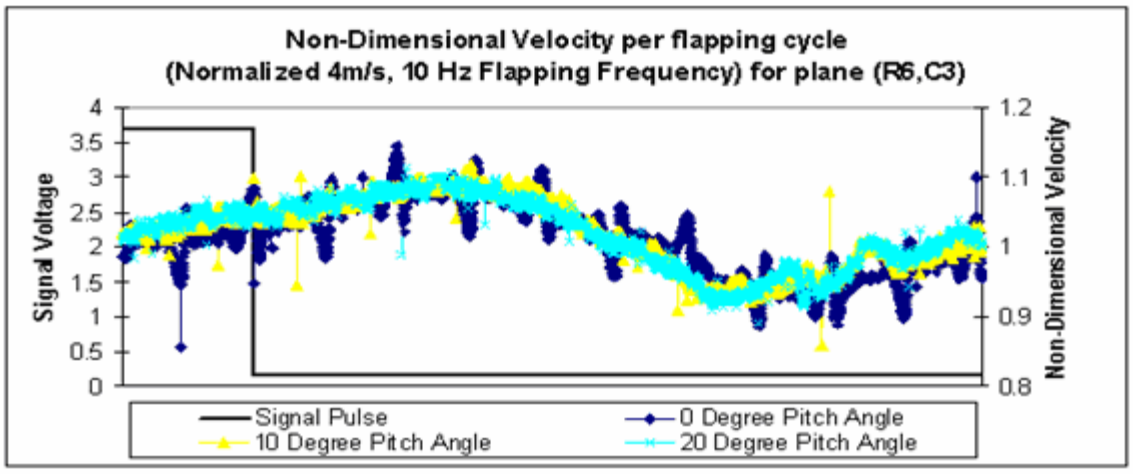
Non-Dimensional Velocity per flapping cycle
(Normalized 4m/s, 10 Hz Flapping Frequency) for plane (R6,C3)
Signal Voltage
Non-Dimensional Velocity
Signal Pulse
0 Degree Pitch Angle
10 Degree Pitch Angle
20 Degree Pitch Angle

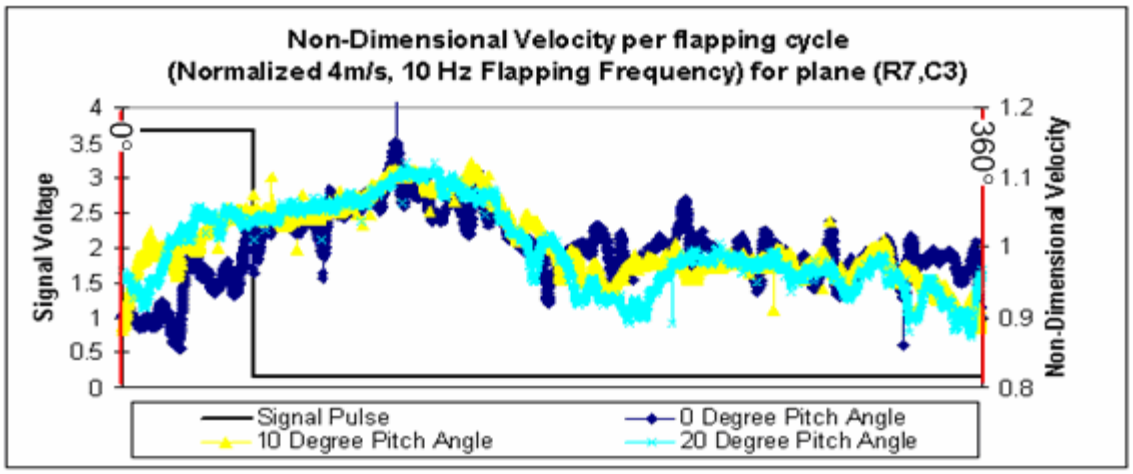
Non-Dimensional Velocity per flapping cycle
(Normalized 4m/s, 10 Hz Flapping Frequency) for plane (R7,C3)
0°
360°
Signal Voltage
Non-Dimensional Velocity
Signal Pulse
0 Degree Pitch Angle
10 Degree Pitch Angle
20 Degree Pitch Angle

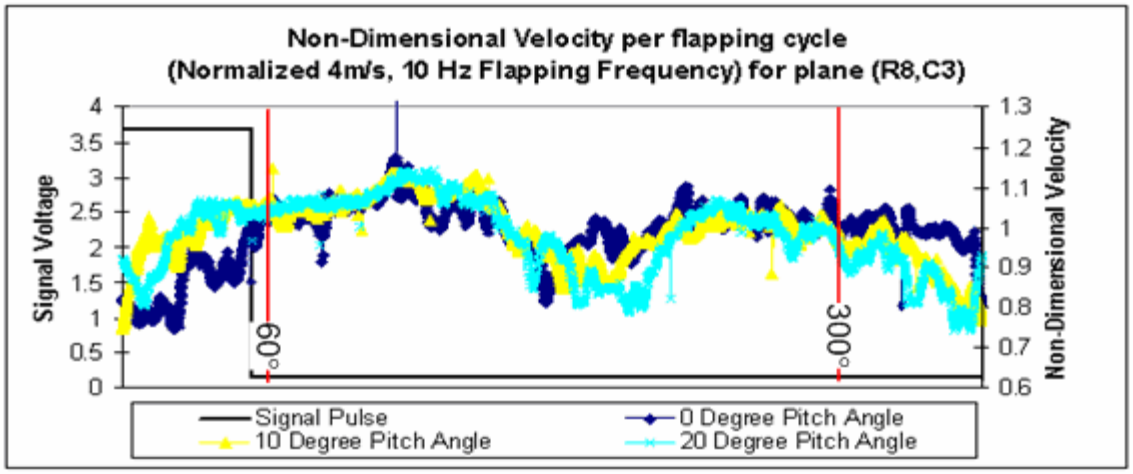
Non-Dimensional Velocity per flapping cycle
(Normalized 4m/s, 10 Hz Flapping Frequency) for plane (R8,C3)
60°
300°
Signal Voltage
Non-Dimensional Velocity
Signal Pulse
0 Degree Pitch Angle
10 Degree Pitch Angle
20 Degree Pitch Angle

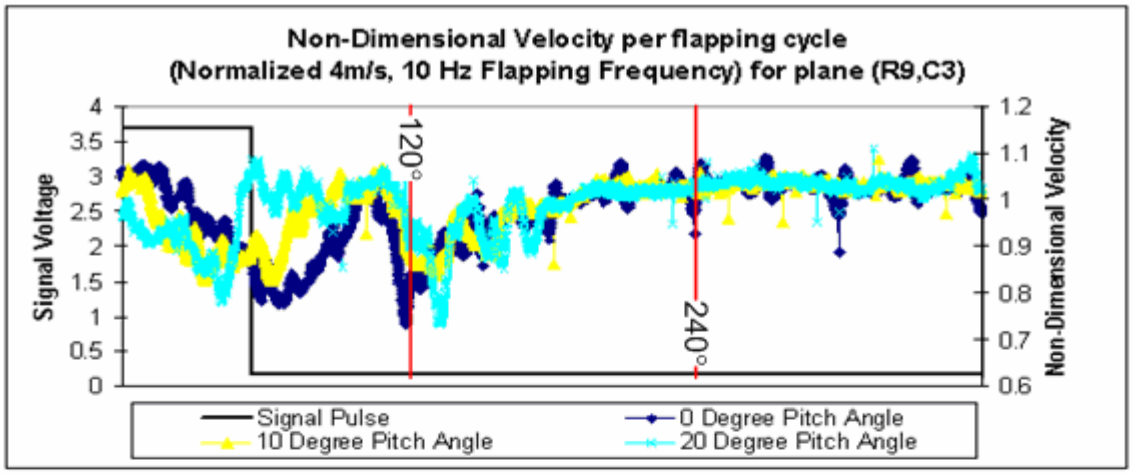
Non-Dimensional Velocity per flapping cycle
(Normalized 4m/s, 10 Hz Flapping Frequency) for plane (R9,C3)
Signal Voltage
Non-Dimensional Velocity
120°
240°
Signal Pulse
10 Degree Pitch Angle
0 Degree Pitch Angle
20 Degree Pitch Angle

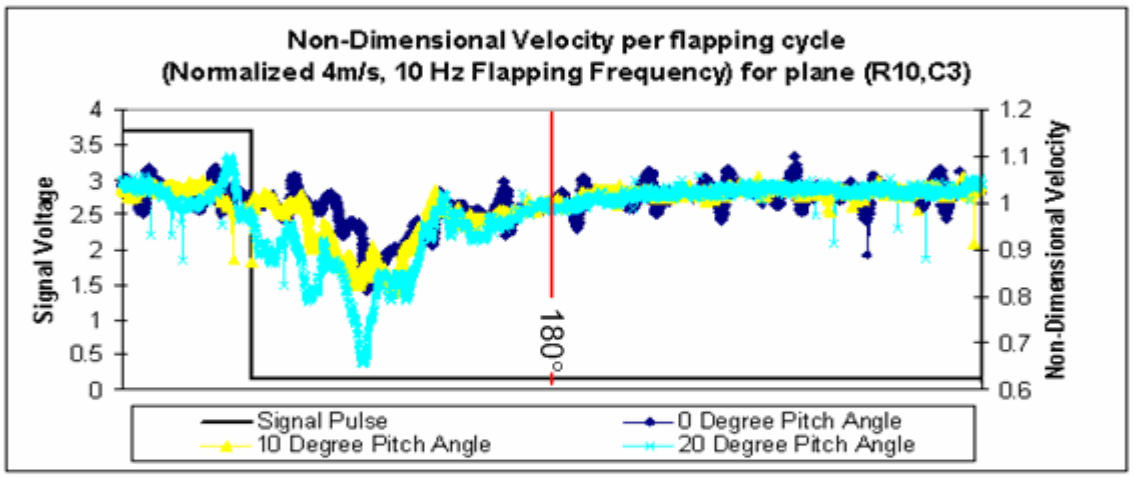
Non-Dimensional Velocity per flapping cycle
(Normalized 4m/s, 10 Hz Flapping Frequency) for plane (R10,C3)
Signal Voltage
Non-Dimensional Velocity
180°
Signal Pulse
10 Degree Pitch Angle
0 Degree Pitch Angle
20 Degree Pitch Angle

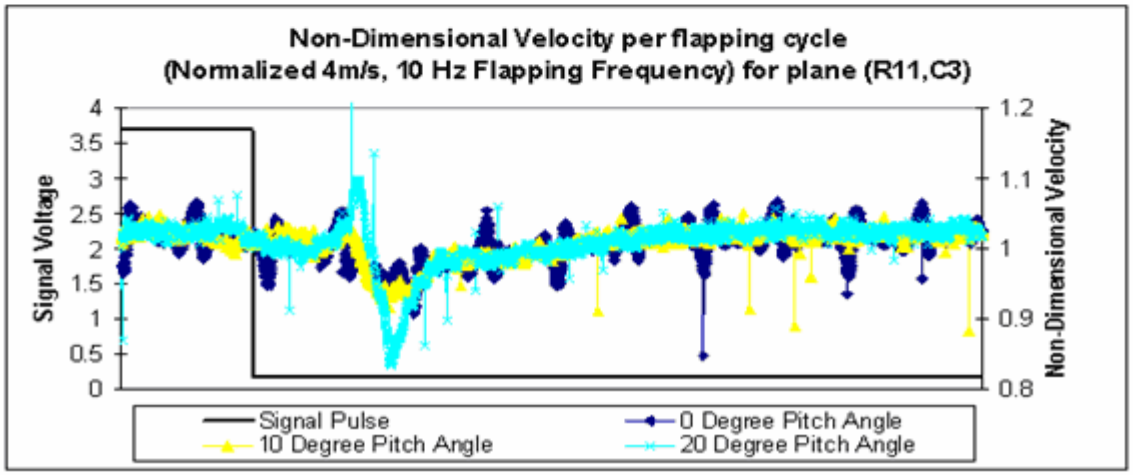
Non-Dimensional Velocity per flapping cycle
(Normalized 4m/s, 10 Hz Flapping Frequency) for plane (R11,C3)
Signal Voltage
Non-Dimensional Velocity
Signal Pulse
10 Degree Pitch Angle
0 Degree Pitch Angle
20 Degree Pitch Angle

TIME-DEPENDANT VELOCITY MAPPING ALONG PLANE C3 FOR VARYING FREE STREAM VELOCITY AND NEUTRAL ANGLE.

6. NORMALIZED 4M/S, 15 HZ FLAPPING FREQUENCY

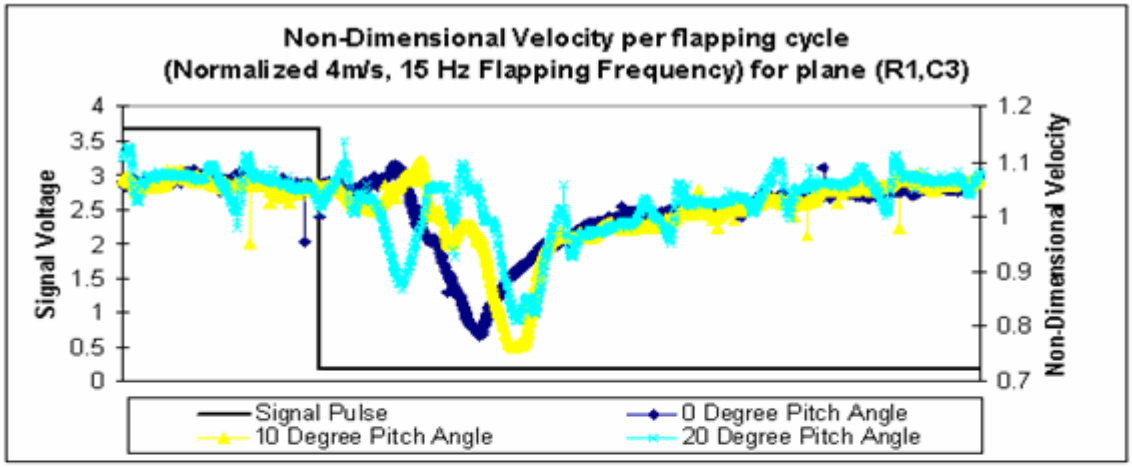

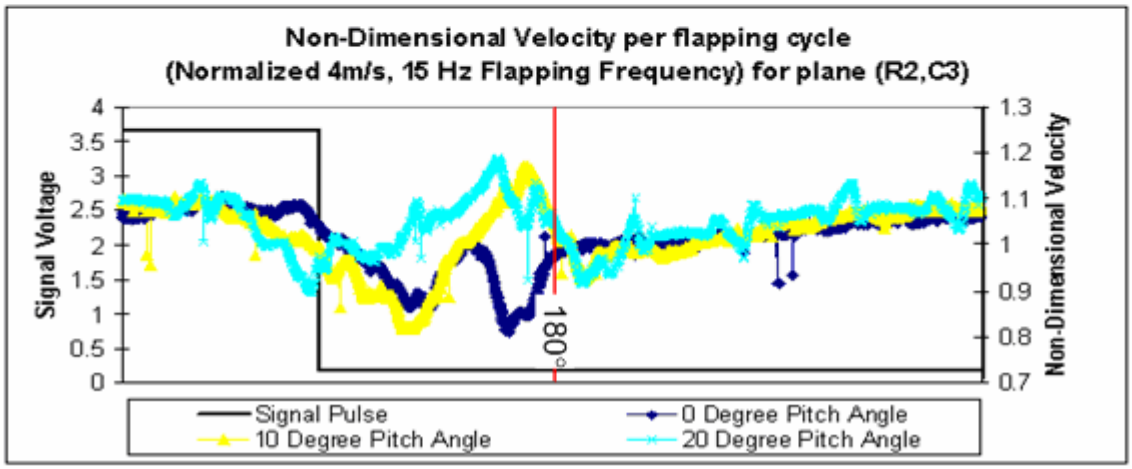

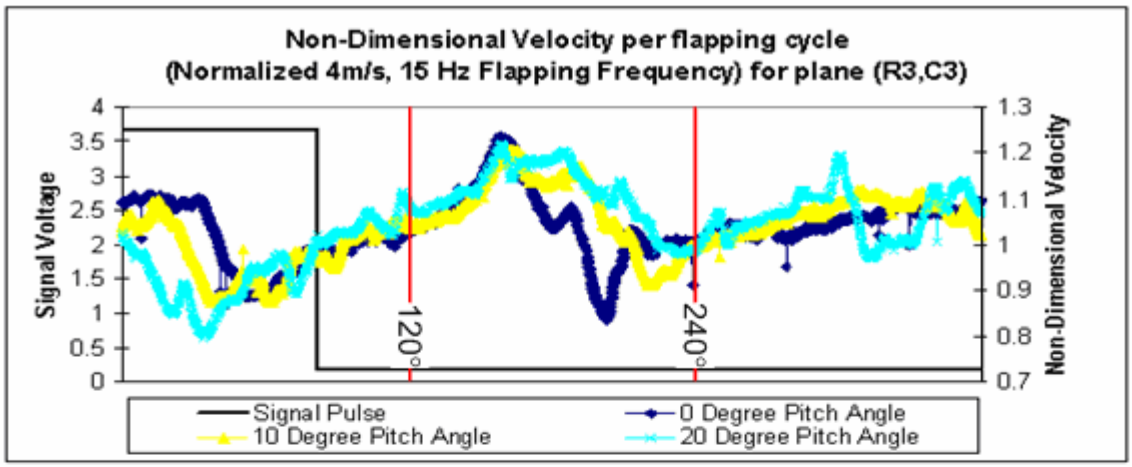
Non-Dimensional Velocity per flapping cycle
(Normalized 4m/s, 15 Hz Flapping Frequency) for plane (R3,C3)
Signal Voltage
Non-Dimensional Velocity
120°
240°
Signal Pulse
10 Degree Pitch Angle
0 Degree Pitch Angle
20 Degree Pitch Angle

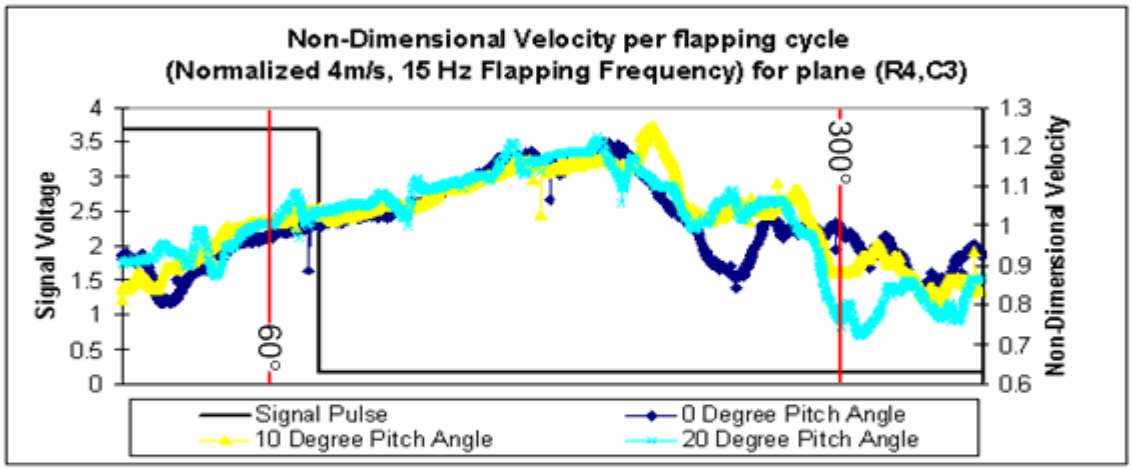
Non-Dimensional Velocity per flapping cycle
(Normalized 4m/s, 15 Hz Flapping Frequency) for plane (R4,C3)
Signal Voltage
Non-Dimensional Velocity
60°
300°
Signal Pulse
10 Degree Pitch Angle
0 Degree Pitch Angle
20 Degree Pitch Angle

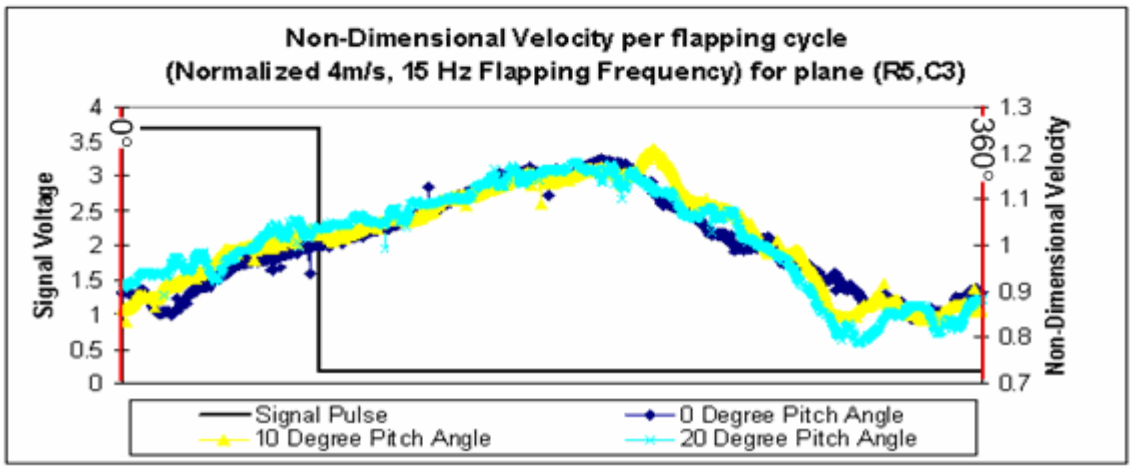
Non-Dimensional Velocity per flapping cycle
(Normalized 4m/s, 15 Hz Flapping Frequency) for plane (R5,C3)
Signal Voltage
Non-Dimensional Velocity
0°
360°
Signal Pulse
10 Degree Pitch Angle
0 Degree Pitch Angle
20 Degree Pitch Angle

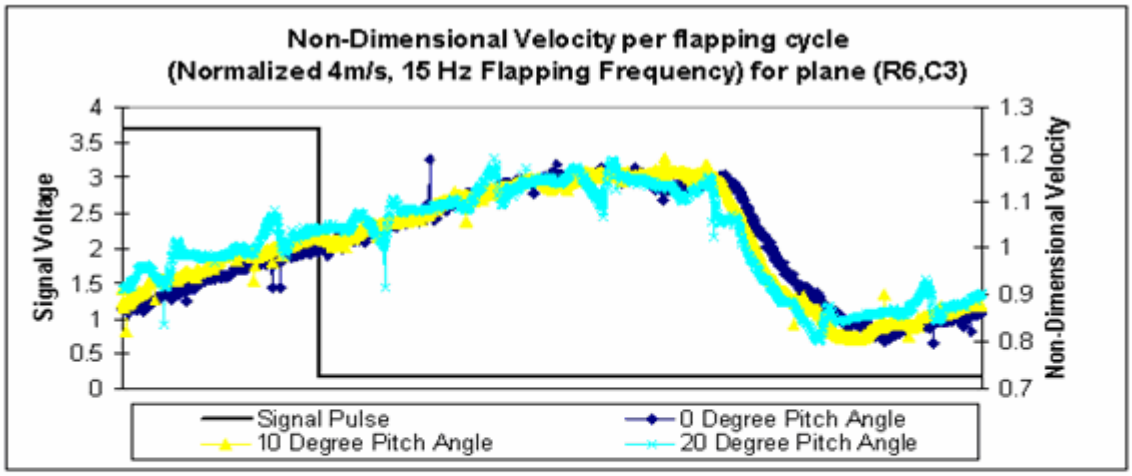
Non-Dimensional Velocity per flapping cycle
(Normalized 4m/s, 15 Hz Flapping Frequency) for plane (R6,C3)
Signal Voltage
Non-Dimensional Velocity
Signal Pulse
0 Degree Pitch Angle
10 Degree Pitch Angle
20 Degree Pitch Angle

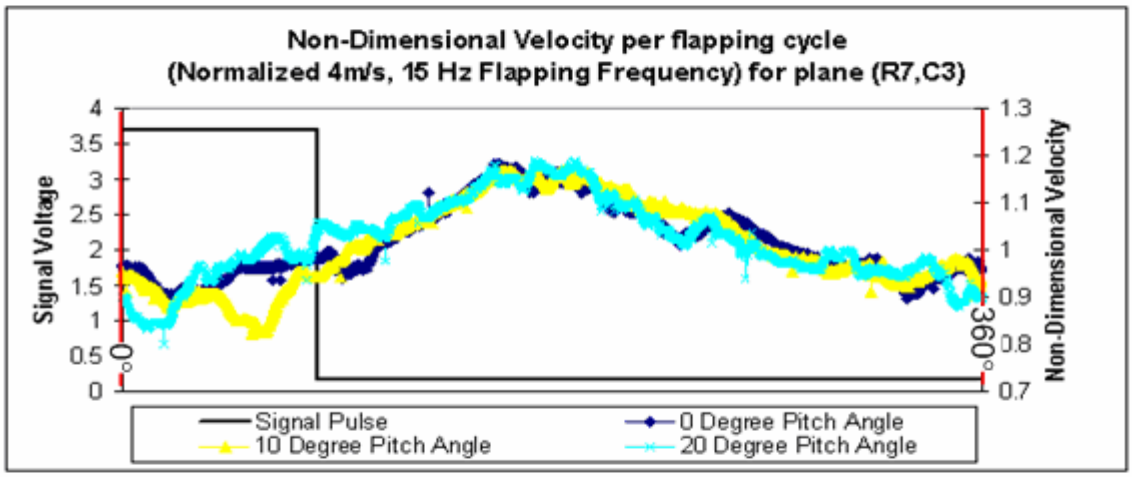
Non-Dimensional Velocity per flapping cycle
(Normalized 4m/s, 15 Hz Flapping Frequency) for plane (R7,C3)
Signal Voltage
Non-Dimensional Velocity
0°
360°
Signal Pulse
0 Degree Pitch Angle
10 Degree Pitch Angle
20 Degree Pitch Angle

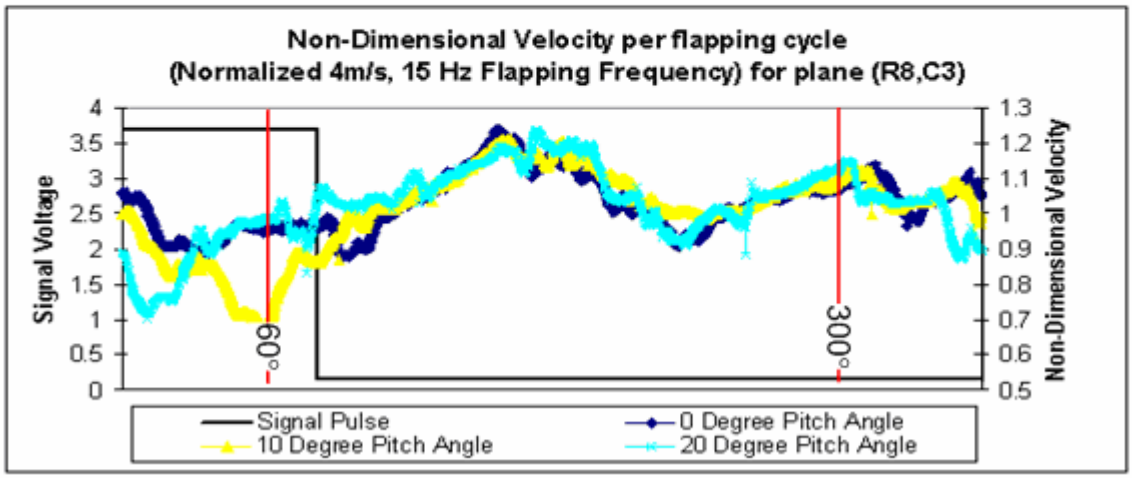
Non-Dimensional Velocity per flapping cycle
(Normalized 4m/s, 15 Hz Flapping Frequency) for plane (R8,C3)
Signal Voltage
Non-Dimensional Velocity
60°
300°
Signal Pulse
0 Degree Pitch Angle
10 Degree Pitch Angle
20 Degree Pitch Angle

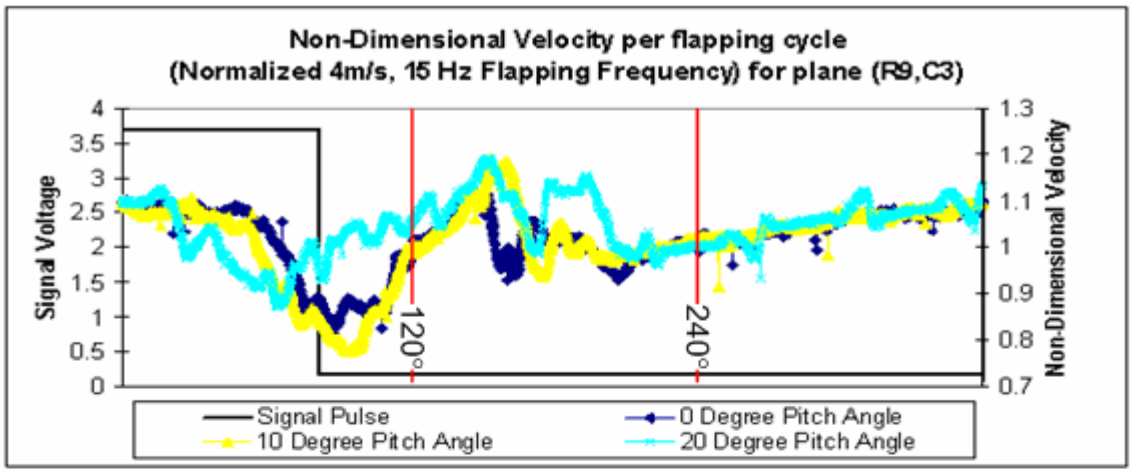
Non-Dimensional Velocity per flapping cycle
(Normalized 4m/s, 15 Hz Flapping Frequency) for plane (R9,C3)
Signal Voltage
Non-Dimensional Velocity
120°
240°
Signal Pulse
10 Degree Pitch Angle
0 Degree Pitch Angle
20 Degree Pitch Angle

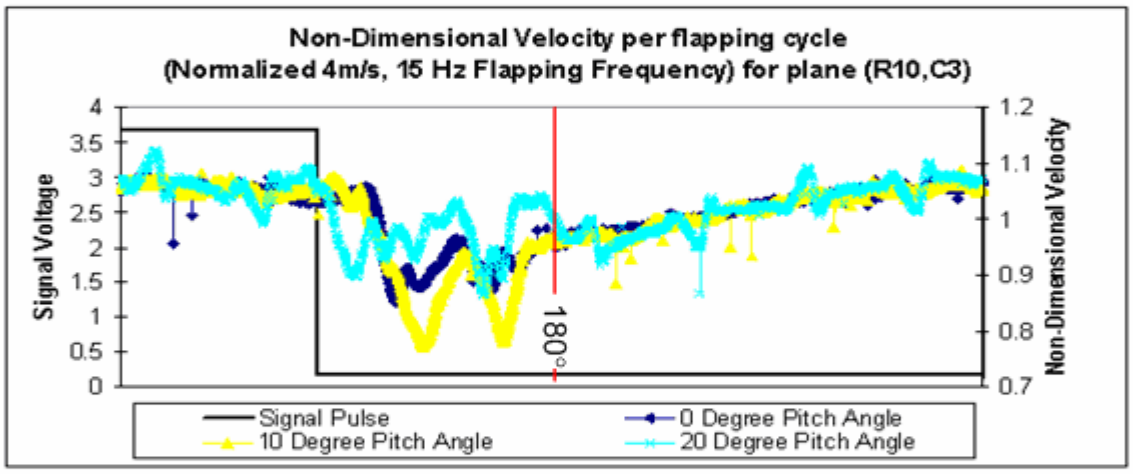
Non-Dimensional Velocity per flapping cycle
(Normalized 4m/s, 15 Hz Flapping Frequency) for plane (R10,C3)
Signal Voltage
Non-Dimensional Velocity
180°
Signal Pulse
10 Degree Pitch Angle
0 Degree Pitch Angle
20 Degree Pitch Angle

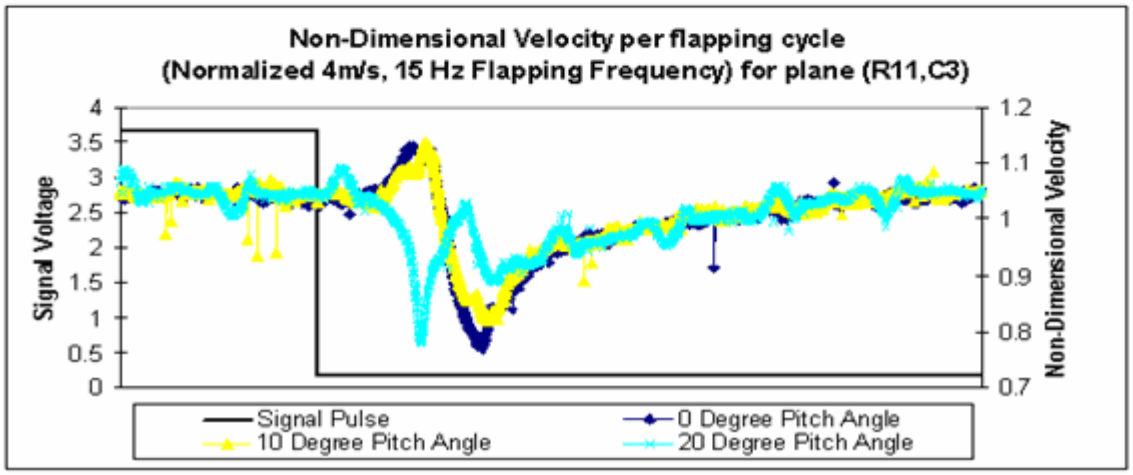
Non-Dimensional Velocity per flapping cycle
(Normalized 4m/s, 15 Hz Flapping Frequency) for plane (R11,C3)
Signal Voltage
Non-Dimensional Velocity
Signal Pulse
10 Degree Pitch Angle
0 Degree Pitch Angle
20 Degree Pitch Angle

APPENDIX D. FORCE BALANCE CALIBRATION

TABULATION OF FORCE BALANCE CALIBRATION

Gram	Run 1			Run 2		
	Voltage		Absolute Voltage	Voltage		Absolute Voltage
	Datum	Measured		Datum	Measured	
0	-5.735	-5.735	0	-5.729	-5.729	0
1	-5.735	-5.762	0.027	-5.729	-5.756	0.027
2	-5.734	-5.788	0.054	-5.727	-5.778	0.051
3	-5.734	-5.814	0.08	-5.726	-5.805	0.079
5	-5.732	-5.87	0.138	-5.727	-5.862	0.135
10	-5.729	-6.003	0.274	-5.725	-5.993	0.268
20	-5.73	-6.275	0.545	-5.725	-6.25	0.525

Gram	Run 3			Run 4		
	Voltage		Absolute Voltage	Voltage		Absolute Voltage
	Datum	Measured		Datum	Measured	
0	-5.725	-5.725	0	-5.721	-5.721	0
1	-5.723	-5.749	0.026	-5.721	-5.747	0.026
2	-5.723	-5.779	0.056	-5.719	-5.773	0.054
3	-5.722	-5.803	0.081	-5.718	-5.799	0.081
5	-5.721	-5.858	0.137	-5.718	-5.854	0.136
10	-5.721	-5.986	0.265	-5.718	-5.996	0.278
20	-5.721	-6.256	0.535	-5.719	-6.247	0.528

Gram	Run 5			Run 6		
	Voltage		Absolute Voltage	Voltage		Absolute Voltage
	Datum	Measured		Datum	Measured	
0	-5.711	-5.711	0	-5.711	-5.711	0
1	-5.711	-5.739	0.028	-5.711	-5.736	0.025
2	-5.711	-5.77	0.059	-5.711	-5.764	0.053
3	-5.713	-5.795	0.082	-5.713	-5.791	0.078
5	-5.715	-5.855	0.14	-5.711	-5.847	0.136
10	-5.718	-5.983	0.265	-5.709	-5.977	0.268
20	-5.719	-6.253	0.534	-5.709	-6.24	0.531

Gram	Run 7			Run 8		
	Voltage		Absolute Voltage	Voltage		Absolute Voltage
	Datum	Measured		Datum	Measured	
0	-5.709	-5.709	0	-5.712	-5.712	0
1	-5.709	-5.738	0.029	-5.712	-5.74	0.028
2	-5.707	-5.763	0.056	-5.714	-5.77	0.056
3	-5.709	-5.797	0.088	-5.712	-5.795	0.083
5	-5.708	-5.843	0.135	-5.715	-5.848	0.133
10	-5.707	-5.975	0.268	-5.713	-5.985	0.272
20	-5.708	-6.244	0.536	-5.713	-6.248	0.535

THIS PAGE INTENTIONALLY LEFT BLANK

APPENDIX E. DIRECT THRUST MEASUREMENT

TABULATION OF FORCE BALANCE MEASUREMENT

A. FREE STREAM AIR VELOCITY 2 M/S

1) Force Balance Measurement for 2m/s Free Stream Velocity

Free Stream Air Velocity 2m/s									
Pitch Angle	Run 1			Run 2			Run 3		
	Voltage			Voltage			Voltage		
	Datum	Measured	Delta	Datum	Measured	Delta	Datum	Measured	Delta
a) Flapping Frequency 10 Hz									
0°	-5.719	-5.715	-0.004	-5.678	-5.680	0.002	-5.675	-5.678	0.003
10°	-5.750	-5.734	-0.016	-5.675	-5.678	0.003	-5.679	-5.679	0.000
20°	-5.740	-5.719	-0.021	-5.681	-5.670	-0.011	-5.680	-5.671	-0.009
b) Flapping Frequency 15 Hz									
0°	-5.720	-5.740	0.020	-5.680	-5.709	0.029	-5.682	-5.711	0.029
10°	-5.734	-5.750	0.016	-5.678	-5.707	0.029	-5.675	-5.708	0.033
20°	-5.730	-5.739	0.009	-5.676	-5.692	0.016	-5.679	-5.694	0.015
c) Flapping Frequency 20 Hz									
0°	-5.721	-5.791	0.070	-5.673	-5.745	0.072	-5.676	-5.744	0.068
10°	-5.726	-5.781	0.055	-5.680	-5.738	0.058	-5.674	-5.737	0.063
20°	-5.732	-5.775	0.043	-5.680	-5.722	0.042	-5.682	-5.722	0.040
d) Flapping Frequency 25 Hz									
0°	-5.722	-5.814	0.092	-5.675	-5.760	0.085	-5.679	-5.764	0.085
10°	-5.721	-5.808	0.087	-5.678	-5.765	0.087	-5.677	-5.765	0.088
20°	-5.719	-5.796	0.077	-5.679	-5.753	0.074	-5.680	-5.754	0.074

2) Force Balance Summary for 2m/s Free Stream Velocity

Free Stream Air Velocity 2m/s						
Flapping Frequency	**Pitch Angle**	**Delta Voltage**			**Average Delta Voltage**	**Curve Fit Y = 0.0271 X**
		Run 1	**Run 2**	**Run 3**		**Extrapolated Thrust (gram-force)**
10 Hz	0°	-0.004	0.002	0.003	0.0003	0.012
	10°	-0.016	0.003	0	-0.004	-0.160
	20°	-0.021	-0.011	-0.009	-0.014	-0.504
15 Hz	0°	0.02	0.029	0.029	0.026	0.959
	10°	0.016	0.029	0.033	0.026	0.959
	20°	0.009	0.016	0.015	0.013	0.492
20 Hz	0°	0.07	0.072	0.068	0.070	2.583
	10°	0.055	0.058	0.063	0.059	2.165
	20°	0.043	0.042	0.040	0.042	1.538
25 Hz	0°	0.092	0.085	0.085	0.087	3.223
	10°	0.087	0.087	0.088	0.087	3.223
	20°	0.077	0.074	0.074	0.075	2.768

B. FREE STREAM AIR VELOCITY 3 M/S

1) Force Balance Measurement for 3m/s Free Stream Velocity

Free Stream Air Velocity 3m/s									
Pitch Angle	Run 1			Run 2			Run 3		
	Voltage			Voltage			Voltage		
	Datum	Measured	Delta	Datum	Measured	Delta	Datum	Measured	Delta
a) Flapping Frequency 10 Hz									
0°	-5.714	-5.692	-0.022	-5.674	-5.649	-0.025	-5.672	-5.647	-0.025
10°	-5.71	-5.685	-0.025	-5.676	-5.653	-0.023	-5.677	-5.647	-0.030
20°	-5.712	-5.672	-0.04	-5.677	-5.635	-0.042	-5.674	-5.637	-0.037
b) Flapping Frequency 15 Hz									
0°	-5.713	-5.713	0.000	-5.678	-5.675	-0.003	-5.672	-5.669	-0.003
10°	-5.712	-5.701	-0.011	-5.675	-5.665	-0.010	-5.672	-5.667	-0.005
20°	-5.715	-5.693	-0.022	-5.679	-5.655	-0.024	-5.672	-5.657	-0.015
c) Flapping Frequency 20 Hz									
0°	-5.717	-5.731	0.014	-5.677	-5.693	0.016	-5.648	-5.688	0.040
10°	-5.716	-5.732	0.016	-5.676	-5.692	0.016	-5.654	-5.682	0.028
20°	-5.712	-5.713	0.001	-5.677	-5.682	0.005	-5.654	-5.678	0.024
d) Flapping Frequency 25 Hz									
0°	-5.717	-5.747	0.030	-5.674	-5.698	0.024	-5.656	-5.691	0.035
10°	-5.715	-5.743	0.028	-5.677	-5.696	0.019	-5.668	-5.696	0.028
20°	-5.717	-5.740	0.023	-5.679	-5.690	0.011	-5.660	-5.678	0.018

2) Force Balance Summary for 3m/s Free Stream Velocity

Free Stream Air Velocity 3m/s						
Flapping Frequency	**Pitch Angle**	**Delta Voltage**			**Average Delta Voltage**	**Curve Fit Y = 0.0271X**
		Run 1	**Run 2**	**Run 3**		**Extrapolated Thrust (gram-force)**
10 Hz	0°	-0.022	-0.025	-0.025	-0.024	-0.886
	10°	-0.025	-0.023	-0.030	-0.026	-0.959
	20°	-0.040	-0.042	-0.037	-0.040	-1.464
15 Hz	0°	0.000	-0.003	-0.003	-0.002	-0.074
	10°	-0.011	-0.010	-0.005	-0.009	-0.320
	20°	-0.022	-0.024	-0.015	-0.020	-0.750
20 Hz	0°	0.014	0.016	0.040	0.023	0.861
	10°	0.016	0.016	0.028	0.020	0.738
	20°	0.001	0.005	0.024	0.010	0.369
25 Hz	0°	0.030	0.024	0.035	0.030	1.095
	10°	0.028	0.019	0.028	0.025	0.923
	20°	0.023	0.011	0.018	0.017	0.640

C. FREE STREAM AIR VELOCITY 4 M/S

1) Force Balance Measurement for 4m/s Free Stream Velocity

Free Stream Air Velocity 4m/s									
Pitch Angle	Run 1			Run 2			Run 3		
	Voltage			Voltage			Voltage		
	Datum	Measured	Delta	Datum	Measured	Delta	Datum	Measured	Delta
a) Flapping Frequency 10 Hz									
0°	-5.712	-5.646	-0.066	-5.666	-5.626	-0.040	-5.668	-5.628	-0.040
10°	-5.712	-5.644	-0.068	-5.668	-5.627	-0.041	-5.641	-5.631	-0.010
20°	-5.714	-5.637	-0.077	-5.661	-5.617	-0.044	-5.661	-5.619	-0.042
b) Flapping Frequency 15 Hz									
0°	-5.713	-5.664	-0.049	-5.671	-5.632	-0.039	-5.655	-5.641	-0.014
10°	-5.712	-5.653	-0.059	-5.643	-5.636	-0.007	-5.651	-5.638	-0.013
20°	-5.698	-5.648	-0.050	-5.673	-5.624	-0.049	-5.658	-5.634	-0.024
c) Flapping Frequency 20 Hz									
0°	-5.697	-5.658	-0.039	-5.658	-5.645	-0.013	-5.671	-5.647	-0.024
10°	-5.701	-5.662	-0.039	-5.644	-5.640	-0.004	-5.671	-5.661	-0.010
20°	-5.705	-5.663	-0.042	-5.646	-5.635	-0.011	-5.659	-5.644	-0.015
d) Flapping Frequency 25 Hz									
0°	-5.688	-5.671	-0.017	-5.648	-5.634	-0.014	-5.656	-5.640	-0.016
10°	-5.679	-5.657	-0.022	-5.671	-5.629	-0.042	-5.666	-5.640	-0.026
20°	-5.680	-5.654	-0.026	-5.659	-5.616	-0.043	-5.656	-5.625	-0.031

2) Force Balance Summary for 4m/s Free Stream Velocity

Free Stream Air Velocity 4m/s						
Flapping Frequency	**Pitch Angle**	**Delta Voltage**			**Average Delta Voltage**	**Curve Fit Y = 0.0271X**
		Run 1	**Run 2**	**Run 3**		**Extrapolated Thrust (gram-force)**
10 Hz	0°	-0.066	-0.040	-0.040	-0.049	-1.796
	10°	-0.068	-0.041	-0.010	-0.040	-1.464
	20°	-0.077	-0.044	-0.042	-0.054	-2.005
15 Hz	0°	-0.049	-0.039	-0.014	-0.034	-1.255
	10°	-0.059	-0.007	-0.013	-0.026	-0.972
	20°	-0.050	-0.049	-0.024	-0.041	-1.513
20 Hz	0°	-0.039	-0.013	-0.024	-0.025	-0.935
	10°	-0.039	-0.004	-0.010	-0.018	-0.652
	20°	-0.042	-0.011	-0.015	-0.023	-0.839
25 Hz	0°	-0.017	-0.014	-0.016	-0.016	-0.578
	10°	-0.022	-0.042	-0.026	-0.030	-1.107
	20°	-0.026	-0.043	-0.031	-0.033	-1.230

LIST OF REFERENCES

1. Madangopal, R.; Khan, Z. A.; and Agrawal, S. K. "Biologically Inspired Design of Small Flapping Wing Air Vehicles Using Four-Bar Mechanisms and Quasi-Steady Aerodynamics." Journal of Mechanical Design, July 2005. http://mechsys4.me.udel.edu/publications/papers/p94.pdf, December 2006.
2. Houssam, SOUEID. "Propulsion by Mobile Wings Aerodynamics and Applications to Micro Air Vehicles." DIAM Internal Report, December 2005.
3. Hickle, C. "Wind Tunnel Renovation, Flow Verification and Flapping Wing Analysis." Naval Postgraduate School: June 2006.
4. Jorgenson, F. "How to Measure Turbulence with Hot-Wire Anemometers – A Practical Guide." Dantec Dynamics, 2005. http://www.dantecmt.com/Download/pdf_files/practicalguide.pdf, December 2006.
5. "Probes for Hot-Wire Anemometry." Dantec Dynamics. http://www.dantecmt.com/Download/pdf_files/238-2-probekatalog.pdf December 2006.
6. "StreamLine CTA Anemometer System." Dantec Dynamics. http://www.dantecmt.com/Download/litterature/pi_StreamLine-CTA-Anemometer-System_119.pdf, December 2006.
7. Barlow, J.; Rae, W. Jr.; and Pope, A. "Low Speed Wind Tunnel Testing." 3rd ed. Wiley, New York, 1999.
8. "National Instruments Products and Services." National Instruments. http://www.ni.com/labview/whatis/, December 2006.
9. T, Theodorsen. "General theory of aerodynamic instability and the mechanism of utter." NACA TR, Volume 496, 1935.

10. **I.E. Garrick. “Propulsion of a flapping and oscillating airfoil.” NACA TR, Volume 567, 1936.**
11. **K.D. Jones.; M.F. Platzer. “AIAA-2000-0897 Flapping-Wing Propulsion For A Micro Air Vehicle.” Naval Postgraduate School: January 2000.**
12. **Papadopoulos, J. “An Experimental Investigation of the Geometric Characteristics of Flapping Wing Propulsion for a Micro Air Vehicle.” Naval Postgraduate School: March 2003.**
13. **Mehta, R., and Bradshaw, P. “Design Rules for Small Low Speed Wind Tunnels.” Aeronautical Journal, November 1979.**

INITIAL DISTRIBUTION LIST

1. Defense Technical Information Center
   Ft. Belvoir, Virginia

2. Dudley Knox Library
   Naval Postgraduate School
   Monterey, California

3. Professor Kevin Jones
   Naval Postgraduate School
   Monterey, California

4. Professor Christopher Brophy
   Naval Postgraduate School
   Monterey, California

5. Professor Yeo Tat Soon
   Director, Temasek Defence Systems Institute
   National University of Singapore
   Singapore

6. Ms. Tan Lai Poh
   Senior Admin Officer (MDTS), Temasek Defence Science Institute
   National University of Singapore
   Singapore

7. Mr. Chin Chee Kian
   Defence Science & Technology Agency
   Singapore